The next frontier in ADME science: predicting transporter-based drug disposition, tissue concentrations and drug-drug interactions in humans

Flavia Storelli[1], Mengyue Yin[1], Aditya R. Kumar[1], Mayur K. Ladumor[1], Raymond Evers[2], Paresh P. Chothe[3], Osatohanmwen J. Enogieru[4,] Xiaomin Liang[5], Yurong Lai[5], Jashvant D. Unadkat[1]*

[1] Department of Pharmaceutics, University of Washington, Seattle, WA, USA

[2] Preclinical Sciences and Translational Safety, Janssen Research & Development, LLC, Spring House, Pennsylvania, USA

[3] Global Drug Metabolism and Pharmacokinetics, Takeda Development Center Americas, Inc. 95 Hayden Avenue, Lexington, Massachusetts, 02421, USA

[4] Pharmacokinetics & Drug Metabolism, Amgen, South San Francisco, CA, USA

[5] Drug Metabolism, Gilead Sciences Inc., Foster City, CA, USA

*Corresponding author:

Jashvant D. Unadkat

Department of Pharmaceutics

Box 357610

University of Washington

Seattle, WA 98195

jash@uw.edu

Abstract

Predicting transporter-based drug clearance (CL) and tissue concentrations (TC) in humans is important to reduce the risk of failure during drug development. In addition, when transporters are present at the tissue:blood interface (e.g., in the liver, blood-brain barrier), predicting TC is important to predict the drug's efficacy and safety. With the advent of quantitative targeted proteomics, *in vitro* to *in vivo* extrapolation (IVIVE) of transporter-based drug CL and TC is now possible using transporter-expressing models (cells lines, membrane vesicles) and the *in vivo* to *in vitro* relative expression of transporters (REF) as a scaling factor. Unlike other approaches based on physiological scaling, the REF approach is not dependent on the availability of primary cells. Here, we review the REF approach and compare it with other IVIVE approaches such as the relative activity factor approach and physiological scaling. For each of these scaling approaches, we review their underlying principles, assumptions, methodology, predictive performance, as well as advantages and limitations. Finally, we discuss current gaps in IVIVE of transporter-based CL and TC and propose possible reasons for these gaps as well as areas to investigate to bridge these gaps.

Keywords: predicting transporter-based drug clearance, predicting transporter-modulated tissue concentrations, *in vitro to in vivo* extrapolation (IVIVE), relative expression factor (REF), relative activity factor (RAF), *in vitro* models

Abbreviations: ADME, absorption, distribution, metabolism, excretion; AUC, area under the concentration-time profile; BBB, blood-brain barrier; BCRP, breast cancer resistance protein; CL, clearance; CL_{int}, intrinsic clearance; CSF, cerebrospinal fluid; DDI, drug-drug interaction; ECM, extended clearance model; ER, efflux ratio; ESF, empirical scaling factor; f_t, fraction transported; IVIVE, *in vitro* to *in vivo* extrapolation; ISEF, intersystem extrapolation factor; J_{max}, maximal rate of transport; K_m, affinity constant; $K_{p,uu}$, ratio of unbound drug concentration in tissue *vs.* plasma at steady-state; MATE, multidrug and toxin extrusion; MPS, microphysiological system; MRP, multidrug resistance protein; NME, new molecular entity; NTCP, sodium-taurocholate co-transporting polypeptide; OAT, organic anion transporter; OATP, organic anion transporting polypeptide; OCT, organic cation transporter; P-gp, P-

glycoprotein; P_{app}, apparent permeability; PBPK, physiologically-based pharmacokinetics; PD, pharmacodynamics; pd, passive diffusion; PET, positron emission tomography; PK, pharmacokinetics; PMUE, protein-mediated uptake effect; PSF, physiological scaling factor; PTM, post-translational modification; QTP, quantitative targeted proteomics; RAF, relative activity factor; RDS, rate-determining step; REF, relative expression factor; SCH, sandwich cultured hepatocytes

Table of Contents

1. Introduction

Drug development is a lengthy and costly process that has a high attrition rate. During the period 1996-2014, 90% of new molecular entity (NME) in Phase 1 trials failed to reach the market (Smietana et al., 2016). This failure rate was higher for small molecules (91%) compared with biologicals (82%) (Hay et al., 2014). Amongst the small molecules, the failure rate during phase 3 clinical trials was particularly high for those targeted to the central nervous system (Kesselheim et al., 2015). The major reason for this failure was lack of efficacy (Hay et al., 2014; Kesselheim et al., 2015). To reduce the failure rate, an integrated understanding of the pharmacokinetics (PK) and pharmacodynamics (PD, including more translatable pharmacology models) of the NME is required (Morgan et al., 2012). The PD (efficacy or toxicity) of an NME is driven by the PK of the NME, both systemic and at the site of action (e.g., target issue). Therefore, predicting the PK of the NME is critical to predicting its PD. In this review, the term PK will be used broadly to imply both systemic and tissue PK and the term drug will be used to imply both a small NME and an approved drug.

During drug development, predicting the systemic PK of the drug is important to estimate the first in human dose and the quantitative impact of drug-drug interactions (DDIs), pharmacogenetics (PGx), disease, age, and other factors on the PK of the drug. Such information is important to design the drug's Phase 2 & 3 clinical trials where the population enrolled is heterogenous. For many drugs, transporters are a significant contributor to not only their absorption and systemic clearance (CL) but also their distribution into tissues where their PD effects manifest (e.g. the brain, liver). If the tissue is not a significant contributor to the systemic CL of the drug, the presence (or modulation by DDI or PGx) of transporters at the tissue:blood barrier (e.g. the blood-brain barrier, BBB) will not affect the systemic CL of drug, but will affect their tissue PK, which drives the drug's efficacy and/or toxicity. Therefore, besides determining (or predicting) systemic PK of a drug, it is also important to predict the tissue PK of the drug. This includes not only the unbound average steady-state drug tissue concentration, but also the dynamic changes in these concentrations. Here, we emphasize the word "predict" as measurement of drug concentrations at the site of its effect is rarely possible in humans.

Prior to first in human dose, prediction of *in vivo* systemic CL of a drug is usually done through *in vitro* to *in vivo* extrapolation (IVIVE). This is because the alternative approach, using animal data and allometry, is fraught with interspecies differences in protein abundance, catalytic activity and substrate selectivity of the transporters and metabolic enzymes that determine the PK of a drug. However, the success of IVIVE of transporter-based drug CL remains elusive (Bowman & Benet, 2016; Soars et al., 2007; Wood et al., 2017). The reasons for this lack of success are multifactorial. First and foremost, there is a conceptual misunderstanding of what determines the systemic and tissue PK of a drug when transporters are present (see section 5 below and Patilea-Vrana & Unadkat, 2016). Second, high quality primary cells or *in vitro* cell models that can be used for IVIVE of transporter-based uptake and efflux CLs are not available routinely for tissues other than liver. Even where available (e.g., hepatocytes), their ability to replicate the activity (and abundance) of transporters found in the corresponding tissue, *in vivo,* is questionable (V. Kumar et al., 2019). Third, until recently, unlike metabolic enzymes (especially cytochrome P450 enzymes), the abundance of transporters in various human tissues was unknown. With the advent of quantitative targeted proteomics (QTP), this challenge has been largely addressed (Prasad et al., 2019). Finally, *in vitro* methods (including scaling factors) to predict transporter-based PK of drugs, have not been thoroughly validated.

Estimating tissue PK of a drug also poses many challenges since unlike systemic CL, tissue PK can rarely be measured in humans. Unlike drugs that passively diffuse across the tissue:blood barrier, the unbound steady-state tissue drug concentration of transporters substrates cannot be assumed to equal that in the plasma when transporters are present at this barrier. Often, the unbound steady-state tissue drug concentration ($C_{u,tissue,ss}$) is expressed relative to the corresponding unbound steady-state concentration in the plasma ($C_{u,plasma,ss}$), i.e., $K_{p,uu}$ (Eq. 1). $K_{p,uu}$ is determined by all the intrinsic (i.e., unbound) entry CLs into the tissue ($CL_{int,in}$) and unbound exit CLs from the tissue ($CL_{int,out}$):

$$K_{p,uu} = \frac{Cu,tissue,ss}{Cu,plasma,ss} = \frac{\sum CL_{int,in}}{\sum CL_{int,out}} \qquad \text{(Eq. 1)}$$

In the absence of tissue metabolism (e.g., the brain), for drugs that passively cross the tissue:blood barrier, $K_{p,uu}$ will equal 1 ($CL_{int,in} = CL_{int,out}$), However, when a drug is transported into or out of the tissue $K_{p,uu}$ will be >1 and <1, respectively. That is, the unbound steady-state tissue concentration can no longer

be assumed to be the same as that in the plasma. In addition, a drug's PD may be determined by its stead-state peak and trough tissue drug concentrations. Such prediction can only be made by estimating all the entry and exit intrinsic CLs (CL_{int}) of the drug (including passive diffusion CL_{int}) for the tissue of interest. In the liver for example, these CL_{int} are the sinusoidal uptake ($CL_{int,s,in}$) and efflux ($CL_{int,s,ef}$), metabolic ($CL_{int,met}$) and biliary efflux ($CL_{int,bile}$).

As outlined above, although predicting PK of transported drugs is challenging, much progress has been made in the last decade to overcome these challenges. These advances have been catalyzed by a better understanding of the role of transporters in the PK of drugs through the extended CL model (ECM) (Gillette & Pang, 1977; Sirianni & Pang, 1997; Shitara et al., 2006a; Camenisch & Umehara, 2012; M. V. Varma et al., 2015; Patilea-Vrana & Unadkat, 2016; Benet et al., 2018), advances in quantification of the abundance of transporters in human tissues using QTP (Prasad et al., 2019), commercial availability of cells/vesicle expressing human drug transporters, and the use of positron emission tomography (PET) imaging data to validate tissue drug PK predictions (including $K_{p,uu,}$ as well as steady-state peak and trough concentrations). In this review, first, we describe in detail current and emerging *in vitro* models that are used for IVIVE of transporter-based and passive diffusion CL_{int}. Second, we propose best experimental and data analysis practices to obtain scalable *in vitro* data. Third, we discuss various IVIVE scaling approaches to predict transporter-based CL, DDI and tissue PK of drugs. For each of these scaling approaches, we review their underlying principles, assumptions, methodology, predictive performance, as well as advantages and limitations. Fourth, we review available studies where predictive performance of these approaches has been assessed. Fifth, we describe how some of the above approaches can be used to predict transporter-based DDI. Finally, we discuss the current gaps in these approaches, and propose possible reasons for these gaps as well as studies that could help fill these gaps.

Of note, in this review we refer to CL and CL_{int} as the product of the surface area of the membrane barrier and the respective total and unbound drug permeability through the membrane barrier. These CLs can be either uptake or efflux. According to the ECM, the combination of multiple CL_{int} (uptake, efflux and metabolic) in an eliminating organ determines the organ CL_{int} (e.g., hepatic or renal) which in turn can be

translated into organ CL by taking into account the unbound fraction of the drug in the blood or plasma and the organ blood flow.

2. *In vitro* models for IVIVE of PK of transporter substrates

To predict the quantitative role of drug transporters (and their modulation by endo- and xenobiotics) in the PK of a drug in humans, *in vitro* models are used, from which data on drug transport and passive diffusion can be extrapolated to *in vivo* (IVIVE). These *in vitro* models can either be primary cells isolated from the human organ of interest, transporter-expressing cells or membrane vesicles. In 2013, the International Transporter Consortium published a comprehensive review on *in vitro* methods to study drug transport (Brouwer et al., 2013). In this section, we provide an update on the *in vitro* models available to perform IVIVE of drug transport once the transporters involved have been identified.

2.1. Primary cells

Except for human hepatocytes, primary human cells have limited availability. Although cells from preclinical species are used to establish *in vitro* to *in vivo* correlation in animals (De Bruyn et al., 2018; N. Li et al., 2020; Matsunaga et al., 2019; Trapa et al., 2019), extrapolation of these data to humans is unlikely to be accurate because of interspecies differences in transporter abundance, localization and substrate specificity (Chu et al., 2013; L. Wang et al., 2015). However, human liver chimeric mouse models have yielded some promising results (Feng et al., 2021; Sanoh et al., 2020).

For accurate IVIVE using human primary cells, where a physiological scaling factor (PSF) is usually used (see section 4), it is critical that transporters of interest are expressed at similar abundance and have similar activity as that in the organ they are isolated from (**Table 1**). While this is often assumed, transporter abundance and activity can differ between primary cells and organ of origin (due to the isolation process, cryopreservation and culture time/conditions) and should be assessed (Y.-A. Bi et al., 2017; Bow et al., 2008; Keemink et al., 2018; Kotani et al., 2011; Ulvestad et al., 2011). As an example, total and plasma membrane abundance of biliary efflux transporters are over-expressed in sandwich-cultured human hepatocytes (SCH) compared to the liver tissue from which the hepatocytes were isolated (V. Kumar et al., 2019). Such assessment can be done by quantifying transport of selective probe substrates (when available) in absence *vs.* presence of selective transporter inhibitors (Y.-A. Bi et al., 2019; De Bruyn et al., 2011; Zhang et al., 2019), quantifying the mRNA expression of the transporter of interest, or, preferably, its abundance (V. Kumar et al., 2019; Lundquist et al., 2014). Such research has

been done for hepatocytes (see studies referenced above), but limited data exist for proximal tubular cells and enterocytes from various regions of the intestine (Brown et al., 2008).

Currently, human hepatocytes, either freshly isolated or cryopreserved, are the most widely available primary cells for ADME (i.e., absorption, distribution, metabolism, excretion) research. Hepatocytes can be used either in suspension, plated or in the sandwich configuration. The first two are used to quantify uptake transport, while the latter is mainly used to quantify biliary (i.e., canalicular) efflux transport. However, as discussed above, overexpression of efflux transporters in SCH could result in overprediction of the efflux CLs at the basal and canalicular membranes. Indeed, correcting the over-prediction of biliary efflux CL of rosuvastatin by the abundance of the biliary membrane transporters, recapitulates the observed *in vivo* biliary CL of the drug as determined by PET imaging (V. Kumar et al., 2019; Storelli et al., 2022a).

Primary enterocytes and kidney proximal tubular epithelial cells are available commercially. However, they are not yet well characterized in terms of the abundance of transporters when cultured *vs*. that present in the corresponding human tissue. Availability of the brain microvascular endothelial cells, that constitute the BBB, represent an even greater challenge as they represent only a small fraction (<3%) of the brain (Lauwers et al., 2008), resulting in low cell yield per gram of tissue. The availability challenge of primary cells is further compounded by the significant interindividual variability in transporter abundance/activity, which results in the need to identify cells from donors that can provide a reasonable estimate of drug transport *in vivo* (e.g. not all hepatocytes are “transporter-qualified” or capable of being used in the SCH, suspended or plated configuration).

2.2. Transporter-expressing cell lines and membrane vesicles

In the absence of transporter-characterized primary cells (e.g. enterocytes or kidney proximal tubular epithelial cells), and due to deficiencies of the human hepatocyte models (described above), immortalized cells and membrane vesicles are alternative *in vitro* models for IVIVE of transporter-based drug PK. Available cell lines are either immortalized human cell lines (e.g., Caco-2, HepaRG, HepG2, HK-2), or human (such as HEK293 cells) or non-human cells (such as CHO, LLC-PK or MDCK cells) expressing a single or multiple human transporter(s) of interest. While the former can be used as models to predict

drug toxicity (e.g., BSEP-related cholestasis in HepaRG cells (Qiu et al., 2016; Woolbright et al., 2016)), they are not suitable for IVIVE due to the fact that not all transporters are expressed, or at abundances similar that in the tissue of interest. For example, organic anion transporting polypeptide (OATP)1B1 is present at a much lower abundance in HepaRG cells than in primary hepatocytes (Kotani et al., 2012), while organic anion transporter (OAT)1 and OAT3 are not at all expressed in HK-2 cells (Jenkinson et al., 2012).

Stable or transiently-transfected cell lines expressing a single transporter or membrane vesicles that are derived from these cells can allow quantitative prediction of the *in vivo* contribution of a particular transport pathway and the effect of genetic polymorphisms on this contribution (Kameyama et al., 2005) without the confounding effect of the presence of other transporters observed in primary cells. Therefore, these cells are the preferred *in vitro* cell models for IVIVE of transporter-based drug CL_{int} using the relative expression factor (REF) or the relative activity factor (RAF) approach (see Section 4 for details about these two approaches). Transfected cell lines and membrane vesicles are commercially available for most clinically relevant drug transporters (uptake and efflux) from different vendors. Cells and vesicles that express the highest abundance of the transporter of interest should be preferred due to increased sensitivity to determine active transport. Also, they should have any endogenous transporter(s) ablated to not confound interpretation of drug transport data (or the endogenous transporter[s] should not contribute significantly to the transport of the drug of interest; **Table 1**). One approach to take endogenous transport activity into account is to subtract transport observed in non-transfected cells from that in transfected *cells* (or the corresponding derived membrane vesicles). This assumes that the activity (and expression) of the endogenous transporter is identical in the transfected cells vs. non-transfected cells. To avoid making this assumption, the endogenous transporter can be knocked out (e.g. canine P-glycoprotein, P-gp, in MDCKII cells) before expressing the human transporter (Karlgren et al., 2017; Simoff et al., 2016; Wegler et al., 2021). Such cells have successfully been used for IVIVE of distribution of P-gp substrate drugs into the human brain and the fetus (Anoshchenko et al., 2021; Storelli, Anoshchenko, et al., 2021).

2.3. Emerging *in vitro* models

Recently, co-culture hepatocyte models (e.g., HepatoPac®, Hμrel®) have received much attention in long-term hepatic metabolism and toxicity studies due to their long-term functional stability (more than 4 weeks). These models have been evaluated for their potential application in phase I and phase II drug metabolism studies especially for low CL drugs (Ballard et al., 2020; Ramsden et al., 2014). These models express and demonstrate activity of major hepatic uptake transporters (Moore et al., 2016; Ramsden et al., 2014) and appear to recapitulate *in vivo* transporter-enzyme interplay in CYP induction. Using this model, prediction of *in vivo* CYP3A induction by rifampicin was better *vs*. the 2D hepatocyte monoculture (Dixit et al., 2016; Moore et al., 2016). Co-cultured models appear to form *in vivo*-like polarized architecture and hold potential in determining biliary excretion of xenobiotics. Biliary excretion of taurocholate has been investigated using the HepatoPac model and is comparable to that in SCH (Hafey et al., 2020). These models utilize smaller number of hepatocytes per well compared with the monoculture model making measuring transporter protein abundance by QTP a significant challenge. Also, because hepatocytes are co-cultured with a feeder cell line consisting of mouse fibroblasts, a control consisting of feeder cells alone (for activity as well as QTP) must be included in each experiment. Also, the accuracy of these models to predict *in vivo* hepatobiliary CL remains to be tested.

Progress has been made in the development of microphysiological models (MPS, or organs-on-chip) for various organs to determine the drug ADME. MPS models can be described as *in vitro* models that go beyond 2D cultures, incorporate primary or stem cell derived cells, include mechanical factors such as flow, and can incorporate components of the immune system (Fowler et al., 2020). The long-term goal in the MPS field is to build a multi-organ chip model by linking MPS for various organs together, but this will first require establishment and qualification of the individual components. Progress has been made to build models for major organs such as the liver (Jang et al., 2019; Sarkar et al., 2017), kidney (W.-Y. Chen et al., 2021), and intestine (Markus et al., 2021). Currently, these models are still in the exploratory phase. Their ability to accurately predict transporter-based PK of drugs is yet to be explored.

Due to the limited availability of primary cells to study drug transport at the BBB, human induced pluripotent stem cell-derived BBB models have been developed and currently being evaluated in predicting the brain penetration of drugs. With rapid progress in differentiation methods, human induced

pluripotent stem cell-derived BBB model has been shown to successfully form tight junctions (Transepithelial/transendothelial electrical resistance ~ 8000 ohm ×cm2) and express efflux transporters such as P-gp and multidrug resistance proteins (MRP) at a functional level (Neal et al., 2019). Further systematic evaluation of such models is needed to understand their potential to predict *in vivo* drug transport across the human BBB. Similarly, induced human intestinal organoids and enterocyte-like cells can express tight junction proteins and efflux transporters present in the intestinal tract. In addition, P-gp activity in this model can be inhibited by verapamil. However, current limitation of such models is the lack of segment-specificity, the need for long time in culture, and also abundance of drug transporters is not well characterized (Arian et al., 2022; Onozato et al., 2018; Ozawa et al., 2015).

3. Best practices to generate *in vitro* data suitable for IVIVE of drug transport PK

To obtain *in vitro* uptake or efflux data that can be used for IVIVE, we provide below some guidelines based on our experience in conducting such studies. An important challenge of IVIVE of transporter-based CL_{int} that does not arise for metabolism is that drug uptake and efflux, both *in vitro* and *in vivo,* is the sum of active transport and passive diffusion. For accurate IVIVE of drug transport from cell models, it is critical that passive diffusion CL_{int} be accurately quantified (except for the ER-REF and $RAF_{in\ vivo}$ approaches in Sections 4.2.1 and 4.2.2, respectively). This is particularly important where the contribution of passive diffusion CL_{int}, both *in vitro* and i*n vivo*, is a significant percent of the total uptake or efflux CL_{int} of the drug. In addition, quantification of passive diffusion *vs.* active CL_{int} of the drug is important for determining the fraction of drug transported (f_t; *i.e.*, the contribution of each transporter in the uptake and/or efflux of a drug) to predict the influence of DDI and transporter pharmacogenetics on transporter-based drug PK. Here we review experimental considerations for both uptake and efflux experiments. Of note, if plasma proteins are not included in the transport buffer, the uptake or efflux CL measured will be the intrinsic CL_{int}. However, when plasma proteins are included (e.g. human serum albumin), the measured uptake/efflux CL should be corrected for binding to translate the CL into CL_{int}.

3.1. Uptake assays

3.1.1. How should the transporter-based uptake CL_{int} be measured?

Two methods can be used to determine transporter-based drug uptake CL_{int} (**Fig. 1**). For both methods, the total drug uptake is measured over a period during which the uptake is linear. It is important to estimate the initial drug uptake rate where the back-flux of the drug from the cells (or vesicles) into the media is minimized and therefore assumed to be negligible. Only if this assumption is correct can the initial uptake rate be translated to uptake CL_{int}. For these reasons, the duration of uptake is short, usually seconds (transporter-transfected cells, vesicles) to several minutes (primary cells), depending on drug properties and the cell model used. Although not explicitly stated, the following assays (including for passive diffusion uptake) also apply to vesicle uptake studies.

In the first method (time-dependent uptake assay), the initial uptake rate is measured at a drug concentration much below its K_m (the affinity constant) for the transporter of interest (**Fig. 1A**). In the second method, the uptake of the drug (at a time when the uptake has been shown to be linear) is measured at different concentrations to generate a concentration-dependent uptake curve (concentration-dependent uptake assay). Though such concentration-dependent uptake could occur for a number of reasons other than Michaelis-Menten, for simplicity, henceforth we will refer to this assay as the Michaelis-Menten assay (**Fig. 1B**).

For the commonly used time-dependent uptake assay, the total (active + passive) uptake CL_{int} can be determined as the initial (linear) slope of the drug uptake (normalized with the initial concentration of the drug in the incubation buffer) *vs*. time plot. Active uptake CL_{int} is then indirectly calculated by subtracting the passive uptake CL_{int} (see below) from the total uptake CL_{int}. We recommend no fewer than three data points (preferably conducted in duplicate) to ensure confidence in the estimated slope. Conducting initial uptake studies can be a challenge since, for some transporters (such as OATPs), linear drug uptake occurs over a short duration such as 5-10 seconds (V. Kumar, Yin, et al., 2020). In this case, data at only two time points may be all that can be obtained to estimate uptake CL_{int}. Use of a single time point is not recommended as it entails assuming that the nonspecific binding of the drug (i.e. intercept) is negligible. Also, such short incubation times can result in increased technical variability due to the time needed to process the sample after quenching the uptake.

The Michaelis-Menten method (**Fig. 1B**) is preferred when the unbound concentration of the drug *in vivo* is likely to span the K_m of the drug transport (e.g., in the gut). That is, where the *in vivo* $CL_{int,active}$ changes with the unbound drug concentration. However, this approach requires more data points (at least 6 different concentrations) to determine K_m and J_{max} (the maximal rate of transport) (see Eq. in **Fig. 1B**). Also, the Michaelis-Menten kinetic parameters cannot be determined for low solubility compounds for which transporter-saturating drug concentrations cannot be achieved.

For both the above assays, it is important to remember that the total uptake is always a combination of active and passive uptake. Thus, if the latter is a significant percent of the total uptake, any inaccuracy in determining the passive and/or total uptake will result in poor confidence in the estimation of active uptake. For this reason, it is important to determine the passive uptake (and total uptake) CL_{int} of the drug with high level of accuracy.

3.1.2. How should passive diffusion CL_{int} be determined?

When using transporter-transfected cells, one can perform a parallel uptake experiment in mock-transfected or non-transfected cells. Then, the active uptake CL_{int} can be obtained by subtracting the passive CL_{int} (measured in mock cells; **Fig. 1Ca**) from the total (active + passive) uptake CL_{int} (measured in the transfected cells). In this case, we assume that the passive diffusion in mock cells is the same as that in the transfected cells. One important consideration is that the measured passive diffusion CL_{int} can be different depending on the cell type used (e.g., HEK293, CHO, or MDCK) (Ishida et al., 2018), perhaps because of differences in cell membrane composition between human and animal cells (Paleocontact et al., 2018; Purushothaman et al., 2016). In this case, for IVIVE, one can take the average of all measured passive diffusion CL_{int} in human cells (V. Kumar, Yin, et al., 2020), although a better practice would be to calibrate the passive diffusion measured in cell lines with that measured in primary cells (methods described below) (R. Li, Bi, et al., 2014).

Other methods to measure passive diffusion apply to both transfected and primary cells (**Fig. 1Cb-d**). First, one can use an inhibitor of the transporter of interest, or if using primary cells, a pan-inhibitor or a cocktail of inhibitors (**Fig. 1Cb**). The advantage of this method (*vs.* using mock cells) is that the passive diffusion is determined in cells used to determine the total uptake of the drug. However, one concern is

whether the inhibitor(s) can inhibit all the transporters involved in drug uptake into the primary cells (e.g. an unidentified transporter may be involved). The second method is to use low temperature (by performing uptake assay at 4°C (on ice), which will suppress the active transport activity (**Fig. 1Cc**). However, as partition/distribution coefficients and passive transcellular permeation can be influenced by temperature, passive uptake measured at 4°C might not reflect that at 37°C (Chothe et al., 2018; Lei et al., 2000). Bi et al. reported, using low canine P-gp expressing MDCK cells, that only about half of a set of 21 compounds showed considerably lower passive uptake at 4°C *vs*. 37°C (i.e., < 50%). In the same study, the effect of temperature on passive uptake varied significantly between compounds and, for some drugs, was as much as 50-fold lower at 4°C *vs.* 37°C. In addition, the authors reported different effect of temperature on passive permeability of drugs between cell types (hepatocytes with rifamycin SV and low-P-gp expression MDCK cells) (Y.-A. Bi et al., 2017). A better understanding of the effect of temperature on passive uptake of drugs is needed to use this method with confidence. The third method is self-inhibition (e.g., by using the labeled drug to perform the uptake experiments, and the unlabeled drug to completely inhibit the active uptake) (**Fig. 1Cd**). This method is advantageous over the use of inhibitors if the presence of an unidentified transporter is suspected or an inhibitor of the transporters involved is not available. The fourth approach, which is specific to concentration-dependent assays (**Fig. 1B**), is to incorporate a passive diffusion component into the Michaelis-Menten equation to simultaneously estimate, via modeling, passive diffusion as well as saturation kinetics parameters, K_m and $J_{max,}$ for the uptake of the drug. This can be done either by simultaneously measuring the uptake of the drug at all concentrations in the absence and presence of complete inhibition of the active uptake or just based on uptake data obtained in the absence of the inhibitor (Brouwer et al., 2013). The latter method is less preferred as it is prone to error especially for drugs with moderate to high passive vs. active uptake CL_{int}.

In conducting both active and passive uptake studies, additional experimental conditions should be taken into consideration to obtain best estimates of these two uptakes. First, after the uptake experiments is complete, the cells are washed with buffer to quench any further uptake and to wash away any nonspecific binding of the drug to cell surface. The latter is particularly important for lipophilic drugs as it is impossible to differentiate drug taken up into the cells from that which is bound to the cell surface. Extensive binding to the cell surface will result in over-estimation of the uptake CL_{int} of the drug. Currently,

there is no consensus on the number of washes (but usually 2-3) nor the volume to be used (but usually bigger than the incubation volume) (Izumi et al., 2022; Kimoto et al., 2017a; V. Kumar, Li, et al., 2020; V. Kumar, Yin, et al., 2020; Miyauchi et al., 2018; Sachar et al., 2020; Watanabe et al., 2011). Both in-house (unpublished) and published data suggest that the number of washes can have impact on the estimate of drug uptake (Yoshikado et al., 2021). Also, to reduce non-specific binding of the drug, some add bovine serum albumin to the washing buffer (Niessen et al., 2009). Of note, uptake into suspended hepatocytes, measured using the oil-spin method, does not involve any washing step. Instead, the transport assay is terminated by rapidly separating the cells from the incubation medium by passaging them through an oil layer. However, this method does not necessarily reduce non-specific binding of highly lipophilic drugs as any drug adsorbed to the cell surface could also passage into the oil layer (Yoshikado et al., 2021). To improve solubility of lipophilic drugs in the uptake buffer, organic solvents are often used (e.g., dimethyl sulfoxide). However, these solvents can affect membranes drug permeability (Mitchell et al., 2019). Therefore, their concentrations should be kept minimal (preferably <1%). In addition, they may differentially affect transporters as we have previously shown with drug metabolizing enzymes (Hickman et al., 1998). Thus, studies are needed to quantify the impact of organic solvents on both passive and active uptake and efflux (see below) of drugs.

3.2. Efflux assays

Determination of drug efflux *in vitro,* for IVIVE*,* is done using either living cells (primary cells, e.g., SCH, or transfected cells) or membrane vesicles. Determination of drug efflux (as opposed to uptake) using cells is complicated by the fact that the drug needs to first permeate into the cells before it can be effluxed. For drugs that are lipophilic, this is not an obstacle. Thus, theoretically, one could determine drug efflux by measuring reduced accumulation (accumulation assay) of a drug in primary or transfected cells expressing the efflux transporter. In practice, due to high passive diffusion of lipophilic drugs and their extensive binding to intracellular proteins and lipids, accumulation assays have low sensitivity to accurately determine drug efflux CL_{int}. Thus, this method is rarely used (X. Chen et al., 2021). Instead, to overcome the above problems, for lipophilic drugs, the efflux ratio (ER) is determined using the Transwell® assay (monolayer of cells grown on a membrane insert). For the less lipophilic drugs,

membrane vesicles made from cells expressing the efflux transporter can be used. These assays are detailed below.

3.2.1. Estimation of efflux CL and efflux ratio (ER) using transfected cell lines

Bidirectional transport assays (Transwell®) using transfected cells (e.g. P-gp or breast cancer resistance protein, BCRP) are widely used to characterize drug ER and efflux CL. In this assay, polarized transfected cells are seeded on a membrane insert facing two chambers: an apical (A) chamber and a basal (B) chamber. Then, the drug is added to either the A or B chamber (*i.e.,* the donor chamber) and its appearance in the receiver chamber is measured over time (**Fig. 2A**). The ER is defined as the ratio of the apparent drug permeability (P_{app}) from the basal-to-apical (B→A) ($P_{app(B\rightarrow A)}$) and the apical-to-basal (A→B) ($P_{app(A\rightarrow B)}$) chamber. Drug ER will be >1 when the drug is effluxed by the efflux transporter localized at the apical membrane, and will equal 1 in the absence of such transport, that is when the drug passively diffuses through the cells (in mock cells that lack any endogenous transport or when the efflux transport is completely inhibited). The P_{app} value is usually determined as the ratio of the cumulative appearance of the drug in the receiver chamber measured at (a) given time point(s) (usually 1-4 hours) and the nominal drug concentration in the donor compartment. However, to take into consideration depletion of the drug in the donor compartment (due to passage into the receiver compartment as well as non-specific binding in the donor compartment), we prefer to determine the ER based on the CL_{int} calculated using the cumulative amount of the drug in the receiver chamber and the area under the concentration-time curve (AUC) of the drug in the donor compartment:

$$ER = \frac{CL_{int,B\rightarrow A}}{CL_{int,A\rightarrow B}} = \frac{cA_{A,R} \times AUC_{A,D}}{cA_{B,R} \times AUC_{B,D}} \qquad \text{(Eq. 2)}$$

where $cA_{A,R}$ and $cA_{B,R}$ are the cumulative amount of the drug appearing in the receiver chamber A or B, respectively, and $AUC_{A,D}$ and $AUC_{B,D}$ are the AUC of the drug in the A or B donor chamber, respectively. This equation assumes identical surface area in the donor and receiver chamber for drug passage and that the P_{app} is independent of the drug concentration (this must be confirmed in preliminary experiments). To determine the ER due to transport alone, the ER is determined in the absence and presence of the inhibitor (usually added to both chambers at inhibitor [inh] concentrations that will completely inhibit the

transporter). When using this bidirectional assay, the integrity of the tight junctions must be ensured by monitoring it using a non-permeability marker (such as lucifer yellow and/or mannitol) and established cut-off values for the permeability of these markers. Paracellular permeability is compound-dependent, and, to our knowledge, there is currently no method available to scale the *in vitro* paracellular permeability to *in vivo*.

The bidirectional assay with determination of the ER using Transwell® is particularly useful for the IVIVE of interstitial tissue drug concentrations (i.e., $K_{p,uu}$) when the unbound steady-state tissue drug concentration is modulated by efflux transporters present at the tissue:blood barrier (e.g., P-gp at the BBB or the placental:blood barrier). Indeed, the Transwell® assay mimics the BBB and placental barriers *in vivo* (**Fig. 2A**). As such, $K_{p,uu}$ can be extrapolated from the ER determined *in vitro* using the REF (see Section 4 for details) without estimating the passive diffusion CL_{int}. Alternatively, the unidirectional CL_{int} (active and passive) can be estimated *in vitro* using the P_{app} values in presence and absence of the transporter inhibitor, or by using mock cells. However, estimation of CL_{int} using $P_{app(B\rightarrow A)}$ and $P_{app(A\rightarrow B)}$ values does not take into account the complexity of the diffusion of the drug through two barriers (apical and basal membranes) and can mislead interpretation of kinetic constants J_{max} and K_m (Tachibana et al., 2010). Therefore, compartmental modeling of the data with ≥ 3 compartments (incl. a cell compartment) is preferred. In this case, simultaneous fitting of the model to the measured drug concentration-time profiles in the donor and receiver chambers (in A→B experiments or in both A→B and B→A experiments), as well as within the cells, in absence and presence of an inhibitor (or in mock cells), over time can provide estimates of the active and passive efflux CL_{int} (Korzekwa et al., 2012; Nagar et al., 2014; Storelli, Anoshchenko, et al., 2021; Zamek-Gliszczynski et al., 2013). Of note, estimation of the efflux CL_{int} (i.e., out of the cell compartment) requires measurement of the unbound drug fraction in the cell (Mateus et al., 2013).

Though the Transwell® assay is suitable for the more lipophilic drugs (for which the use of vesicles is limited, see below), highly lipophilic drugs represent a challenge if the drug binds extensively within the intracellular compartment. In this case, very little drug will reach the receiver compartment making estimation of the ER impossible (X. Chen et al., 2021). In contrast, study of drug efflux of low permeability

drug using the Transwell® assay will likely necessitate the use of a double-transfected cells (expressing an uptake transporter for the drug in addition to the efflux transporter of interest).

3.2.2. Estimation of efflux CL_{int} using membrane vesicles

Membrane vesicles are useful to study efflux transport by the ATP-binding cassette transporters (e.g. P-gp, BCRP, MRP2/3) because a significant fraction of the membrane vesicles is in the inside-out configuration (**Fig. 2B**), allowing the transporter cofactor (ATP) in the assay buffer to directly interact with the cofactor binding site. As a result, data analysis is comparable to that of uptake assays. Active transport is determined by subtracting the drug uptake into vesicles in the presence of adenosine monophosphate (passive uptake) from drug uptake in the presence of adenosine triphosphate (total uptake). Passive drug uptake can also be determined using mock vesicles and adenosine triphosphate. To use vesicles for IVIVE of the ER or efflux CL_{int}, the percentage of inside-out vesicles in the vesicles must be determined (e.g. by assessing the activity of an ectoenzyme such as 5'-nucleotidase in the vesicle mixtures before and after lysis (C. Y. Li et al., 2019)).

Vesicles are best used for efflux assays when the drug has low passive permeability. They are not suitable to study efflux of lipophilic compounds which are likely to have high permeability or high nonspecific binding to the filter/vesicles. This is because these phenomena will result in passive uptake being a large fraction of the total uptake making it difficult to quantify the active uptake with confidence. Also, compounds with significant passive permeability can show significant back-flux of the drugs into the incubation medium, therefore requiring very short incubation times (< 30 seconds) to enable measurement of the initial uptake rate. Nonspecific binding to the filter/vesicles can be reduced by optimizing the number of washes and the volume of washing solution, and by adding albumin in the quenching solution. When determining drug efflux, membrane vesicles have a number of advantages over cells (Transwell® assay). First, the use of cells requires more complex compartmental modeling of the data (see above). Second, unlike cells, membrane vesicles do not need culturing and can be dosed at high drug concentrations which might be toxic to the cells.

3.2.3. Determination of biliary CL using sandwich-cultured hepatocytes (SCH)

SCH are traditionally used to estimate biliary drug efflux CL. To do so, experiments are conducted in the absence and presence of calcium (Ca^{2+})/ magnesium (Mg^{2+}). When Ca^{2+}/ Mg^{2+} is present in the incubation buffer, the amount of drug quantified in the cell lysate represents the amount that accumulates in both the SCH and in the bile canaliculi. Exclusion of Ca^{2+}/ Mg^{2+}- from the incubation buffer (over short duration) results in disruption of SCH tight junctions and therefore the bile canaliculi. In this case, the amount of drug quantified in the cell lysate represents drug accumulated in only the SCH and not in the bile canaliculi. Then, a 3-compartment model is usually used to estimate the sinusoidal and biliary efflux CLs (Ishida et al., 2018; Jones et al., 2012; V. Kumar, Li, et al., 2020; Pfeifer et al., 2013; Storelli et al., 2022a; Zamek-Gliszczynski et al., 2013). The compartments are the buffer, cells and the bile canaliculi. Note that to obtain intrinsic CLs (i.e., unbound), the fraction unbound of the drug in the cells and in the buffer (if containing proteins) must be determined and incorporated in the model. The *in vitro* biliary efflux CL_{int} ($Cl_{int,bile}$) can also be determined by measuring the canalicular accumulation of the drug over a given period as well as the unbound drug AUC in the hepatocytes ($AUC_{hep.u}$) during that same time, as follows:

$$CL_{int,bile} = \frac{Accumulation\ (+\ Ca^{2+}/Mg^{2+}) - Accumulation\ ((-)\ Ca^{2+}/Mg^{2+})}{AUC_{hep.u}} \qquad \text{(Eq. 3)}$$

In this case, $AUC_{hep,u}$ is estimated based on the measured amount of drug in the cell lysates and cell volume (usually estimated based on cell number or total protein content). $AUC_{hep,u}$ is preferred over $C_{hep,u}$ when steady-state conditions are not achieved. Note that biliary $CL_{int,bile}$ should be estimated (Eq. 3) using drug concentration in the cells rather than in the buffer, because the former drives biliary efflux and the latter may not be representative of the unbound cell drug concentration due to the involvement of active transport at the sinusoidal membrane of the SCH (Nakakariya et al., 2012). Also, several challenges, discussed by Kumar et al., (V. Kumar, Li, et al., 2020), need to be considered when conducting SCH experiments. First, if the incubation in the absence of Ca^{2+}/ Mg^{2+} is short, the canalicular tight junctions may reform and could prevent accurate estimation of biliary CL. However, prolonged incubation in the absence of Ca^{2+}/ Mg^{2+} is not an option as this condition is toxic to the cells (V. Kumar, Li, et al., 2020). Second, depletion of Ca^{2+}/ Mg^{2+} downregulates the sodium-taurocholate co-transporting polypeptide (NTCP) transporter, a confounding factor when interpreting hepatic uptake CL of drugs mediated (at least in part) by this transporter.

4. *In vitro to in vivo* scaling approaches

Scaling factors for IVIVE of transporter-based drug uptake or efflux CL_{int} will depend on the *in vitro* model used (**Fig. 3**).

4.1. Scaling factors when using primary cells

Physiological scaling

Most commonly, the *in vivo* uptake or efflux CL_{int} ($CL_{int,\ in\ vivo}$) is obtained by scaling the CL_{int} determined *in vitro* ($CL_{int,\ in\ vitro}$) in primary cells using a physiological scaling factor (PSF) (**Fig.3**, left panel):

$$CL_{int,in\ vivo} = CL_{int,in\ vitro} \times PSF \qquad \text{(Eq. 4)}$$

When transport is measured using the Michaelis-Menten approach (see Section 3 above), $CL_{int,\ in\ vitro}$ (J_{max}/K_m when drug concentration << K_m) can be scaled as in Equation 4. If the unbound drug concentration *in vivo* is likely to approach or exceed the unbound *in vivo* K_m, the concentration-dependent $CL_{int,\ in\ vivo}$ can be computed by scaling J_{max} assuming that unbound K_m is identical *in vitro* and *in vivo*. In this event, $CL_{int,\ in\ vivo}$ can be computed for every *in vivo* unbound drug concentration (C_u), e.g. in physiologically-based PK (PBPK) modeling and simulation, as:

$$CL_{int,in\ vivo} = \frac{J_{max}}{K_m + C_u} \times PSF \qquad \text{(Eq. 5)}$$

where PSF includes the number of cells in the tissue of interest or the membrane/total protein content (i.e., mg membrane/total protein or million cells per gram of tissue and tissue weight); C_u is the unbound drug concentration *in vivo*. PSF is considered by many as the preferred approach for IVIVE for compounds in discovery due to its ease of implementation. This PSF approach assumes that the transporter activity *in vitro* in the primary cells is the same as that *in vivo*. With this approach, the identity of the transporter(s) does not need to be known. The PSF approach is limited by the availability of primary cells, as well as significant interindividual variability (as discussed in Section 2). Moreover, this approach seems to underpredict transporter-based hepatic uptake *in vivo* (Jones et al., 2012; R. Li, Barton, et al., 2014; Sachar et al., 2020; Storelli et al., 2022a).

Empirical Scaling

To address the issue of underprediction of transporter-based CL_{int} by primary cells, the use of empirical scaling factors (ESF) has been proposed, where:

$$CL_{int,in\ vivo} = CL_{int,in\ vitro} \times PSF \times ESF \quad \text{(Eq. 6)}$$

These ESF can be obtained either from studies in animals or in humans. In the first case, the ESF approach utilizes preclinical animal data to inform IVIVE for humans (De Bruyn et al., 2018; Matsunaga et al., 2019). This approach assumes that the magnitude of misprediction of transporter-based CL_{int} in humans is the same as that in the preclinical species. A significant disadvantage of the approach is the need to conduct both *in vitro* animal cell-based and *in vivo* animal experiments in conjunction with *in vitro* studies with human primary cells or transporter-transfected cells. In the second case, the best possible ESF is determined from both *in vitro* (e.g. hepatocytes) and *in vivo* (e.g. hepatic CL) transport studies of multiple drugs substrates for a given transporter or class of transporters (e.g., OATPs) (Jones et al., 2012; R. Li, Barton, et al., 2014). However, these ESFs are often drug-dependent and cannot be generalized to other drugs. Therefore, more mechanistic scaling approaches are needed, such as RAF or REF described below.

4.2. Scaling factors when using transfected cells or vesicles

RAF or REF can be used as scalars for IVIVE of transporter-based CL_{int} when using transporter-expressing cells and/or membrane vesicles provided the transporters involved are known. RAF and REF respectively account for the difference in intrinsic transporter activity and expression between *in vitro* models and human tissue. In addition, passive diffusion of drugs needs to be scaled from *in vitro* to *in vivo*. An exception is when using RAF for drugs transported predominately by a single transporter. In this case, both the *in vitro* active and passive diffusion CL_{int} can be simultaneously scaled to *in vivo* without using a PSF (as detailed below in Section 4.2.2). However, with both approaches, when multiple transporters are involved, active and passive CL_{int} are separately scaled (see Section 4.2.2), and the *in vitro* passive diffusion CL ($CL_{int,pd,\ in\ vitro}$) is scaled to that *in vivo* ($CL_{int,pd,\ in\ vivo}$) using PSF, as follows:

$$CL_{int,pd,in\ vivo} = CL_{int,pd,in\ vitro} \times PSF \quad \text{(Eq. 7)}$$

4.2.1. Relative expression factor (REF)

With the advent of QTP and availability of transporter abundance data (Prasad et al., 2019), the REF approach has recently gained a lot of attention (Anoshchenko et al., 2021; Deng et al., 2021; A. R. Kumar et al., 2021; V. Kumar et al., 2018, 2018; Nozaki & Izumi, 2020; Sachar et al., 2020; Sato et al., 2021a; Storelli, Anoshchenko, et al., 2021; Storelli et al., 2022a; Trapa et al., 2019; Vildhede et al., 2016). CL_{int} via a transporter is defined as the ratio of J_{max} over K_m (when the drug concentration is < K_m). J_{max} is the product of its turnover rate (k_{cat}; rate at which substrates are actively translocated across the cell membrane) and its abundance (concentration). The REF approach assumes that the difference in transporter activity *in vitro vs. in vivo* is due to the difference in transporter abundance, and that K_m and k_{cat} are identical *in vitro* and *in vivo.* This assumption is supported by data showing that OATP1B1 and BCRP transporter activity correlates well with their abundance (or expression) in cell lines (V. Kumar et al., 2015). Therefore, transporter-based CL_{int} and (and $K_{p,uu}$) can be scaled from *in vitro* to *in vivo* by using the REF (unitless) (**Figure 3**, middle panel), as described below:

$$CL_{int,in\ vivo,active} = [\sum_{i=1}^{n} CL_{int,in\ vitro,i} \times REF_i] \times PSF \qquad \text{(Eq. 8)}$$

$$REF_i = \frac{TA_{tissue,i}}{TA_{in\ vitro,i}} \qquad \text{(Eq. 9)}$$

where $TA_{tissue,i}$ and $TA_{in\ vitro,i}$ are the abundance of the i^{th} transporter in human tissue and the *in vitro* model, respectively. Therefore, REF requires measurement of transporter abundance for each drug transporter protein of interest, in both *in vitro* models and *ex vivo* tissue.

The REF approach has also been used to extrapolate the tissue:plasma unbound drug concentration ratio, $K_{p,uu,}$ from the ER determined in the presence and absence of inhibitors (inh), as follows (see also **Fig. 2A**) :

$$K_{p,uu} = \frac{1}{[\sum_{i=1}^{n}\left(ER_{(-)inh_i} - ER_{(+)inh_i}\right)\cdot REF_i]+1} \qquad \text{(Eq. 10)}$$

When multiple transporters are involved, the ER and REF are estimated using cell lines, each expressing a single transporter (e.g. P-gp and BCRP-transfected cells), in absence and presence of complete inhibition of the respective transporter. This approach is named the ER-REF approach and can be used to determine the steady-state parameter $K_{p,uu,}$ either after multiple (to steady-state) or single dose

administration provided the drug concentration is << K_m of the transporter. Although this approach is applied when efflux transport is expected to affect drug concentrations in the tissue it could easily be modified when active uptake into the tissues is involved. The ER-REF approach has the major advantage of not requiring extrapolation of passive diffusion, as only the active component of the ER (characterized by the difference in the ER in the absence and in presence of the transporter inhibitor) is extrapolated to *in vivo*.

To predict the dynamic (rather than static) changes in tissue drug concentrations, the sum of input and exit drug CL_{int} is required (Eq. 1). In that event, the *in vivo* passive diffusion CL_{int} can be estimated using a passive diffusion marker as a calibrator, for which *in vitro* and *in vivo* CL_{int} data are available (e.g., midazolam). Then, the active CL_{int} of the drug can be estimated from passive diffusion CL_{int} and $K_{p,uu}$ based on the following equations:

$$CL_{int,passive,in\ vivo,drug\ X} = P_{app,drug\ X} \cdot \frac{CL_{int,in\ vivo,marker}}{P_{app,marker}} \qquad \text{(Eq. 11)}$$

$$K_{p,uu} = 1 - f_t = \frac{CL_{int,passive}}{CL_{int,passive} + CL_{int,active}} \qquad \text{(Eq. 12)}$$

So far, the ER-REF approach has been validated in humans to successfully predict the cerebral and fetal systemic concentrations of drugs modulated by P-gp efflux at the BBB and the placental:blood barrier respectively (Anoshchenko et al., 2021; Storelli, Anoshchenko, et al., 2021). Validation is needed for situations where other transporters (e.g. BCRP) are involved in modulating tissue drug concentrations.

An elegant advantage of the REF approach is that it is capable of handling multiple drug transporters (if transfected cells are available and the transporters of interest can be quantified in the human tissue of interest). This versatility, in contrast to the RAF approach, results in additional advantage. It does not need to assume that uptake is the rate-determining step (RDS) for the CL of the drug via the organ of interest. Also, it is not limited by the availability of primary cells (not available for the kidney, intestine or the BBB) or by availability of selective probe substrates (used by the RAF approach). Additionally, the IVIVE of the CL_{int} of the drug by a given transporter is not limited to a single organ when transporter abundance is available for different organs. This approach, however, has limitations. , When multiple

transporters are involved, the uptake by these transporters, individually expressed in transporter-expressing cells, need to be measured to arrive at a REF for each. This is because there is large inter-laboratory variability in the reported drug transporter abundance values likely due to the use of different QTP methodologies (Badée et al., 2015; Harwood et al., 2016; Prasad et al., 2019). Therefore, we recommend measuring transporter abundance in the tissue of interest in the same laboratory as where the *in vitro* CL_{int} is measured.

To obtain reliable REF value using QTP, we recommend several best practices. First, whenever sensitivity of the LC-MS/MS assay allows, the relative abundance of the transporters in cell or tissue lysate (vs. crude membrane preparation) should be measured to avoid the need to correct for loss of membrane during the membrane preparation which can introduce error (V. Kumar et al., 2019). Second, if lack of sensitivity of the assay requires membrane preparation to enrich the transporter concentration, we recommend the use of a membrane marker, such as Na^+-K^+-ATPase, to correct for membrane loss during the membrane preparation (Storelli, Billington, et al., 2021). Third, all peptide standards (labeled and unlabeled) and reagents must be of the highest purity available. Fourth, maximal digestion of the protein to liberate the peptide of interest using an enzyme, such as trypsin, must be optimized. Fifth, we recommend including a biological control, such as albumin, to confirm consistent and reproducible digestion of proteins. Sixth, we recommend including another biological control, such as a pooled membrane preparation isolated from multiple organs (e.g. livers), which also goes through the digestion process at the same time as the membrane of interest. Quantification of transporters in this biological control membrane preparation (e.g. OATPs) should be consistent and reproducible for every assay. Finally, when using the above approaches to quantify the abundance of transporters, all the transporters quantified are assumed to be expressed in the plasma membrane and functional. But, as pointed out in Section 7.3 this may not be the case. Therefore, confirming this assumption, using a method such as biotinylation, is important (V. Kumar et al., 2017).

4.2.2. Relative activity factor (RAF)

The RAF approach relies on the availability of data on selective probe drug transport CL_{int}, both *in vitro* (in primary cells or in transporter-transfected cells) and *in vivo* (e.g. Mathialagan et al., 2017) (**Figure 3**, right panel). Selectivity means that the probe drug must be predominantly transported *in vivo* and *in vitro* by a single transporter (rarely the case). If it is, the difference in transporter activity/expression and passive diffusion CL_{int} in primary or transfected cells and *in vivo*, yields the value of the scaling factor, $RAF_{in\ vivo}$:

$$RAF_{in\ vivo} = \frac{CL_{int,in\ vivo,probe\ substrate}}{CL_{int,in\ vitro,probe\ substrate}} \qquad \text{(Eq. 13)}$$

Then, the *in vitro* CL_{int} of another drug (e.g., drug X), in the same cells as that used to measure the *in vitro* CL_{int} of the probe drug, and transported by the same transporter as the probe drug, is scaled to *in vivo* as follows:

$$CL_{int,in\ vivo} = CL_{int,in\ vitro} \times RAF_{in\ vivo} \qquad \text{(Eq. 14)}$$

$RAF_{in\ vivo}$ assumes either that the passive diffusion clearance of the drug is negligible or that the ratio of the *in vitro* passive and active CL_{int} of drug X is identical to that of the probe drug. Consequently, this scalar does not need a PSF as this is implicitly included in Eq. 13 and 14. Therefore, it is less prone to any errors in PSF which can have significant inter-laboratory variability (Barter et al., 2007). However, if the *in vitro* passive diffusion CL_{int} of drug X is a significant fraction of its total *in vitro* $CL_{int,}$ and this fraction differs from that of the probe drug then the $RAF_{in\ vivo}$ scalar will be incorrect. Also, the use of $RAF_{in\ vivo}$ is more complicated when multiple transporters are involved. In this event, *in vivo* data on probe drugs selectively transported by each transporter involved must be available (rarely the case). And, if the *in vitro* and *in vivo* passive diffusion CL_{int} of the probe drug and drug X can be assumed to be negligible, then the $RAF_{in\ vivo}$ for each selective probe drug can be determined and used to predict the *in vivo* CL_{int} of a drug as:

$$CL_{int,in\ vivo} = [\sum_{i=1}^{n} CL_{int,in\ vitro,i} \times RAF_{\ in\ vivo,i}] \qquad \text{(Eq. 15)}$$

where I represents the i^{th} transporter.

Since the *in vivo* CL_{int} data for a selective transporter probe(s) are rarely available, or if the passive diffusion CL of drug X is significant, an alternative scalar, $RAF_{in\ vitro}$, can be used:

$$RAF_{in\ vitro,i} = \frac{Cl_{int,in\ vitro,probe\ substrate,primary\ cells,i}}{Cl_{int,in\ vitro,probe\ substrate,transfected\ cells,i}} \quad \text{(Eq. 16)}$$

$$CL_{int,in\ vivo} = ([\sum_{i=1}^{n} CL_{int,in\ vitro,i} \times RAF_{\ in\ vitro,i}] + CL_{int,pd,in\ vitro}) \times PSF \quad \text{(Eq. 17)}$$

The $RAF_{in\ vitro,i}$ scalar (which scales only the active transport CL of the drug via the i^{th} transporter) requires the availability of primary cells and therefore can be used to estimate only *in vivo* hepatic transporter-based CL_{int} (Izumi et al., 2018; Mitra et al., 2018). Briefly, the active $CL_{int,in\ vitro}$ of the probe drug via each transporter can be determined in the single-transporter transfected cells as well as hepatocytes to arrive at the $RAF_{in\ vitro}$ for each transporter (Eq. 16). Then, the active $CL_{int,in,vitro}$ of drug X in transfected cell line, via each transporter, can be individually scaled using the respective RAF value and summed (Eq 17). This summed $CL_{int,in\ vivtro}$ plus the $CL_{int,pd,\ in\ vitro}$ of drug X can then be scaled to obtain $CL_{int,in\ vivo}$ using a PSF (Eq. 17). Similar to the PSF approach, the use of $RAF_{in\ vitro}$ assumes that the transport activity *in vitro* in the hepatocytes is identical to that *in vivo.*

When using either of the above RAF scalars, the assumption made is that the estimated *in vivo* CL_{int} is the rate-determining step (RDS) for the CL of that drug via the organ of interest (e.g. renal secretory CL). For example, in Mathialagan et al. (2017), where $RAF_{in\ vivo}$ scalars were applied to predict the renal secretory CL of OAT substrates, the authors assumed that there was no significant passive CL_{int} of the probe drugs used (tenofovir for OAT1, acyclovir and ganciclovir for OAT2, and benzylpenicillin and oseltamivir acid for OAT3) and that basal uptake of these drugs (mediated by the respective OATs) was the RDS in their renal secretory CL. This assumption and the challenges of validating it are further discussed in Section 5.

4.2.3. Inter-system extrapolation factor (ISEF)

As an alternative, the use of the ISEF has been proposed (Burt, Riedmaier, et al., 2016; Harwood et al., 2013). The ISEF is a hybrid between the RAF and REF approaches, and as such require both transporter abundance data and probe substrates' activity data, which limits its use for transporters because of the paucity of transporter specific substrates (as described for the RAF approach).

5. Predictive performance of IVIVE approaches: a review of existing data

To use IVIVE approaches with confidence when predicting transporter-based CL and TC, they must first be validated. This can be done using probe substrates of selected transporters. Once validated, the approaches can be applied with confidence to the prediction of transporter-based CL_{int} and tissue concentrations of other drugs transported by the transporters for which the validation was performed. In this section, we review important principles to consider when validating IVIVE transporter-based drug CL_{int} and TC. Then, we review studies that have conducted such validation and whether they have adhered to these important principles.

5.1. Principles to consider when validating IVIVE approaches for transporter-based CL and tissue drug concentrations

5.1.1. IVIVE of transporter-based CL_{int}

When conducting IVIVE of transporter-based CL_{int} it is critical to consider the RDS in the systemic CL of the drug. First, it is important to note that the systemic CL of a drug is summation of both the hepatic and extrahepatic (e.g. renal) CL of the drug. Therefore, systemic CL can be equated to hepatic CL only if the extrahepatic CL of the drug is negligible. For the purposes of this section, we will assume that this is the case; however, the principles enunciated here can also be applied to renal CL. Therefore, according to the ECM (Eq. 18-20), hepatic drug CL is determined by all individual CL_{int} pathways (Patilea-Vrana & Unadkat, 2016; Shitara et al., 2006b; Sirianni & Pang, 1997):

$$CL_{h,b} = \frac{Q_h \cdot f_{u,b} \cdot CL_{int,h}}{Q_h + f_{u,b} \cdot CL_{int,h}} \qquad \text{(Eq. 18)}$$

where

$$CL_{int,h} = \frac{CL_{int,s,in} \cdot (CL_{int,met} + CL_{int,bile})}{CL_{int,s,ef} + CL_{int,met} + CL_{int,bile}} \qquad \text{(Eq. 19)}$$

consequently:

$$CL_{h,b} = \frac{Q_h \cdot f_{u,b} \cdot CL_{int,s,in} \cdot (CL_{int,met} + CL_{int,bile})}{Q_h \cdot (CL_{int,s,ef} + CL_{int,met} + CL_{int,bile}) + f_{u,b} \cdot CL_{int,s,in} \cdot (CL_{int,met} + CL_{int,bile})} \qquad \text{(Eq. 20)}$$

where $CL_{h,b}$ is the hepatic CL from blood, Q_h is the hepatic blood flow, $f_{u,b}$ is the fraction unbound of the drug in the blood, $CL_{int,h}$ is the intrinsic hepatic CL, $CL_{int,s,in}$ is the sinusoidal influx clearance, $CL_{int,s,ef}$ is the sinusoidal efflux clearance, $CL_{int,bile}$ biliary (canalicular efflux) clearance, $CL_{int,met}$ is the metabolic clearance.

Of note, each of these CL_{int} are the summation of both active and passive CL_{int} of the drug. To predict the whole organ drug CL, all these CL_{int} need to be extrapolated to *in vivo* from *in vitro* data. However, many studies that have conducted IVIVE of hepatic CL of OATP-transported drugs erroneously assume that the sinusoidal uptake is the RDS of the hepatic CL (i.e. $CL_{int,s,ef}$ is << $CL_{int,met}$+$CL_{int,bile}$ and therefore $CL_{int,s,in}$=$CL_{int,h}$). Consequently, they equate the hepatic CL of the drug to its uptake CL ($CL_{s,in}$), as follows:

$$CL_{h,b} = CL_{s,in} = \frac{Q_h \cdot f_{u,b} \cdot CL_{int,s,in}}{Q_h + f_{u,b} \cdot CL_{int,s,in}} \quad \text{(Eq. 21)}$$

As Patilea-Vrana and Unadkat have demonstrated, OATP-mediated transport alone (even when co-administration of rifampicin results in a large DDI with the drug) is not in itself sufficient to assume that the uptake is the RDS in its hepatic CL (Patilea-Vrana & Unadkat, 2016). It will be the RDS only if $CL_{int,s,ef}$ << $CL_{int,met}$+$CL_{int,bile}$ and only under this scenario is the whole organ CL equal to $CL_{s,in}$. Determining $CL_{int,s,ef}$ << $CL_{int,met}$+$CL_{int,bile}$ is possible *in vitro* through SCH studies, by using transfected cells and REF or *in vivo* by imaging studies. Unfortunately, determination of various CLs by SCH has limitations that have been described in Sections 2 and 3.

Elucidating the correct RDS is very important to correctly interpret the accuracy of IVIVE of hepatic drug CL. Consider the situation where all hepatobiliary CLs (i.e., uptake, efflux and metabolic) are RDS. In this case, hepatic CL predicted by IVIVE assuming uptake is the RDS will be overpredicted (see Eq. 20 & 21). However, as has been repeatedly shown, if IVIVE underpredicts $CL_{s,in}$, then the hepatic CL will be erroneously assumed to be well-predicted when that is far from the truth. This is an excellent example of comparing “apples” with “apples” and not with “oranges”. That is, the IVIVE of $CL_{s,in}$ should be compared with *in vivo* $CL_{s,in}$ (obtained by imaging) rather than hepatic CL (V. Kumar, Yin, et al., 2020). Assuming uptake is the RDS and CL_h=$CL_{s,in}$ without evidence to support this assumption is an important limitation of IVIVE of hepatic CL of drugs based solely on *in vitro* determination of $CL_{int,s,in}$ (which is often the case,

see **Tables 2 and 3**). The only solution to this dilemma is to estimate all the hepatobiliary CLs by PET imaging (Billington et al., 2019; Hernández Lozano & Langer, 2020) (**Fig. 4A**). Therefore, when such data are available, they should be used over hepatic CL data to validate prediction of transporter-based drug disposition. In addition, tissue drug concentrations can be validated ONLY by obtaining these concentrations using imaging.

5.1.2. What endpoints should IVIVE of transporter-based CL use for validation?

Two different endpoints have been used to validate *in vivo* drug CL predictions from *in vitro* studies (**Fig. 4B**). The first endpoint (endpoint 1) is where the observed *in vivo* organ CL is compared with that predicted from *in vitro* studies (**Fig. 4Ba**). The second endpoint (endpoint 2) is where the *in vivo* CL_{int}, deconvoluted from the observed *in vivo* organ CL, is compared with that predicted from *in vitro* studies (**Fig. 4Bb**). Specifically, for endpoint 1, the *in vitro* CL_{int} of a compound is first determined in primary or transporter-expressing cells or vesicles. Then, the CL_{int} is scaled to *in vivo* using PSF/RAF/REF (as described in Section 4), and the organ CL is estimated based on extrapolated CL_{int} and a model of drug CL (e.g. parallel tube model; Pang et al., 2019) such as organ blood flood, blood to plasma concentration ratio and unbound fraction in plasma or blood. The predicted organ CL (endpoint 1) is subsequently directly compared with that observed *in vivo*. This is the most frequently used (but not preferred; see below) approach to validate predictions of organ CL from *in vitro* data (**Fig. 4Ba**). In contrast, for endpoint 2, the CL_{int} estimated from the *in vitro* studies is directly compared to the CL_{int} deconvoluted (by retrograde calculations) from the observed organ CL (**Fig. 4Bb**). We prefer this approach as it correctly compares “apples” with “apples” especially for intermediate to high extraction ratio compounds (A. R. Kumar et al., 2021; V. Kumar, Yin, et al., 2020; Peng et al., 2021). For such drugs, mis-prediction of transporter-based *in vivo* organ CL (endpoint 1) from *in vitro* CL_{int} will be dampened by blood flow, which can be a significant determinant of organ CL for such drugs (Billington et al., 2019). Consequently, such mis-predictions may erroneously look accurate when in fact they are not.

5.1.3. How should predictions of tissue concentrations be validated?

Prediction of $K_{p,uu}$ as well as the dynamic changes in the unbound tissue concentrations is important to inform drug safety and toxicity. For a drug that is transported (influxed or effluxed) across the tissue:blood

barrier (e.g. BBB, placental:blood barrier) and/or metabolized in the tissue (e.g. liver), $K_{p,uu}$ can be significantly less than 1 (see **Eq. 1**). For such a drug, irrespective of how much systemic PK information of the drug is available, its unbound tissue concentrations cannot be predicted (or validated) based solely on its systemic PK data (L. Wang et al., 2021). Instead, such predictions can be validated using imaging, usually PET imaging (**Fig. 4A**). Imaging studies should be used for validation only after considering the following potential confounders and limitations. They cannot be employed routinely as they are cost prohibitive, and not all drugs can be radiolabeled for PET imaging; only a limited number of PET imaging studies are available in humans to validate predictions (Billington et al., 2019; Eyal et al., 2010; Kaneko et al., 2018; Kreisl et al., 2010; Maeda et al., 2019; Nakaoka et al., 2022; Takashima et al., 2011, 2012; Tournier et al., 2019). PET imaging studies cannot distinguish between the parent drug and the labeled metabolite or the total and the unbound drug tissue concentrations. Therefore, for validation, PET imaging studies are conducted with drugs that are not extensively metabolized (Billington et al., 2019), or if metabolized, data over a duration where such metabolism is minor are used (Eyal et al., 2010; Sasongko et al., 2005). In addition, the total tissue drug concentration measured by imaging needs to be corrected for the fraction bound in the tissue homogenate or in the *in vitro* cell lysate (assuming that this reflects drug binding in the tissue *in vivo*) (Storelli, Anoshchenko, et al., 2021). Imaging data should also be corrected for the amount of drug present in the blood within the tissue (Hernández Lozano & Langer, 2020; Sachar et al., 2020). For example, 30% of liver volume is blood (Hwang et al., 2002), which can significantly affect estimation of tissue concentrations (and for that matter, estimation of hepatobiliary CLs). PET imaging of hepatic drug concentrations cannot differentiate between drug in hepatic tissues from that in the bile ducts. In this case, modeling of data, including distinct hepatocytes and intrahepatic bile duct compartments, can be useful (Hernández Lozano et al., 2019; L. Wang et al., 2021). Besides imaging, another approach that has been described to predict tissue drug concentrations is PK/PD modeling (K. Riccardi et al., 2017). In this approach, the unbound tissue drug concentration at the site of effect is estimated from the observed PD data.

5.2. Predictive performance of IVIVE approaches for transporter-based CL and tissue dug concentrations

Here, we summarize the performances of the different scaling approaches described in Section 4 to predict tissue distribution and hepatic/renal CL of transported drugs. Because there are limited data on the validation of IVIVE of drug absorption mediated by transporters, this aspect is not discussed here.

It is noteworthy to mention that success of IVIVE approaches can vary between different studies, based on three aspects: (i) the available validation dataset (e.g., systemic PK data, PET imaging, PK/PD modeling); (ii) the parameter used for validation (e.g., systemic or tissue concentration-time profiles, whole organ CL, uptake/efflux CL_{int}, and $K_{p,uu}$); and (iii) the acceptance criteria used (predicted parameter falling within boundaries that range from 1.25-to-5-fold of the observed value or falling within 90% or 95% confidence interval of observed data) (**Tables 2-4**). In this regard, the authors' view is that acceptance criteria should be preset, clearly stated and be dependent on the primary purpose for IVIVE (i.e., whether it is to screen candidates with desirable PK profiles, predict first-in-human dose or to predict TC for optimizing drug dosing regimen). The anticipated therapeutic index should also be considered. For example, if the approach is to be used to predict drug dosing regimens without additional PK studies in the population of interest, then the validation of the approach must be more stringent. Likewise for prediction of TC of the drug of interest, as these usually cannot be routinely measured (see below).

Regarding IVIVE of hepatic CL or hepatic uptake CL (**Table 2**), most have studied OATPs or dual OATPs/NTCP substrates with one exception, an organic cation transporter (OCT)1 substrate, metformin. While OCT1-mediated uptake of metformin is well predicted with the REF approach (using plasma membrane OCT1 abundance), plated hepatocytes underpredict this CL pathway. For OATP substrates, despite heterogeneity in assessing success, most studies underpredict hepatic uptake CL. This underprediction is observed both with hepatocytes (suspended, plated and sandwich-cultured) using PSF and transporter-expressing cells using REF or RAF. These data suggest that an endogenous factor present *in vivo* and absent in *in vitro* studies might enhance the *in vivo* activity of OATPs. This is discussed in more detail in Section 7.

There are different ways to estimate biliary efflux CL_{int}: (i) by using the concentration of the drug in blood or plasma (*in vivo*) or in the incubation buffer (*in vitro*); or (ii) by using intracellular unbound hepatocyte concentrations. The use of the latter is pharmacokinetically correct as it is the driving force and not

confounded by disequilibrium between unbound blood/incubation buffer and tissue/intracellular concentrations due to active uptake or sinusoidal efflux transporters. Using the latter, both Jones *et al.*, 2012 and Storelli et al., 2022 found overprediction of biliary efflux using SCH, likely due to the overexpression of efflux transporters in SCH reported by Kumar *et al.*, 2019. In contrast, the application of the REF approach and measuring transport in vesicle containing the relevant transporters resulted in excellent prediction of CL_{bile} (Storelli et al., 2022a).

For renal CL, available studies evaluated OAT transporters as well as OCT2 (**Table 3**). Transfected cells were used for all studies and the REF or RAF scalar or both was used. While the overall predictions were good for OAT and OCT2 substrates, all studies assumed that the basal uptake was the RDS of the renal secretory CL, and that tubular reabsorption was negligible. More studies are needed to validate the predictions of each individual renal secretory CL transporter pathway of drugs, as well as that of drug concentrations in the proximal tubular cells. Here, the 5-8 mm discrimination capacity of PET imaging (Tournier et al., 2018) will preclude measurement of drug concentrations in these cells.

Finally, regarding drug distribution modulated by transporters, the collected studies include prediction of drug partitioning into the brain or the liver. Due to limited availability of imaging data, only a few studies have validated their brain $K_{p,uu}$ predictions (**Table 4**). Most studies have used P-gp or BCRP expressing cells (LLC-PK1 or MDCK) and *in vitro* efflux ratio using the REF to extrapolate either the absolute active efflux CL_{int} (J. Li et al., 2017; Verscheijden et al., 2021) or the static brain $K_{p,uu}$ (Nicolaï et al., 2020; Sato et al., 2021a; Storelli, Anoshchenko, et al., 2021). Overall, brain $K_{p,uu}$ predictions have been good to excellent for selective P-gp and dual P-gp/BCRP substrates demonstrating the validity of these approaches. While PET imaging or measurement of the brain interstitial fluid concentration by microdialysis are ideal approaches to validate brain $K_{p,uu}$ predictions, such studies are not routinely possible. Therefore, cerebrospinal fluid (CSF) drug concentrations are often used to validate brain drug concentration predictions. However, brain interstitial fluid and CSF drug concentrations can differ for many reasons (e.g. cerebral metabolism or CSF bulk flow), including when drugs are substrates of efflux transporters expressed at the apical membrane of the choroid plexus (Kodaira et al., 2011; Nagaya et al., 2020; Shen et al., 2004). Therefore, caution should be used when using this approach (Loryan et al.,

2020). For example, in a macaque study, the P-gp inhibitor zosuquidar increased brain nelfinavir (a P-gp substrate) concentration by >100-fold without affecting its CSF concentration obtained by lumbar puncture (Kaddoumi et al., 2007).

For predicting liver partitioning, two approaches have been used (**Table 4**). In the first, hepatic $K_{p,uu}$ is estimated by measuring steady-state total and unbound drug concentrations in hepatocytes (K. Riccardi et al., 2017). In the second, hepatic concentrations were predicted using estimates of all hepatobiliary CLs obtained from either hepatocytes or transporter-expressing cells and vesicles (C. Y. Li et al., 2019; Storelli et al., 2022a). The first approach, the use of hepatocytes, is straightforward, but can only provide an estimate of $K_{p,uu}$ but not the dynamic changes in hepatic concentrations such as peak (C_{max}) and trough (C_{min}) concentrations. These peak and trough concentrations could be important determinants of drug safety and efficacy. Also, this approach can be used only when primary cells are available (mostly for the liver). The second approach overcomes these challenges because it does not require primary cells and it can predict both $K_{p,uu}$ and the dynamic changes in tissue concentrations. However, it is more time-consuming and challenging to implement because all hepatobiliary CLs must be determined.

In another approach, using PK/PD and hepatocyte data to validate predictions, Riccardi *et al*. showed that hepatic $K_{p,uu}$ was underpredicted for pravastatin and overpredicted for rosuvastatin (K. Riccardi et al., 2017); this could be due to incorrect estimation of unbound drug concentration in the hepatocytes or incorrect estimation of the *in vivo* IC_{50} against HMG-CoA reductase that was used for validation. Using hepatic rosuvastatin concentrations measured in humans by PET imaging, we found that the REF approach (using transporter-expressing cells and vesicles) just barely underpredicted rosuvastatin hepatic uptake CL and concentrations while the SCH (using the PSF) underpredicted them to a much greater extent because SCH overestimated both the rosuvastatin sinusoidal and biliary efflux CLs (Storelli et al., 2022a).

6. Prediction of transporter-based DDIs

To predict drug-drug interactions (DDIs) related to transporter-based drug disposition, an important parameter to predict/estimate is f_t. This parameter informs the sensitivity of a drug to alterations in transporter activity/abundance due to the effect of a co-administered drug (inhibition/induction) or genetic

polymorphism (Prasad & Unadkat, 2015; Zamek-Gliszczynski et al., 2009). When using primary cells, the contribution of each transporter can be estimated *in vitro* using selective inhibitors of transporters (Y. Bi et al., 2013; Y.-A. Bi et al., 2019). Provided the abundance of the transporter in the primary cells is equal to that in the tissue, one can assume that the *in vitro* f_t will be the same as that *in vivo*. In this case, no scaling of transporter activity/abundance is required. However, the lack of selectivity of transporter inhibitors can preclude determination of f_t via a specific transporter. At first sight, the significant inter-lot variability in f_t when using primary cells could be interpreted as a limitation; it is not. Such variability provides vital information on possible inter-individual variability in transporter activity *in vivo*.

In contrast, when using transfected cells or membrane vesicles, scaling of all extrapolated intrinsic CLs of transporters involved using REF or RAF, as well as passive diffusion, is required, prior to estimating ft:

$$f_{t,i} = \frac{CL_{int,active,i}}{\sum_{i=1}^{n} CL_{int,active,i} + CL_{int,pd}} \qquad \text{(Eq. 22)}$$

where $f_{t,i}$ is the fraction transported by the i^{th} transporter.

The f_t via a given transporter provides a number (akin to fraction metabolized) that can readily be used to determine the likely magnitude of the change in transporter-based CL_{int} of a drug (due to inhibition or induction). For example, if the f_t of a drug via the hepatic OATP transporters is 0.9, then complete inhibition of these transporters will result in 10-fold increase in the plasma AUC of the drug, provided the OATPs are the RDS in the hepatic CL of the drug and non-hepatic CL is negligible.

To predict inhibitory DDIs *in vivo*, f_t is used in conjunction with inhibition potency (unbound IC_{50} or K_i), as described for competitive inhibition in Eq. 23 below. These parameters are preferably based on measured (uptake assays or membrane vesicles assay) or estimated (cell efflux assays) concentrations rather than nominal concentrations.

$$CL_{int,(+)inh} = CL_{int,(-)inh} \cdot \left[\sum_{i=1}^{n} \frac{f_{t,i}}{1 + {}^{[I]}/_{K_{i,i}}} + f_{pd} \right] \qquad \text{(Eq. 23)}$$

Where $CL_{int,(-)inh}$ and $CL_{int,(+)inh}$ are the CL_{int} (sum of all active and passive CL_{int}) in absence and in presence of an inhibitor, respectively, [I] is the unbound concentration of the inhibitor at the transporter

binding site, and $K_{i,i}$ is the unbound inhibition constant of the inhibitor for the i^{th} transporter, and f_{pd} is the fraction of $CL_{int,(-)inh}$ mediated by passive diffusion.

To predict DDI based on induction of transporters (e.g. intestinal P-gp by rifampin), information on the relationship between the magnitude and time course of increase in tissue transporter abundance (e.g. by QTP) and the concentration of the inducing drug is needed. Such data can be obtained from biopsies obtained after initiating administration of the inducing drug (Greiner et al., 1999). If multiple transporters are induced, the contribution of each in *in vivo* drug absorption, distribution or clearance of the drug can be predicted using REF and transporter-expressing cells/vesicles as detailed in Section 4.2.1. Alternatively, such information can be obtained, *in vitro*, using primary cells (e.g. hepatocytes) by exposing them to different concentration of the inducing drug for several days Dixit et al., 2007). Then, the magnitude and time course of increase in tissue transporter abundance (e.g. by QTP) or activity and the concentration of the inducing drug can be measured (Dixit et al., 2007). From these data the EC_{50} of the inducing drug and its maximal potential to induce the transporter (E_{max}) can be obtained. Using these data as well as the degradation half-life of the transporter, transporter-based DDI with the inducing agent can be predicted using PBPK modeling and simulation (Hanke et al., 2018a). To date, such predictions have mostly focused primarily on DDI caused by induction of P-glycoprotein in the intestine (Hanke et al., 2018a). Though some claim that hepatic OATPs can be induced by rifampin, both *in vitro* and *in vivo* evidence have challenged this claim (Dixit et al., 2007; Rodrigues et al., 2020).

In **Table 5**, we review published studies that have performed validation of transporter-based DDIs. Though most of these studies are focused on inhibitory DDI, some do include DDI where simultaneous inhibition and induction of transporters occurs (Hanke et al., 2018a). Such predictions were often done using a static model, such as described in Eq. 23 above, in which the maximal concentration of the inhibitor is used for [I]. The static model assumes that the concentration of the inhibitor does not change over time, and thereby reflects a worst-case scenario. In addition, many studies assume a f_t of 1, which likely overestimates the magnitude of DDIs. In recent years, PBPK modeling (i.e., dynamic approach), has been increasingly used to predict DDI magnitude over the entire plasma concentration-time profile of a substrate with dynamically varying inhibitor concentration, [I]. In principle, this dynamic approach

enables incorporation of inhibiting/inducing metabolites, dose staggering, concomitant use of multiple inhibiting drugs, net effect of inhibition and induction, and interplay of multiple enzymes and transporters. A summary of research articles that have used PBPK modeling to predict transporter-based DDIs is provided in **Table 5**. In most cases, the transporter-based CL_{int} of victim drugs was either estimated from systemic PK data or incorporated an ESF applied to the *in vitro*-determined transporter-based intrinsic CL. In addition, the inhibition potential of the perpetrator (K_i, IC_{50}) was optimized from that experimentally determined *in vitro* to best recapitulate the extent of DDIs observed in humans. Also, in many cases, there was no full characterization of the contribution of different transporters to the transporter-based CL (e.g., active sinusoidal uptake CL was assumed to be mediated solely by OATP1B1). This highlights the current limitations of these approaches to predict transporter-based DDIs using IVIVE-linked PBPK models. In contrast, using PET imaging, our group successfully predicted the extent of inhibition of sinusoidal uptake of rosuvastatin by cyclosporin (V. Kumar, Yin, et al., 2020, summarized in **Table 5**). In this case the contributions (f_t) of OAT1B1, 1B3, 2B1, NTCP and passive diffusion to rosuvastatin sinusoidal hepatic uptake were predicted using transfected cells and the REF approach, and the extent of inhibition of these transporters by cyclosporin A was determined *in vitro* at the same cyclosporin A concentration as that measured *in vivo* (in the PET imaging study used to validate prediction), rather than determining IC_{50} or Ki. Although more studies are needed (the study mentioned here was limited in sample size, n=3), this suggests that the REF approach appears to predict well the f_t of drugs by different transporters, and that misprediction of DDIs using IVIVE-linked PBPK models (without the use of ESF) might be due to misprediction of f_t and/or inhibition potential of the perpetrator. In addition, inconsistency in the *in vitro* inhibition studies may be a contributing factor. First, pre-incubation of cells with inhibitors may be necessary. For example, Yoshikado *et al.* and Pahwa *et al.* demonstrated that the *in vitro* Ki values of OATP inhibitors following pre-incubation are close to their *in vivo* Ki values (Pahwa et al., 2017; Yoshikado et al., 2016). Second, substrate-dependent inhibition (due to multiple binding sites) (Belzer et al., 2013; Gerk et al., 2004; Izumi et al., 2013) may occur. In several studies, the victim drugs used *in vitro* were probe substrates of transporters, which were not the target victim drugs in the DDI prediction. If the inhibitory capacity of perpetrator is substrate-dependent, this will result in a discrepancy in the *in vitro-in vivo* translation of DDI with the target drugs. Thus, if possible, to avoid bias due to substrate-dependent

inhibition, *in vitro* inhibition data should be obtained for the clinically relevant perpetrator-victim pair. Therefore, a harmonized *in vitro* experimental design and precise acceptance criteria should be considered for accurate prediction of transporter-based DDI.

7. Principles and experimental factors to consider to improve accuracy of IVIVE of transporter-based drug disposition and tissue concentrations

In recent years, significant advances have been made in predictions of transporter-based drug disposition and tissue concentrations. In particular, the REF approach was validated with PET imaging data for both prediction of transporter-based CL and tissue concentrations and appears superior to the use of primary cells (suspended or plated) and physiological scaling. However, for both approaches, further refinements is needed to predict transporter-based drug CL, especially for OATP substrate drugs. Here, we discuss principles and experimental factors that could improve accuracy of IVIVE of transporter-based drug disposition, many of them challenging the assumption that the *in vitro* intrinsic activity of transporters (corrected for transporter abundance) is similar to that *in vivo*.

7.1. Is the mechanism of transport *in vivo* replicated *in vitro*?

This is critical for success in IVIVE of transporter-based drug disposition, irrespective of whether cells or vesicles are used for *in vitro* studies (**Table 1**). Among mechanisms of transport are the presence of a co-transported substrate(s) (e.g. Na+ for NTCP, α-ketoglutarate for OATs), protons (e.g. pH effect on multidrug and toxin extrusion, MATE, transporters), or membrane potential (e.g. OCTs). For example, when using membrane vesicles, the activity of MRP1-4 can require inclusion of the co-transported glutathione (Borst et al., 1999; Loe et al., 1996). For OATPs, where CL by these transporters is underpredicted by current IVIVE approaches, the co-transported compound is unknow, but likely involves the exchange with an anionic intracellular compound (Stieger & Hagenbuch, 2014). Where this co-transported compound is unknown (e.g. OATPs), vesicles cannot be used to measure transport activity. An *in vitro* to *in vivo* discrepancy in the intracellular concentration of this co-transported substance could potentially help explain the current underpredictions of OATP-mediated hepatic uptake CL. When measuring *in vitro* transport by electrogenic transporters (e.g. OCT), incorporation of the *in vitro* to *in vivo*

difference in membrane potential has been shown to improve IVIVE and prediction of OCT-mediated drug disposition *in vivo* ((Burt, Neuhoff, et al., 2016; Kikuchi et al., 2021; V. Kumar et al., 2018)).

Allosterism is an example of another mechanism that should be considered. OATP transporters are allosteric (Gerk et al., 2004; Kindla et al., 2011). Therefore, it is possible that *in vivo* constituents in blood (a soluble factor or a protein – see below) can bind to the OATPs transporters, causing a conformational change of the transporter and thereby alter the drug's affinity to the transporter. In this case, if this endogenous allosteric factor is absent *in vitro*, the drug's $CL_{int,in\ vitro}$ will not replicate its $CL_{in,in\ vivo}$. However, in preliminary studies in our laboratory, human plasma filtrate (Yin et al., 2022) did not affect statin uptake by OATP1B1-expressing cells, indicating an absence of an allosteric effect on OATP1B1-mediated transport of statins by soluble constituents of plasma. Choosing the type of cells used or adjusting the experimental design for cell or vesicle uptake experiments, that replicates the mechanisms of transport *in vivo,* is critical for successful IVIVE of transporter-based drug disposition.

7.2. Is the unbound drug concentration at the site of transport *in vivo* replicated *in vitro?*

According to the free drug hypothesis, only unbound drug can passively diffuse or be transported across the cell membrane. Hence, an accurate estimation of the *in vivo* unbound fraction in plasma (for uptake transporters) or in the cells (for efflux transporters), at the site of transport, is important for successful IVIVE. Numerous publications have questioned whether the drug unbound fraction measured *in vitro* accurately represents that present *in vivo* at the site of transport (Bowman & Benet, 2018; Bteich et al., 2019; Francis et al., 2021). Instead, they have postulated a "protein-mediated uptake effect (PMUE)", where the presence of plasma (proteins) in the *in vitro* studies, increases the apparent uptake CL of drugs by OATPs, thereby partially bridging the under prediction of the *in vivo* hepatic uptake CL by these transporters (Y.-A. Bi et al., 2020; N. Li et al., 2020; Liang et al., 2020). Several possible mechanisms for the PMUE have been proposed. Most of these postulate an increase in the *in vivo* drug unbound concentration (not captured by the *in vitro* protein binding studies) at the transport site caused by an interaction between the drug-protein complex and the lipid membrane of the cells or the membrane transporter itself (Bowman et al., 2019; Kim et al., 2019). As a result, the transport CL measured *in vitro* will be lower than that *in vivo*. However, our studies with OATP1B1-transfected HEK293 cells indicate

that for the majority of statins studied, the supposed PMUE is likely an artifact of non-specific binding of the statin-albumin complex to the cells/labware (Yin et al., 2022). Additional studies are needed to determine if the same is true for the PMUE on OATP-mediated uptake of drugs by hepatocytes.

7.3. Is post-translational transporter regulation in the *in vitro* cell models the same as *in vivo*?

Post-translational modifications (PTMs), protein-protein interactions or protein-lipid interactions (i.e., scaffolding) can affect membrane transporter activity and abundance (Czuba et al., 2018; Lee et al., 2020; Stieger & Hagenbuch, 2014). Isolation of plasma membrane from cell homogenates using a biotinylation method and quantification of transporter abundance at the plasma membrane can improve IVIVE of transporter-mediate drug CL_{int} (V. Kumar et al., 2017; V. Kumar, Yin, et al., 2020; Sachar et al., 2020). However, a limitation of this method is that it can only be used for cells and not tissues. Thus, this approach requires an assumption about the plasma membrane abundance of the transporters in tissues. PTMs can also affect transporter function without altering transporter membrane abundance, as recently shown for OCTs (Sprowl et al., 2016). Whether transporters are differentially post-translationally modified in primary cells, transfected cells (hence in vesicles) and *in vivo*, and if they are, the impact of such PTMs on transporter activity needs to be assessed.

7.4. Does the lack of blood flow in the in the in vitro model affect active and passive uptake of drugs?

A major difference between *in vitro* (suspended or plated cells) and *in vivo* conditions is the flow and shear stress imposed on the endothelial cells of the organ of interest (e.g. kidneys, brain, liver) by blood. While the effect of such factors on transporter-based CL_{int} needs to be investigated, it has been shown previously that the unstirred water layer present in the static *in vitro* model affects permeability above a given permeability threshold (Korjamo et al., 2008, 2009). In this regards, MPS might offer potential advantages as they are designed to recapitulate the tissue environments with respect to fluid flow and shear stress (Chang et al., 2016).

7.5. How does the choice of the CL model used to predict the *in vivo* CL of drug affect accuracy of IVIVE of transport-mediated CL?

For intermediate to high extraction drugs, the predicted organ CL extrapolated from *in vitro* studies can depend on the choice of the CL model used. Because of its simplicity, the well-stirred model is the most widely used model and is the basis of the ECM. However, the use of more physiologically relevant models taking into account a gradual decrease in tissue concentrations along the organ (e.g., from the periportal to the perivenous regions of the liver), such as the parallel-tube or the dispersion model or a 5-compartment liver PBPK model, can yield better predictions of organ CL for intermediate to high extraction drugs (Pang et al., 2019; Watanabe et al., 2009). But the choice of these models cannot bridge the gap between predicted and observed CL data for low extraction drugs. Recently, we compared the ability of the well-stirred model and the parallel tube model to predict the hepatic uptake CL of rosuvastatin (extraction ratio of around 0.6), and found only slight differences in the predicted values (Storelli et al., 2022a). Of note, the validity of predicting drug CL (from systemic concentrations) by inputting *in vitro* to *in vivo* extrapolated intrinsic CL into one of the above-mentioned CL models is the subject of much debate (Benet & Sodhi, 2021; Rowland et al., 2022).

8. Conclusions

Predicting transporter-based drug CL, tissue concentrations and DDIs from *in vitro* studies is challenging and requires further refinement. Nevertheless, within the last decade, enormous progress has been made in successfully predicting *in vivo* transporter-based drug CL, tissue concentrations and DDI, including the use of transporter-transfected cells and membrane vesicles using the REF (and in some cases the RAF) approach. It is important to keep in mind that each of the approaches outlined above to predict transporter-based drug CL and tissue concentrations, once validated for a given transporter, provides confidence to use that approach for any other drug transported by the same transporter. For example, once the REF approach has been thoroughly validated for OATP-transported drugs using imaging, it can be used with confidence to predict OATP-mediated hepatic uptake of another drug without conducting imaging studies for that drug. Although we have validated the REF approach for hepatic uptake (rosuvastatin, metformin) and efflux (rosuvastatin) as well as renal OAT transport of some drugs, validation with additional drugs that interrogate the same and other transporters (e.g. MATE1, MATE2-K) is needed before the approach can be widely used to predict transporter-based drug CL and tissue

concentrations. Going forward, we are confident that such additional research and validation will be conducted to enhance the success of the REF approach in predicting transporter-based CL and tissue concentrations of a wide variety of drugs. At that juncture, the REF approach can easily be combined with current approaches for IVIVE of metabolic clearance of drugs (Houston & Galetin, 2008) to predict *in vivo* clearance of drugs that are eliminated from the body by both transporters and metabolic enzymes.

9. Conflicts of interest

The authors declare no conflict of interest. R.E., P.P.C., O.J.E., X.L., and Y.L. are all employees of their respective companies and hold stock or stock options in the company.

10. Acknowledgement

The authors acknowledge support from the University of Washington Research Affiliate Program, funded by Gilead Sciences, Amgen, Takeda and Janssen, the National Institute of Health (P01 DA032507, R01 HD102786, Certara's Simcyp Grant & Partnership Scheme, and the Bill & Melinda Gates Foundation). Authors would like to thank Stephanie Kourula (Janssen Research & Development) for her valuable suggestions on the manuscript. BioRender (https://biorender.com/), and Microsoft Office Excel and PowerPoint (https://www.office.com/) were used to create the figures.

11. Figures

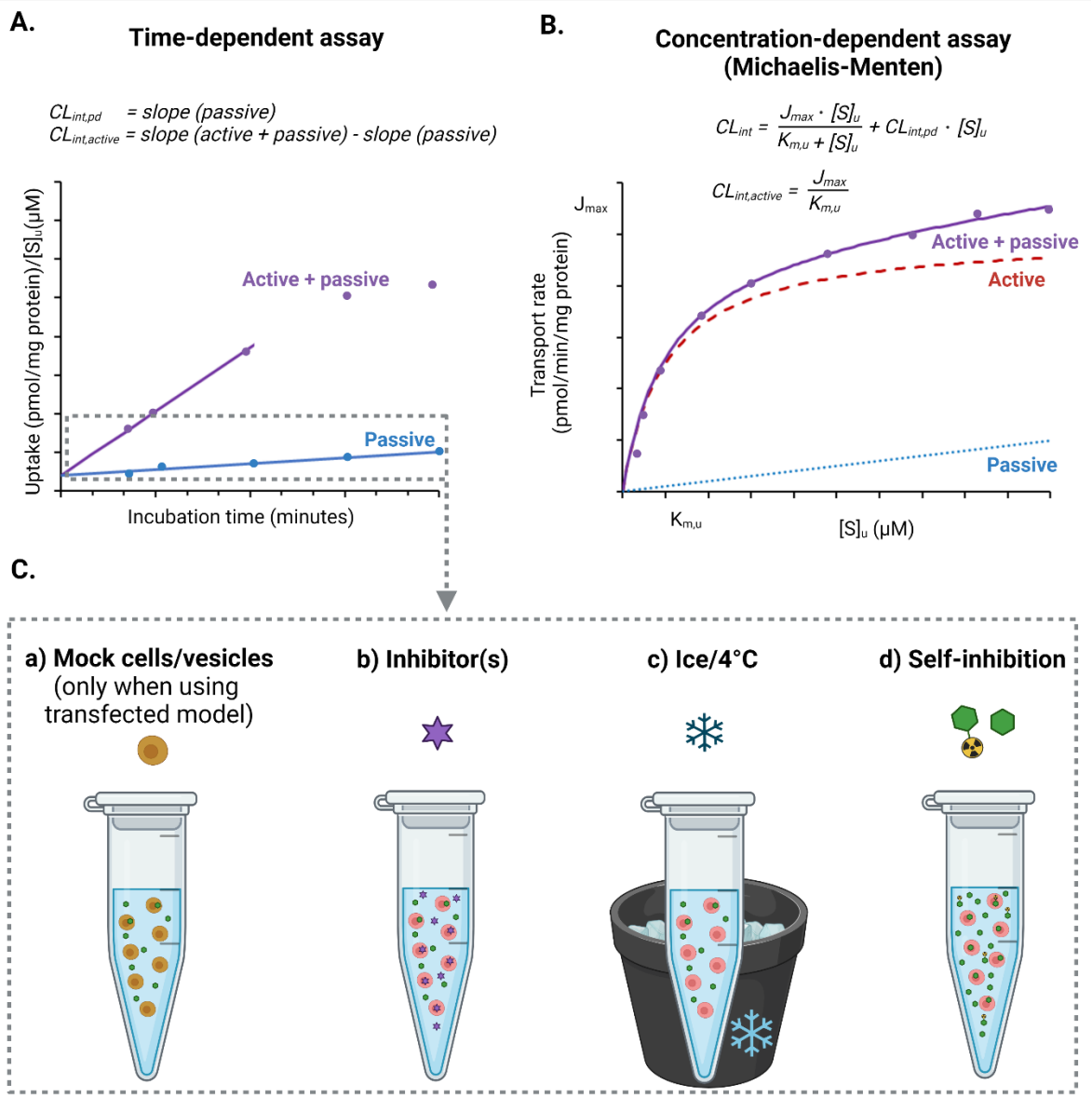

Figure 1. Determination of *in vitro* active ($CL_{int,active}$) and passive ($CL_{int,pd}$) intrinsic clearance using cells or vesicles. $CL_{int,active}$ and $CL_{int,pd}$ can be determined *in vitro* using either a time-dependent assay (A) or a concentration-dependent (or Michaelis-Menten) assay (B) over time when the uptake is linear. Passive diffusion CL of the drug can either be estimated by fitting a Michaelis-Menten model, incorporating both saturable (active) and non-saturable (passive) components, to the observed concentration-dependent data (panel B) or by fitting a linear model to the data obtained by one of the methods illustrated in panel C (applicable for both types of assays). That is, uptake determined using a) mock cells/vesicles not expressing the transporter of interest; b) transfected cells/vesicles or primary cells

co-incubated with an inhibitor(s) at a concentration that completely inhibits the transporter(s); c) transfected cells/vesicles or primary cells incubated at 4 °C (on ice); d) self-inhibition (i.e., where the uptake of the labeled drug is measured in presence of saturating concentration of the non-labeled drug). The investigational drug is shown as a green hexagon, the inhibitor(s) is/are shown as a purple star. J_{max}, maximal transport rate; $K_{m,u}$, unbound affinity constant; $[S]_u$, unbound substrate concentration in the incubation buffer.

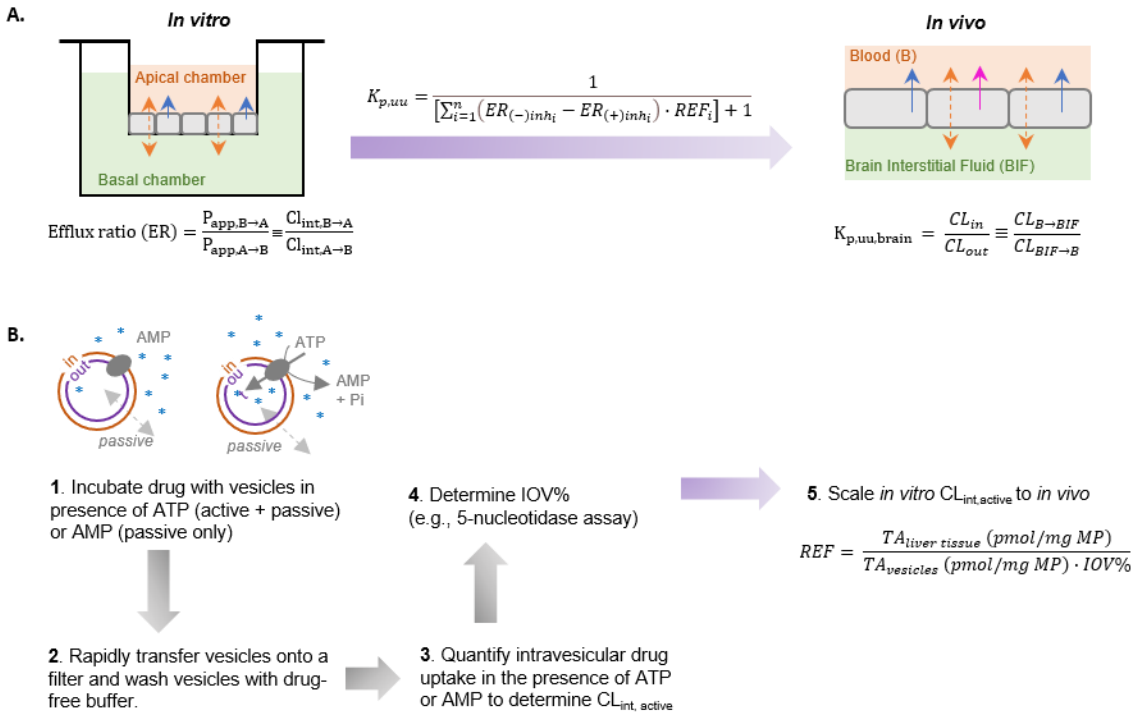

Figure 2. Determination of efflux ratio (ER) and efflux clearance (CL) *in vitro*. (A) The ER is determined *in vitro* by the ratio of the apparent permeability of the drug from the basal to apical chamber ($P_{app,B\to A}$) and from the apical to the basal chamber ($P_{app,A\to B}$). This ratio is equivalent to the ratio of the B→A and A→B intrinsic CLs ($CL_{int,B\to A}$ and $CL_{int,A\to B}$, respectively). The ER is an *in vitro* inverse equivalent of the BBB; the apical chamber represents the blood compartment and the basal chamber represents the brain interstitial fluid (BIF). Assuming that drug efflux from the BIF is mainly mediated by the back flux of the drug from the BIF to the blood (i.e., negligible metabolism and bulk flow), $K_{p,uu}$ can be extrapolated from the active ER (i.e., difference between ER in absence of inhibitor, ($ER_{(-)inh,i}$) and ER in presence of inhibitors ($ER_{(+)inh,i}$) or in mock cells) using the relative expression factor (REF). (B) Active efflux intrinsic CL can also be determined using membrane vesicles. The *in vitro* active intrinsic CL ($CL_{int,active}$) is determined by the difference between the vesicular uptake of the drug in the presence of ATP (active + passive) and that in the presence of AMP or mock vesicles (passive only). Because the inside-out vesicles are a fraction of the total vesicles used, the percentage of inside-out vesicles (IOV%) must be determined for *in vitro* to *in vivo* extrapolation. IOV% can be estimated using an ectoenzyme (eg., 5-nucleotidase). The IOV% is then integrated into the REF for scaling of *in vitro* intrinsic CL to *in vivo*. AMP, adenosine monophosphate;

ATP, adenosine triphosphate; Pi, phosphate; MP, membrane protein; TA, transporter abundance; Pi, phosphate.

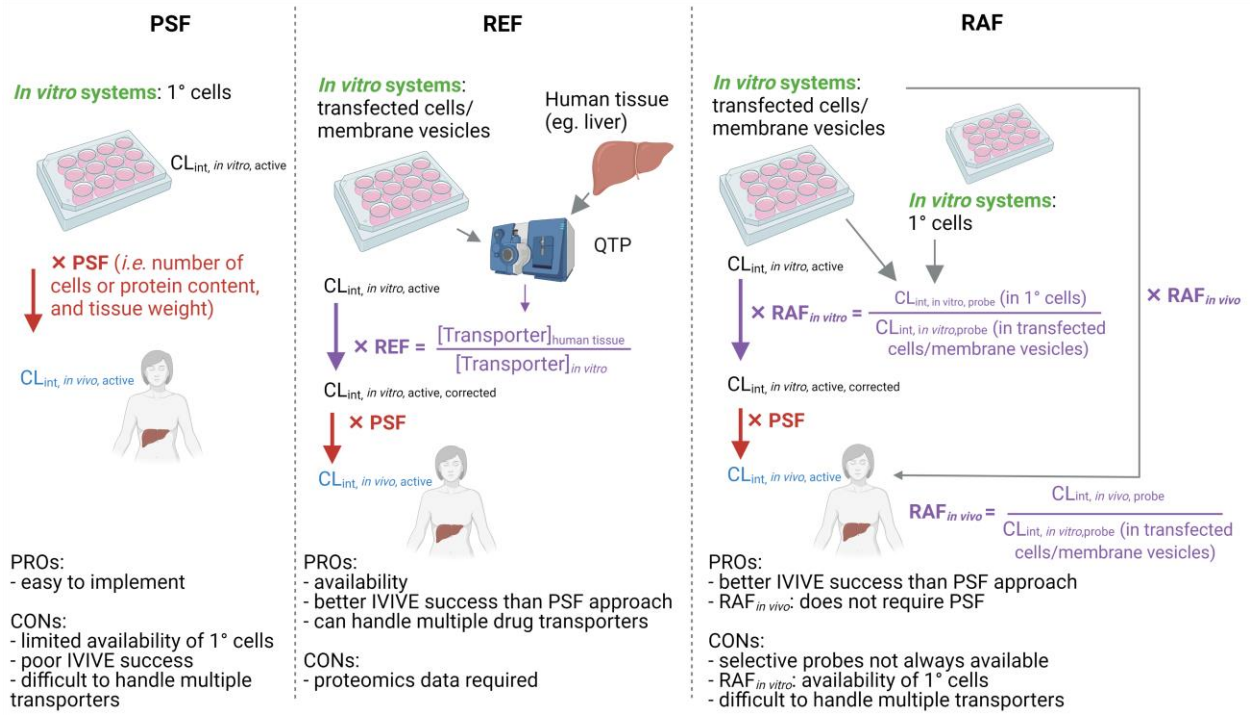

Figure 3. Schematic framework of different scaling approaches for IVIVE of transporter-mediated intrinsic clearance. 1°, primary; $CL_{int,\ in\ vitro,\ active}$, *in vitro* active intrinsic clearance; $CL_{int,\ in\ vitro,\ active,\ corrected}$, *in vitro* active intrinsic clearance corrected by REF or RAF; $CL_{int,\ in\ vitro\ probe}$, *in vitro* intrinsic clearance of the probe substrate; $CL_{int,\ in\ vivo\ probe}$, *in vivo* intrinsic clearance of the probe substrate used for the $RAF_{in\ vivo}$ approach; PSF, physiological scaling factor; QTP, quantitative targeted proteomics; RAF, relative activity factor; $RAF_{in\ vitro}$, *in vitro* relative activity factor; $RAF_{in\ vivo}$, *in vivo* relative activity factor; REF, relative expression factor.

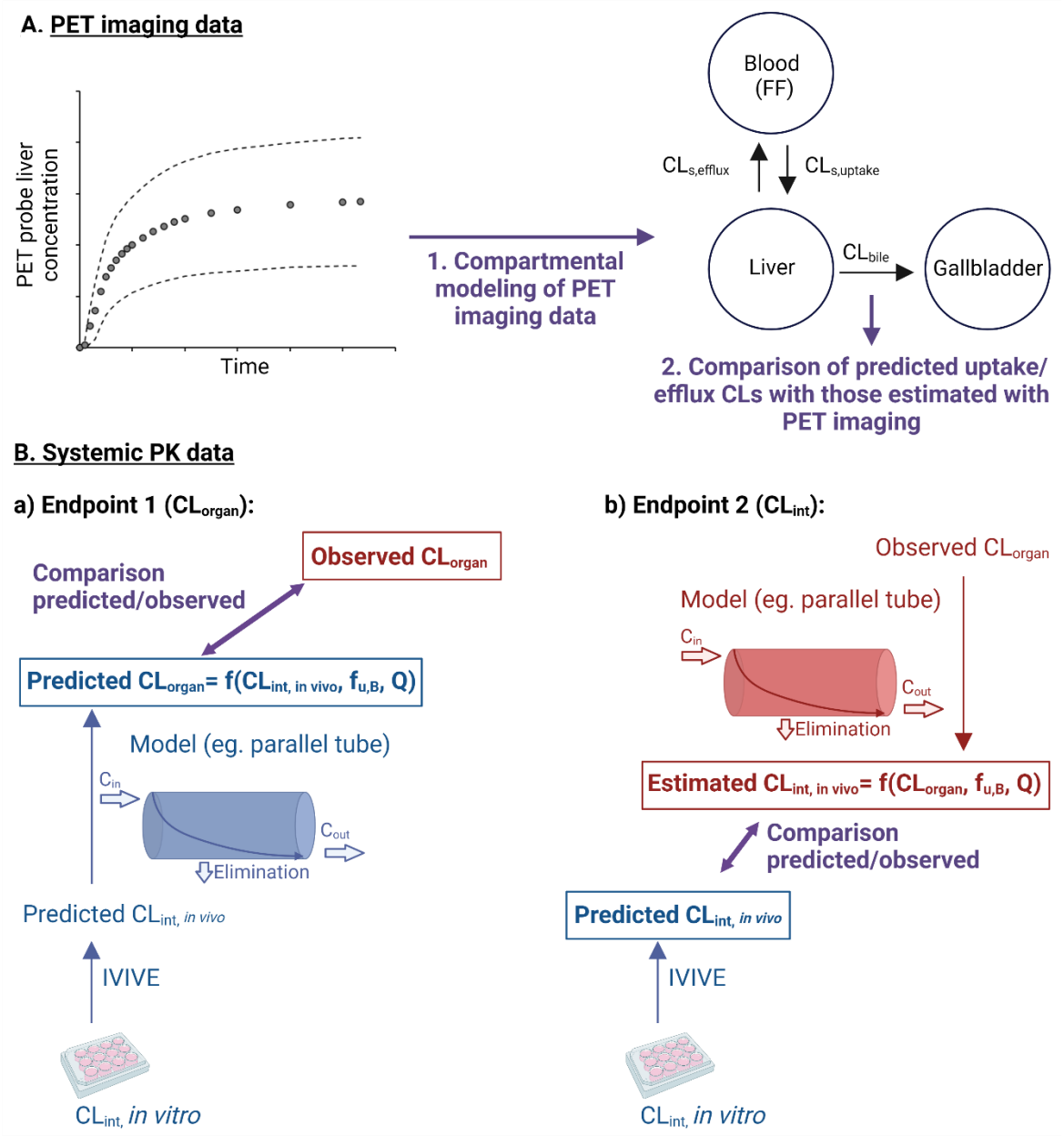

Figure 4. Validation of *in vitro* t***o*** *in vivo* extrapolation (IVIVE) of clearances (CL) using imaging (e.g. positron emission tomography [PET] imaging) or systemic PK data. (A) PET imaging data taken over a period of time, when metabolism is negligible, are used to estimate the *in vivo* uptake and efflux CLs using a compartmental model. These estimated CLs are then compared with those predicted using IVIVE methods. (B) Using systemic PK data (e.g. using FF, forcing function, to estimate the CLs), two endpoints can be used to validate IVIVE of transporter-mediated CLs. For endpoint 1, the whole organ CL (CL_{organ}) observed in humans is compared to the one predicted based on the extrapolated intrinsic CL ($CL_{int,\ in\ vivo}$)

and a CL model (e.g., parallel-tube or well-stirred model). For endpoint 2, the *in vivo* intrinsic CL used for validation is estimated based on the CL_{organ} and a CL model (e.g. parallel-tube or well-stirred model). This value is then compared to the predicted $CL_{int,\ in\ vivo}$. The two endpoints are expected to yield similar outcomes for low extraction compounds. However, validation outcomes can differ for intermediate to high extraction compounds, for which blood flow (Q) plays a significant role in determining whole organ CL. For such drugs, mis-prediction of transporter-mediated *in vivo* organ CL from *in vitro* CL_{int} will be dampened by blood flow, which is a significant determinant of organ CL for such drugs. Consequently, such mis-predictions may erroneously look accurate when using endpoint 1 when in fact they are not.

12. List of tables

Table 1. Requirements of primary cells for successful *in vitro* to *in vivo* extrapolation (IVIVE) of transporter-mediated drug disposition

Requirement	**Primary cells**	**Transfected cells/ membrane vesicles**
Recapitulation of *in vivo* mechanism of transport (e.g., membrane potential, co-transported substrate)	Yes; more likely to do so than transfected cells/membrane vesicles	Yes
Recapitulation of *in vivo* total and plasma membrane transporter abundance	Yes, if using physiological scaling If no, use a transporter-abundance correction factor (RAF/REF)	No, but need to use a transporter-abundance correction factor (REF/RAF)
Human origin	Yes	No, but need to express the human transporters in a cell of human or non-human origin
Endogenous transporters ablated	No, but recognize that transport of a drug be mediated by multiple transporters present in the cells	Yes, unless the contribution of the endogenous transporter is not significant in the transport of drug of interest

RAF, relative activity factor; REF, relative expression factor

Table 2. Predictive performances of *in vitro* to *in vivo* extrapolation (IVIVE) approaches for predicting hepatic clearance (CL_h) of transported drugs

Transporters involved	Drug	*In vitro* system	SF	CL model	Predicted parameter	Validation method	Predictive performance	Comments	Study
OATPs	19 OATP1B1 substrates including atorvastatin, pitavastatin, rosuvastatin, bosentan *etc.*	PH	PSF	WSM & PTM	CL_h	Systemic PK (endpoint 1)	*WSM:* 5% and 16% of predicted values fell within 2-fold of observed values in the absence and presence of plasma, respectively *PTM:* 11% and 21% of predicted values fell within 2-fold of the observed values in the absence and presence of plasma, respectively	Assuming uptake was RDS of CL_h PMUE included	(Y.-A. Bi et al., 2020)
					CL_{int}	Systemic PK (endpoint 2)	*WSM and PTM:* 5% and 16% of predicted values		

							fell within 2-fold of observed values in the absence and presence of plasma, respectively		
OATP1B1, OATP1B3, OATP2B1, NTCP	Rosuvastatin	OATP1B3/NTCP (HEK293 cells), OATP1B1 (CHO cells), OATP2B1 (MDCKII cells)	REF	WSM	$CL_{s,uptake}$	PET imaging	Underprediction (outside the 2-fold success criterion, unless uptake transporter-mediated CL was determined in presence of 5% HSA)		(V. Kumar, Yin, et al., 2020)
OATP1B1, OATP1B3, OATP2B1, NTCP	Rosuvastatin	PH/ SH/ SCH	PSF	WSM	$CL_{s,uptake}$	PET imaging	Underprediction (outside 2-fold range of the average observed value)	Predicted $CL_{s,uptake}$ were comparable between PH, SH and SCH	(V. Kumar, Yin, et al., 2020)
OATPs	8 OATPs-substrates including pitavastatin, rosuvastatin *etc.*	SH (+/- 10% human serum)	PSF	Estimated using PBPK modeling	$CL_{int,s,uptake}$ (active)	Systemic PK	0/8 predictions fell within 3-fold of the observed values; 1/8 predictions fell within 3-fold of the	PMUE included	(Liang et al., 2020)

							observed values in the presence of 10% human serum		
OCT1	Metformin	PH	PSF	WSM	$CL_{s,uptake}$	PET imaging	Fell outside the 2-fold range of the observed value (i.e. P/O < 0.50)	Corrected for PMA of OCT1	(Sachar et al., 2020)
OCT1	Metformin	OCT1-expressing HEK293 cells	REF	WSM	$CL_{s,uptake}$	PET imaging	Predicted $CL_{h,uptake}$ was within 2-fold of the observed value	REF determined based on PMA of OCT1. When REF determined based on total OCT1 abundance, predicted $CL_{s,uptake}$ was < 50% of the average observed value	(Sachar et al., 2020)
OATPs	11 OATPs-substrates including pitavastatin, rosuvastatin, repaglinide, *etc.*	SH	PSF	WSM or DM	$CL_{h,int,all}$	Systemic PK (endpoint 2)	27% compounds fell within 5-fold of observed data when $CL_{int,uptake}$ was quantified in buffer; 90% compounds fell within 5-fold of observed data when $CL_{int,uptake}$ was quantified in the	Assuming uptake was RDS of CL_h PMUE included	(Kim et al., 2019)

							presence of 5%HSA		
OATPs	32 OATPs-substrates, including pitavastatin, repaglinide, telmisartan, glyburide	SH	PSF	ECM	CL_h	Systemic PK (endpoint 1)	method A: 21 out of 32 fell within 3-fold of observed value; method B: 8 out of 32 fell within 3-fold of the observed value	Method A assumes that *in vitro* $CL_{int,s,uptake}$ values with BSA are equivalent to the in vivo $CL_{int,s,uptake}$ values, and *in vitro* $CL_{int,met}$ and $CL_{int,pd}$ values with (or without) BSA are equivalent to the *in vivo* values. Method B assumes that *in vitro* $CL_{h,int,met}$, $CL_{h,int,pd}$, and $CL_{int,s,uptake}$ clearance values without BSA are equivalent to the *in vivo* clearance values. $CL_{int,bile}$ is assumed to be zero for both method.	(K. A. Riccardi et al., 2019)
					CL_{int}	Systemic PK (endpoint 2)	method A: 17 out of 32 fell within 3-fold of the observed value; method B: 7 out of 32 fell within 3-fold of the observed value		
OATPs	1-anilino-8-naphthalene sulfonate,	SH	PSF	DM	$CL_{h,int,all}$	Systemic PK (endpoint 2)	Predicted values fell outside 3-fold of observed data	Assumed uptake is the RDS of CL_h	(Miyauchi et al., 2018)

	Pitavastatin								
OATPs, MRP2, BCRP, MDR1	17 compounds, incl. OATP substrates such as rosuvastatin, pravastatin, valsartan	SCH	PSF	WSM	$CL_{int,bile}$	Systemic PK study with CL_{bile} measured as the ratio of amount excreted in feces *vs*. plasma AUC	$CL_{int,bile}$: 8/17 predictions were within 3-fold of the observed values	Biliary CL *in vitro* was estimated using drug concentration in the medium, rather than the intracellular concentration	(Kimoto et al., 2017b)
OATP1B1, OATP1B3, OATP2B1	Rosuvastatin	SH, OATP1B1/OATP1B3/OATP2B1-transfected HEK293 cells	REF	DM	$CL_{h,int,all}$	Systemic PK (endpoint 2)	P/O=0.96 using SH; P/O=0.97 using transfected cells	Assuming uptake is the RDS of CL_h	(Bosgra et al., 2014)
OATPs	7 OATPs-substrates including pitavastatin, rosuvastatin, valsartan	SCH	PSF	Fitted value using PBPK modeling	$CL_{int,s,uptake}$ (active) $CL_{int,bile}$	Systemic PK	$CL_{int,s,uptake}$ (active): Underpredicted by 12-to-161 fold $CL_{int,bile}$: Overpredicted by 3- to 41- fold	Assuming active sinusoidal efflux was 0	(Jones et al., 2012)

AUC, area under the concentration-time profile; BSA, bovine serum albumin; CL, clearance; $CL_{int,all}$, intrinsic clearance (function of all hepatobiliary CLs); $CL_{int,bile}$, intrinsic biliary clearance; $CL_{int,met}$, intrinsic metabolic clearance; $CL_{int,pd}$, intrinsic passive diffusion clearance; $CL_{int,s,uptake}$, intrinsic sinusoidal uptake clearance; C-T, concentration-time; DM, dispersion model; ECM, extended clearance model; H/BSA, human/bovine serum albumin; PBPK, physiologically based pharmacokinetic model; PET, positron emission tomography; PH, plated hepatocytes; PMA, plasma membrane abundance; PMUE, protein-mediated uptake effect; PK, pharmacokinetics; PSF, physiological scaling factor; PTM, parallel-tube model; P/O, predicted over observed; RAF, relative activity factor; REF, relative expression factor; RDS, rate-determining step; SCH, sandwich-cultured hepatocytes; SF, scaling factor; SH, suspended hepatocytes; WSM, well-stirred model.

Table 3. Predictive performances of *in vitro* to *in vivo* extrapolation (IVIVE) approaches for predicting renal clearance of transported drugs

Transporters involved	Drug	*In vitro* system	SF	CL model	Predicted parameter	Validation method	Predictive performance	Comments	Study
OATs?, OCT2	Morphine and morphine-6-glucuronide	Vascularized human renal proximal tubule MPS	PSF	-	CL_r	Systemic PK (endpoint 1)	P/O between 0.5-2	PBPK model was also used and predicted well the systemic C-T profile of morphine and morphine 6-glucuronide using the MPS, but not with plated PTC.	(Imaoka et al., 2021)
		PTCs (2D plated)					P/O < 50%		
OCT2; MATE1; MATE2K	Metformin	HEK293 cells	REF	*In vitro* K_m and J_{max}, and REF values were input into a PBPK model for IVIVE	C_{max}; AUC	Systemic PK	C_{max}: P/O between 0.5-2 AUC: P/O between 0.5-2	Prediction was corrected for OCT2 PMA and for the membrane potential	(Kikuchi et al., 2021)
OAT1; OAT2; OAT3	Acetazolamide; Adefovir; Amoxicillin;	HEK293 cells	REF, RAF	WSM; CL_r = ($CL_{r,sec}$ +	CL_r	Systemic PK (endpoint 1)	REF: RMSE= 2.0 ($CI_{95\%}$ 0.15-3.8)	Assumed F_{reabs} and passive diffusion are negligible.	(A. R. Kumar et al., 2021)

	Bumetanide; Captopril; Cefazolin; Cefdinir; Cefotaxime; Cilostazol; Cimetidine; Famotidine; Fexofenadine; Furosemide; Gemfibrozil; Gemfibrozil Glucuronide; Hydrochlorothiazide; Ketoprofen; Ketorolac; Methotrexate; Olmesartan; Penciclovir; Pravastatin; Rosuvastatin; Sitagliptin; Torsemide; Zalcitabine			CL_{filt}) * (1 – F_{reabs})			ME= 0.50 ($CI_{95\%}$ - 0.40-1.2) RAF: RMSE=1.6 ($CI_{95\%}$ 0.058-3.1) ME= 0.015 ($CI_{95\%}$ - 0.65-0.67)		
					$CL_{int,r,sec}$	Systemic PK (endpoint 2)	REF: RMSE= 15 ($CI_{95\%}$ 3.1-26) ME= 3.0 ($CI_{95\%}$ - 2.9-9.0) RAF: RMSE= 9.8 ($CI_{95\%}$ 0.97-18) ME= -3.3 ($CI_{95\%}$ - 7.1-0.45)		

OCT2	Metformin	OCT2 transfected HEK293 cells and MDCKII cells	REF	---	$CL_{r,sec}$	Systemic PK (endpoint 2)	Predicted value within the observed range	Prediction was corrected for OCT2 PMA and for the membrane potential	(V. Kumar et al., 2018)
OAT1-3	Acetazolamide; Adefovir; Amoxicillin; Bumetanide; Captopril; Cefazolin; Cefdinir; Cefotaxime; Cilostazol; Cimetidine; Famotidine; Fexofenadine; Furosemide; Gemfibrozil; Gemfibrozil Glucuronide; Hydrochlorothiazide; Ketoprofen; Ketorolac; Methotrexate; Olmesartan;	OAT1-3 transfected HEK293 cells	RAF	WSM; $CL_r = (CL_{r,sec} + CL_{filt}) * (1 - F_{reabs})$	CL_r	Systemic PK (endpoint 1)	AFE = 1.4	Assumed F_{reabs} is negligible.	(Mathialagan et al., 2017b)
					$CL_{r,sec}$	Systemic PK (endpoint 2)	AFE = 1.89		

	Penciclovir; Pravastatin; Rosuvastatin; Sitagliptin; Torsemide; Zalcitabine								
OCT2, MATE1, MATE2K, OAT1, OAT3, MRP2, MRP4, BCRP, OCTN1, OCTN2	Desipramine; Imipramine; Propranolol; Quinidine; Quinine; Verapamil; Atorvastatin; Cyclosporine A ; Ketoconazole; Amantadine; Atenolol; Chloroquine; Cimetidine; Digoxin; Fexofenadine; Metformin; Methotrexate; Pravastatin;	LLC-PK1 cells (bidirectional assay)	PSF	WSM; $CL_r = (CL_{r,sec} + CL_{filt}) * (1 – F_{reabs})$	CL_r	Systemic PK (endpoint 1)	AFE = 1.47	F_{reabs} was predicted from GFR and extrapolated intrinsic CL (apical to basolateral)	(Kunze et al., 2014)

	Tetracycline; Valsartan								
OAT1, OAT3	Rosuvastatin, Pravastatin, Pitavastatin, Valsartan, Olmesartan, Trichlormethiazide, *P*-Amino-Hippurate, Fexofenadine, Methotrexate, Benzylpenicillin	Human kidney slices	PSF	DM	$CL_{r,sec}$	Systemic PK (endpoint 1)	9/10 fell within 3-fold range	Assumed that basolateral uptake is RDS of tubular secretion, and that F_{reabs} is negligible.	(Watanabe et al. 2011)
					$CL_{int,r,sec}$	Systemic PK (endpoint 2)	Predicted value were 10-fold underestimated compared to observed value		

2D, two dimensions; AFE, average fold error; AUC, area under the concentration-time profile; CL, clearance; C-T, concentration-time; $CI_{95\%}$, 95% confidence interval; CL_{filt}, filtration clearance; CL_r, renal clearance; $CL_{r,sec}$, renal secretory clearance; $CL_{int,r,sec}$, intrinsic renal secretory clearance; C_{max}, maximal concentration; DM, dispersion model; F_{reabs}, fraction of the drug reabsorbed; GFR, glomerular filtration rate; PBPK, physiologically based pharmacokinetic model; ME, mean error; MPS, microphysiological system; PET, positron emission tomography; PH, plated hepatocytes; PK, pharmacokinetics; PMA, plasma membrane abundance; PMUE, protein-mediated uptake effect; PSF, physiological scaling factor; PTC, proximal tubular cells; PTM, parallel-tube model; *P/O, predicted over observed;* RAF, relative activity factor; REF, relative expression factor; RMSE, root mean square error; RDS, rate-determining step; SH, suspended hepatocytes; SCH, sandwich-cultured hepatocytes; WSM, well-stirred model.

Table 4. Predictive performances of *in vitro* to *in vivo* extrapolation (IVIVE) approaches for predicting absorption and tissue concentrations of transported drugs

Organ	**Transporters involved**	**Drug**	***In vitro* system**	**SF**	**Predicted parameter**	**Validation method**	**Predictive performance**	**Comments**	**Study**
Absorption									
Intestine	P-gp	Digoxin	Caco-2	REF	CL_{po}	Comparison of predicted and observed systemic C-T profiles	5/10 predicted CL_{po} were within 1.25-fold of the observed value 10/13 predictions for IV studies were within 1.25-fold of the observed value	REF taken from a published study	Neuhoff *et al.*, 2013
Distribution – tissue or interstitial concentrations									
Brain	P-gp and/or BCRP	Delavirdine, erlotinib, etoposide, indomethacin, metoprolol, nelfinavir, pefloxacin, topiramate, verapamil, zidovudine	MDCK-MDR1 and MDCK-BCRP (ER)	REF to scale ER to $K_{p,uu,brain}$ Other passive CLs were estimated by best fit of data to model	$K_{p,uu,brain}$ $K_{p,uu,CSF}$	PET imaging ($K_{p,uu,brain}$) and CSF sampling ($K_{p,uu,CSF}$), and binding data	$K_{p,uu,brain}$: 4/4 within 3-fold the observed value $K_{p,uu,CSF}$: 78% within 3-fold the observed value	REF was not measured but estimated based on available REF value normalized using a probe substrate's ER data from the authors study *vs.* REF from another study 3C model incl. plasma, brain ISF and brain CSF	Sato *et al.*, 2021

Brain	P-gp and/or BCRP	Delavirdine, erlotinib, etoposide, indomethacin, metoprolol, nelfinavir, pefloxacin, topiramate, verapamil, zidovudine	MDCK-MDR1 and MDCK-BCRP (ER)	ESF on ER that provides best fit to full human dataset Other passive CLs were estimated by best fit of model to datal	$K_{p,uu,brain}$ $K_{p,uu,CSF}$	PET imaging ($K_{p,uu,brain}$) and CSF sampling ($K_{p,uu,CSF}$), and binding data	$K_{p,uu,brain}$: 4/4 within 3-fold the observed value $K_{p,uu,CSF}$: 9/10 within 3-fold the observed value	3C model incl. plasma, brain ISF and brain CSF	Sato *et al.*, 2021
Brain	P-gp	Morphine	MDCKII-MDR1 (ER)	REF to scale CL_{efflux} from *in vitro* data (ER and passive permeability)	Brain ISF C-T profile	Microdialysis	Observed pseudoequilibrium ISF concentration within 90% CI of simulated data	Morphine is a weak P-gp substrate (ER=1.3)	Verscheijden *et al.*, 2021
Brain	P-gp	Verapamil, metoclopramide and desmethyl loperamide	MDCK-MDR1$^{cP\text{-}gp\text{-}KO}$ (ER)	REF to scale ER to $K_{p,uu,brain}$	$K_{p,uu,brain}$	PET imaging (cER or $K_{p,brain}$, as available) and binding data if using $K_{p,brain}$	All predicted $K_{p,uu,brain}$ values fell within 2-fold of the observed value, 2/3 were within 95% CI of the observed value		Storelli *et al.*, 2021

Brain	P-gp	Verapamil, metoclopramide and desmethyl loperamide	MDCK-MDR1$^{cP\text{-}gp\text{-}KO}$	REF to scale active and passive CL from *in vitro* (estimated by modeling) to *in vivo*	$K_{p,uu,brain}$	PET imaging (cER or $K_{p,brain}$, as available) and binding data if using $K_{p,brain}$	Predicted $K_{p,uu,brain}$ values for 2/3 drugs fell within 2-fold of the observed value	While $K_{p,uu,brain}$ was relatively well predicted, unbound brain C-T profiles were underpredicted (5C model including membranes)	Storelli *et al.*, 2021
Brain	P-gp	Verapamil, desmethyl loperamide and zolmitriptan	Mock and MDR1-transfected LLC-PK1 Cells (ER)	REF to scale ER to $K_{p,uu,brain}$	$K_{p,uu,brain}$	PET imaging	P/O were 0.42 for verapamil, 0.68 for desmethyl loperamide and 0.57 for zolmitriptan	Authors used an incorrect definition of the net ER for scaling, which might have resulted in erroneous use of 0.1 correction factor on passive diffusion Also, not all drugs are selective P-gp substrates (only 2/6) and 3/6 drugs had an in vivo $K_{p,uu,brain} > 1$ indicating that transporters may not be involved at the human BBB	Nicolaï *et al.*, 2020
Brain tumor (glioblastoma)	P-gp and BCRP	AZD1775	MDCK-MDR1 and MDCK-BCRP (ER)	REF to scale CL_{efflux} from *in vitro* to *in vivo*	$K_{p,uu,brain\ tumor}$	$K_{p,uu,brain\ tumor}$ estimated from $K_{p,brain\ tumor}$ (from tumor resection) and binding data	Predicted $K_{p,uu,brain\ tumor}$ was 24% of the average observed value	P-gp BBB abundance from healthy subjects was used instead of that from subjects with brain tumor	Li *et al.*, 2017

Brain	P-gp and/or BCRP	Verapamil, diazepam, bupropion, lamotrigine, metoprolol, atenolol, levofloxacin, indomethacin, methotrexate	Brain-like endothelial cells (generated from stem cells) grown on filter	No scaling needed	$K_{p,uu,brain}$	CSF sampling ($K_{p,uu,CSF}$)	r^2=0.84 for the correlation between in vitro $K_{p,uu}$ and in vivo $K_{p,uu,CSF}$	CSF concentrations used as a surrogate for brain concentrations	(Cecchelli et al., 2014)
Liver	OATPs, NTCP, BCRP, MRP2, P-gp	Rosuvastatin	SCH	PSF to scale all *in vitro* passive and active hepatobiliary CLs from *in vitro* to *in vivo*	Liver AUC	PET imaging	P/O liver AUC: 0.08-0.14	PTM resulted in slightly better predictions than WSM Underprediction of liver AUC was the result of underprediction of $CL_{s,uptake}$ and overprediction of $CL_{s,efflux}$ and CL_{bile}	(Storelli et al., 2022b)
Liver	OATPs, NTCP, BCRP, MRP2, P-gp	Rosuvastatin	Transfected HEK293 or CHO or MDCKII cells (OATP1B1, 1B3, 2B1, NTCP) and HEK293 membrane	REF	Liver AUC	PET imaging	P/O liver AUC: 0.43-0.72	PTM resulted in slightly better predictions than WSM;incubation with HSA or plasma improved predictions (PMUE) Underprediction seems to be explained by underprediction of $CL_{s,uptake}$	(Storelli et al., 2022b)

			vesicles (BCRP, MRP2, P-gp)						
Liver	OATPs, NTCP	Telmisartan	SCH	PSF+ESF to scale *in vitro* passive and active hepatobiliary CLs from *in vitro* to *in vivo* (ESFs estimated from a set of 7 OATPs substrates)	Liver C-T profile	PET imaging	Predicted liver concentration-time profile agreed with the observed data (visual check)	Simulated and observed liver concentrations included both parent compound and glucuronide metabolite	(R. Li, Ghosh, et al., 2014)
Liver	OATPs, NTCP	Pravastatin, rosuvastatin	SH	No scaling needed	$K_{p,uu,liver}$	$K_{p,uu,liver}$ estimated from PK/PD modeling ($IC_{50,in\ vivo}$/ $IC_{50,in\ vitro}$ for 3-hydroxy-3-methylglutaryl-CoA reductase inhibition)	P/O=0.43 for pravastatin and 3.9 for rosuvastatin		(K. Riccardi et al., 2017)

3C, three compartments; 5C, five compartments; AAFE, average absolute fold error; AUC, area under the concentration-time profile; BBB, blood brain barrier; cER, cerebral extraction ratio; CL, clearance; CL_{bile}, biliary CL; $CL_{s,efflux}$, sinusoidal efflux CL; CL_{efflux}, efflux CL; $CL_{s,uptake}$, uptake CL; CL_{po}, oral clearance; C-T, concentration-time; ER, efflux ratio; ESF, empirical scaling factor; HSA, human serum albumin; IC_{50}, concentration to achieve 50% inhibition; ISF, interstitial fluid; IV, intravenous; $K_{p,uu,brain}$, ratio of unbound drug concentration in brain *vs*. plasma; $K_{p,uu,CSF}$, ratio of unbound drug concentration in cerebrospinal fluid *vs*. plasma;

$K_{p,uu,brain\ tumor}$, ratio of unbound drug concentration in brain tumor *vs*. plasma; P/O, predicted-over-observed ratio; PET, positron emission tomography; PMUE, protein-mediated uptake effect; PSF, physiological scaling factor; PTM, parallel-tube model; RAF, relative activity factor; REF, relative expression factor; CSF, cerebrospinal fluid; RMSE, root mean square error; SCH, sandwich-cultured hepatocytes; SH, suspended hepatocytes; SF, scaling factor, WSM, well-stirred model

Table 5: Predictive performances of *in vitro* to *in vivo* extrapolation (IVIVE) approaches for predicting transporter-based drug-drug interactions (DDIs). Unless otherwise indicated, predictions were validated using systemic PK data.

Organ	Transporters involved	Perpetrator	Victim	*In vitro* system	Model	Predicted parameter	Predictive performance	Comments	Study ID
Liver, kidney, intestine	BCRP, OATP1B1/3	Rifampicin, cyclosporine, gemfibrozil, fenebrutinib, fostamatinib, capmatinib, grazoprevir, grazoprevir+elbasvir, darolutamide, velpatasvir, itraconazole	Rosuvastatin	Perpetrator's IC_{50}: OATP1B1- and OATP1B3-transfected HEK293 cells; BCRP membrane vesicles Victim's $CL_{int,T}$: Hepatic: SCH + ESF Kidney: transfected HEK293 cells + ESF Intestine: optimized to recover PK	PBPK modeling	AUCR, $C_{max}R$, C-T profiles	Rifampicin IV: AUCR P/O = 0.96–1.07 $C_{max}R$ P/O = 0.55–0.87 Rifampicin PO: AUCRo P/O = 0.89–1.20 $C_{max}R$ P/O = 0.62–0.76 Cyclosporine: AUCR P/O = 0.73–0.55 $C_{max}R$ P/O = 0.50–0.59 Gemfibrozil: AUCR P/O = 1.06 $C_{max}R$ P/O = 1.16 Fenebrutinib: AUCR P/O = 0.81 $C_{max}R$ P/O = 0.91 Fostamatinib: AUCR P/O = 1.90 $C_{max}R$ P/O = 2.99 Capmatinib:	Included preincubation of perpetrator (30 min)	(Costales et al., 2021)

							AUCR P/O = 1.05 C_{max}R P/O = 1.47 Grazoprevir: AUCR P/O = 0.79 C_{max}R P/O = 0.36 Grazoprevir + Elbasvir: AUCR P/O = 0.92 C_{max}R P/O = 0.56 Darolutamide: AUCR P/O = 2.70 C_{max}RP/O = 2.35 Velpatasvir: AUCR P/O = 1.05 C_{max}RP/O = 1.55 Itraconazole: AUCR P/O = 0.90 C_{max}R P/O = 0.81		
Liver, kidney, intestine	OATP2B1, P-gp, BCRP, OATP1B1/1B3 and OAT3	Rifampicin, gemfibrozil, probenecid	Rosuvastatin	Perpetrator's IC_{50} and K_i: collected from literature Victim's $CL_{int,T}$: Optimized to recover PK data	PBPK modeling	AUCR, C_{max}R	Rifampicin: AUCR GMFE = 1.19 (range: 1.01-1.59) C_{max}R GMFE = 1.28 (range: 1.07-1.55) Gemfibrozil: AUCR GMFE = 1.33 C_{max}R GMFE = 1.32		(Hanke et al., 2021)

							Probenecid: AUCR GMFE = 1.15 C_{max}R GMFE = 1.54		
Liver	OATP1B1	Cyclosporin, rifampicin	Pemafibrate	Perpetrator's Ki: HEK293 cells + ESF Substrate $CL_{int,T}$: Cryopreserved human hepatocytes HEK293 cells	PBPK modeling	C-T profiles	Good fit between predicted and observed C-T profiles (visual inspection)	Pre-incubation of perpetrator included PMUE included	(Park et al., 2021)
Liver, kidney	OAT3, MRP4, OATP1B1	Furosemide, rifampicin	Probenecid	Perpetrator's Ki: Perpetrator Ki: Transfected HEK293 cells Victim's $CL_{int,T}$: Optimized to recover PK data	PBPK modeling	C_{max}R AUCR	Probenecid -furosemide: AUCR GMFE=1.17 C_{max}R GMFE =1.09 Probenecid - rifampicin: AUCR GMFE =1.19 C_{max}R GMFE =1.85		(Britz et al., 2020)

Liver, intestine	BCRP, OATP1B1/3	Fenebrutinib	Rosuvastatin	Victim's $CL_{int,T}$: Data collected from literature Perpetrator's IC50: OATP1B1, OATP1B3, or OAT3 – expressing HEK293 cells, BCRP-expressing MDCKII cells	PBPK modeling	CmaxR AUCR	AUC ratio P/O = 0.61 Cmax ratio P/O = 1.02	IC_{50} values determined with probes substrate	(Y. Chen et al., 2020)
Liver, intestine	P-gp, OATP1B1	Rifampin	Elagolix	Perpetrator's Ki: Used literature reported validated model Victim's $CL_{int,T}$: Estimated based on PK data	PBPK modeling	CmaxR AUCR	CmaxR % PE = 14-27 AUCR % PE = 28-39		(Chiney et al., 2020)
Liver, intestine	P-gp	Elagolix	Digoxin	Perpetrator's Ki: Estimated based on DDI data Victim's $CL_{int,T}$:	PBPK modeling	C_{max}R AUCR	C_{max} ratio % PE = 0.6-1 AUC ratio % PE = 6-8		(Chiney et al., 2020)

				Used literature reported validated model					
Liver	OATP1B1/3, OATP2B1, NTCP	Cyclosporin	Rosuvastatin	Transfected HEK293 and MDCKII cells (REF approach)	-	% inhibition of rosuvastatin uptake	The predicted % inhibition of rosuvastatin uptake by cyclosporin fell with the 95% CI of that observed *in vivo*	The inhibitor concentration and preincubation duration *in vitro* was kept the same as *in vivo; Validated by PET imaging*	(V. Kumar, Yin, et al., 2020)
Liver, kidney, intestine	P-gp, BCRP, MRP2, OATPs	Cyclosporin	Atorvastatin, cerivastatin, pravastatin, rosuvastatin, fluvastatin, simvastatin, lovastatin, repaglinide, bosentan	Perpetrator's Ki: collected from multiple literature sources Victim's $CL_{int,T}$: Optimized to recover PK data	PBPK modeling	$C_{max}R$ AUCR	96% predicted PK parameters fell within 0.5–2.0 fold of observed ones		(Yang et al., 2020)
Liver, intestine	OATP1B1, P-gp	Telaprevir	Maraviroc	Perpetrator's Ki: Optimized to recover DDI with probe drugs	PBPK modeling	AUCR	AUCR P/O= 0.83		(Kimoto et al., 2019)

				Victim's $CL_{int,T}$: SCH, SH, HEK293 cells + ESF					
Liver	OATP1B1, OATP1B3	GDC-0810, rifampicin, cyclosporine, gemfibrozil	Pravastatin	Perpetrator's Ki: HEK293 cells Victim's $CL_{int,T}$: OATP1B1/OATP1B3-expressing HEK293 cells	PBPK modeling	$C_{max}R$ AUCR	GDC-0810 $C_{max}R$ P/O= 0.84-1.7 AUCR P/O= 0.74-1.58 Rifampicin $C_{max}R$ P/O= 1.31 AUCR P/O= 1.53 Cyclosporine $C_{max}R$ P/O= 0.32 AUCR P/O= 0.17 Gemfibrozil $C_{max}R$ P/O= 1.63 AUCR P/O= 1.52	Included preincubation of perpetrator. K_i values determined with probes substrate	(Y. Chen et al., 2018)
Liver, kidney, intestine	P-gp	Rifampicin, clarithromycin	Digoxin	Perpetrator's IC50: Rifampicin: LLC-MDR1 cell Clarithromycin: Caco-2 cells Victim's $CL_{int,T}$: Optimized to recover PK data	PBPK modeling	$C_{max}R$ AUCR	**Rifampicin:** 6/7 AUCR P/O within 2-fold 4/5 $C_{max}R$ P/O within 2-fold **Clarithromycin:** 4/4 AUCR P/O within 2-fold 2/2 $C_{max}R$ P/O within 2-fold		(Hanke et al., 2018b)

Liver	OATP1B1, OATP1B3	Sacubitril	Atorvastatin and simvastatin	Perpetrator's K_i: OATP1B1 transfected HEK293 cells Victims' $CL_{int,T}$: SH (pooled) + ESF for atorvastatin and top-down estimation for simvastatin	PBPK	AUCR, $C_{max}R$	Atorvastatin $C_{max}R$ P/O= 0.98 AUCR P/O= 1.05 Simvastatin $C_{max}R$ P/O= 1.25 AUCR P/O= 1.23	K_i values determined with probe substrate, E217ß-G	(Lin et al., 2017)
Liver	OATP1B1, OATP1B3	Rifampicin	Pravastatin	Perpetrator's IC_{50}: transfected HEK293 cells Victim's $CL_{int,T}$: default Simcyp model (version 15) – not reported	PBPK	AUCR, $C_{max}R$	AUCR P/O= 1.18 $C_{max}R$ P/O= 1.04	Included preincubation (60 minutes); IC_{50} was determined with another victim drug, E217ß-G	(Pahwa et al., 2017)
Intestine, liver, kidney	OATP1B1, OATP1B3, OATP2B1,	Cyclosporine, rifampin, gemfibrozil	Rosuvastatin	Perpetrators' K_i: collected from literature and	PBPK	AUCR, $C_{max}R$	Cyclosporine AUCR P/O= 0.71 $C_{max}R$ P/O: 0.67 Rifampin	K_i values determined with probes substrates	(Q. Wang et al., 2017)

	BCRP, NTCP, OAT3			optimized to recover DDI data Victim's $CL_{int,T}$: optimized to recover PK, contribution determined from transfected cells, RAF and REF (collected from literature)			AUCR P/O = 1.26 C_{max}R P/O = 0.85 Rifampin IV AUC ratio P/O = 1.10 C_{max}R P/O = 0.74 Gemfibrozil AUC ratio P/O = 0.95 C_{max}R P/O = 0.92		
Intestine, liver	OATP1B1, BCRP	Fostamatinib, eltrombopag, darunavir, lopinavir, clopidogrel, ezetimibe, fenofibrate	Rosuvastatin	Perpetrators' K_I: Caco-2 cells (BCRP), OATP1B1 transfected cells Victim's $CL_{int,T}$: Estimation using a middle-out approach (*in vivo* PK and *in vitro* hepatocytes data)	Static	AUCR	AUC ratio P/O= Fostamatinib: 1.03 Eltrombopag: 1.03 Darunavir: 0.98 Lopinavir: 1.02 Clopidogrel: 1.03, 1.04 Ezetimibe: 1.07 Fenofibrate: 0.99	AUCR due to intestinal BCRP inhibition; K_i values determined with probes substrates	(Elsby et al., 2016)

Liver, kidney	OATP1B1, OAT3	Gemfibrozil and glucuronide metabolite	Atorvastatin, pitavastatin, rosuvastatin, pravastatin, montelukast, cerivastatin, repaglinide	Perpetrators' K_i: K_i data collected from literature (hepatocytes, oocytes) Victims' $CL_{int,T}$: SCH + ESF	Static	AUC ratio	AUCR P/O= Atorvastatin: 1.93 Pitavastatin: 1.87 Rosuvastatin: 1.42 Pravastatin: 1.10 Cerivastatin:0.98 Repaglinide: 0.41-1.06	Prediction improved by including inhibition by glucuronide metabolite	(M. V. S. Varma et al., 2015)
			Repaglinide, cerivastatin (dual OATP and CYP2C8/3A substrates)	Perpetrators' Ki: see above Victims' $CL_{int,T}$: SCH +ESF	PBPK	C-T profiles	Good fit between predicted and observed C-T profiles (visual inspection)	Inhibition of renal OAT3 not included	
Liver	OATP1B1	Rifampicin (IV and PO)	Glyburide	Perpetrator's Ki: sourced from literature, optimized to recover PK data Victim's $CL_{int,T}$: SCH +ESF	PBPK	C-T profiles, AUCR	Good fit between predicted and observed C-T profiles (visual inspection); AUCR P/O was within 0.8-1.25	K_i values determined with probes substrates	(M. V. S. Varma et al., 2014)
Liver	OATP1B1, OATP1B3, OATP2B1	Cyclosporine	Repaglinide	Perpetrator's IC_{50}: transfected HEK293 cells;	PBPK	C-T profiles	Good fit between predicted and observed C-T profiles (visual inspection)	Included preincubation;	(Gertz et al., 2013)

				Victim's $CL_{int,T}$: PH + ESF (f_t estimated based on in vivo PGx data)				IC_{50} values determined with probes substrates	
Kidney	OAT1, OAT3	Probenecid, S44121	S44121, Tenofovir, Ciprofloxacin	Perpetrator's IC50: OAT1-/OAT3-transfected *Xenopus laevis* oocytes Victim's $CL_{int,T}$: OAT1-/OAT3-transfected HEK293 cells RAF (S44121)	PBPK modeling	AUCR CL_rR $CL_{nr}R$	**S44121 as victim:** AUCR P/O=0.73, 0.71 CL_rR P/O=1.29, 1.36 $CL_{nr}R$ P/O=1.41, 1.14 **Tenofovir as victim:** AUCR P/O=1.12 CL_rR P/O=0.94 $CL_{nr}R$ P/O=0.8 **Ciprofloxacin as victim:** AUCR P/O=1.0 CL_rR P/O=1.0 $CL_{nr}R$ P/O=0.83	IC_{50} values determined with probes substrate	(Ball et al., 2017)
Kidney	MATE1/2-K, OCT2	Cimetidine	Metformin	Perpetrator's IC_{50}: transfected HEK293 cells Victim's $CL_{int,T}$: transfected HEK293 cells	PBPK	AUCR	Underpredicted (SA revealed K_i values needed to be decreased 8-fold to recover observed AUCR)	Membrane potential of OCT2 was accounted for	(Burt, Neuhoff, et al., 2016)

Kidney	OAT1, OAT3	Probenecid	13 renally cleared OATs substrates	Perpetrator's Ki: Transfected cells (OAT1, OAT3)	Static	AUCR	7/13 predicted AUCR were within 25% and 12/13 within 50% error of observed values	K_i values determined with probes substrates	(Feng et al., 2013)
Intestine	P-gp	Itraconazole, verapamil, clarithromycin	Dabigatran etexilate	Perpetrators' K_i: itraconazole: HEK293 membranes vesicles, clarithromycin: MDCK cells, verapamil: Caco-2 cells ; Victim's $CL_{int,T}$: K_m from Caco-2 cells and V_{max} estimated to recover PK	PBPK	AUCR, $C_{max}R$	Itraconazole $C_{max}R$ P/O= 1.20 AUCR P/O= 0.85; Verapamil $C_{max}R$ P/O= 0.69, 0.90 AUCR P/O= 0.75, 0.86 Clarithromycin $C_{max}R$ P/O= 0.74, 1.32, 1.17 AUCR P/O= 0.77, 1.44, 1.07	Included inhibitory potencies of metabolites of itraconazole and verapamil	Lang *et al.*, 2021

Unless otherwise mentioned, administration route of perpetrators and victim drugs is oral (PO). *AUCR, ratio of area under the systemic concentration-time profile in the presence and absence of the inhibitor; C-T, concentration-time; $CL_{int,T}$, transporter-mediated clearance; $C_{max}R$, ratio of maximal (systemic) concentrations in the presence and absence of the inhibitor; CLrR, ratio of renal clearance in the presence and absence of the inhibitor; CLnrR, ratio of non-renal clearance in the presence and absence of the inhibitor. GMFE, geometric mean fold error; % PE, percentage prediction error; DDI, drug-drug interaction; E217ß-G, estradiol 17β-d*

glucuronide; ESF, empirical scaling factor; f_t, fraction transported; GMFE, fold error on the geometric mean; IC_{50}, concentration of inhibitor that inhibits 50% of transporter activity; IV, intravenous; K_i, inhibition constant; K_m, affinity constant; P/O, predicted over observed; PBPK, physiologically-based pharmacokinetics; PGx, pharmacogenetic; PH, plated hepatocytes; PMUE, protein-mediated uptake effect; PK, pharmacokinetics; RAF, relative activity factor; REF, relative expression factor; SA, sensitivity analysis; SCH, sandwich-cultured hepatocytes; SF, scaling factor; SH, suspended hepatocytes; V_{max}, maximal velocity (equivalent to J_{max}, maximal transport rate).

13. References

Anoshchenko, O., Storelli, F., & Unadkat, J. D. (2021). Successful Prediction of Human Fetal Exposure to P-gp Substrate Drugs Using the Proteomics-informed Relative Expression Factor Approach and PBPK Modeling and Simulation. *Drug Metabolism and Disposition: The Biological Fate of Chemicals*, DMD-AR-2021-000538. https://doi.org/10.1124/dmd.121.000538

Arian, C. M., Imaoka, T., Yang, J., Kelly, E. J., & Thummel, K. E. (2022). Gutsy science: In vitro systems of the human intestine to model oral drug disposition. *Pharmacology & Therapeutics*, *230*, 107962. https://doi.org/10.1016/j.pharmthera.2021.107962

Badée, J., Achour, B., Rostami-Hodjegan, A., & Galetin, A. (2015). Meta-analysis of expression of hepatic organic anion-transporting polypeptide (OATP) transporters in cellular systems relative to human liver tissue. *Drug Metabolism and Disposition: The Biological Fate of Chemicals*, *43*(4), 424–432. https://doi.org/10.1124/dmd.114.062034

Ball, K., Jamier, T., Parmentier, Y., Denizot, C., Mallier, A., & Chenel, M. (2017). Prediction of renal transporter-mediated drug-drug interactions for a drug which is an OAT substrate and inhibitor using PBPK modelling. *European Journal of Pharmaceutical Sciences: Official Journal of the European Federation for Pharmaceutical Sciences*, *106*, 122–132. https://doi.org/10.1016/j.ejps.2017.05.055

Ballard, T. E., Kratochwil, N., Cox, L. M., Moen, M. A., Klammers, F., Ekiciler, A., Goetschi, A., & Walter, I. (2020). Simplifying the Execution of HepatoPac MetID Experiments: Metabolite Profile and Intrinsic Clearance Comparisons. *Drug Metabolism and Disposition: The Biological Fate of Chemicals*, *48*(9), 804–810. https://doi.org/10.1124/dmd.120.000013

Barter, Z. E., Bayliss, M. K., Beaune, P. H., Boobis, A. R., Carlile, D. J., Edwards, R. J., Houston, J. B., Lake, B. G., Lipscomb, J. C., Pelkonen, O. R., Tucker, G. T., & Rostami-Hodjegan, A. (2007). Scaling factors for the extrapolation of in vivo metabolic drug clearance from in vitro data: Reaching a consensus on values of human microsomal protein and hepatocellularity per gram of liver. *Current Drug Metabolism*, *8*(1), 33–45. https://doi.org/10.2174/138920007779315053

Belzer, M., Morales, M., Jagadish, B., Mash, E. A., & Wright, S. H. (2013). Substrate-Dependent Ligand Inhibition of the Human Organic Cation Transporter OCT2. *Journal of Pharmacology and Experimental Therapeutics*, *346*(2), 300–310. https://doi.org/10.1124/jpet.113.203257

Benet, L. Z., Bowman, C. M., Liu, S., & Sodhi, J. K. (2018). The Extended Clearance Concept Following Oral and Intravenous Dosing: Theory and Critical Analyses. *Pharmaceutical Research*, *35*(12), 242. https://doi.org/10.1007/s11095-018-2524-0

Benet, L. Z., & Sodhi, J. K. (2021). Can In Vitro–In Vivo Extrapolation Be Successful? Recognizing the Incorrect Clearance Assumptions. *Clinical Pharmacology & Therapeutics*, *n/a*(n/a). https://doi.org/10.1002/cpt.2482

Bi, Y., Qiu, X., Rotter, C. J., Kimoto, E., Piotrowski, M., Varma, M. V., Ei-Kattan, A. F., & Lai, Y. (2013). Quantitative assessment of the contribution of sodium-dependent taurocholate co-transporting polypeptide (NTCP) to the hepatic uptake of rosuvastatin, pitavastatin and fluvastatin. *Biopharmaceutics & Drug Disposition*, *34*(8), 452–461. https://doi.org/10.1002/bdd.1861

Bi, Y.-A., Costales, C., Mathialagan, S., West, M., Eatemadpour, S., Lazzaro, S., Tylaska, L., Scialis, R., Zhang, H., Umland, J., Kimoto, E., Tess, D. A., Feng, B., Tremaine, L. M., Varma, M. V. S., & Rodrigues, A. D. (2019). Quantitative Contribution of Six Major Transporters to the Hepatic Uptake of Drugs: “SLC-Phenotyping” Using Primary Human Hepatocytes. *The Journal of Pharmacology and Experimental Therapeutics*, *370*(1), 72–83. https://doi.org/10.1124/jpet.119.257600

Bi, Y.-A., Ryu, S., Tess, D. A., Rodrigues, A. D., & Varma, M. V. S. (2020). Effect of Human Plasma on Hepatic Uptake of Organic Anion-Transporting Polypeptide 1B Substrates: Studies using Transfected Cells and Primary Human Hepatocytes. *Drug Metabolism and Disposition: The Biological Fate of Chemicals*. https://doi.org/10.1124/dmd.120.000134

Bi, Y.-A., Scialis, R. J., Lazzaro, S., Mathialagan, S., Kimoto, E., Keefer, J., Zhang, H., Vildhede, A. M., Costales, C., Rodrigues, A. D., Tremaine, L. M., & Varma, M. V. S. (2017). Reliable Rate Measurements for Active and Passive Hepatic Uptake Using Plated Human Hepatocytes. *The AAPS Journal*, *19*(3), 787–796. https://doi.org/10.1208/s12248-017-0051-2

Billington, S., Shoner, S., Lee, S., Clark-Snustad, K., Pennington, M., Lewis, D., Muzi, M., Rene, S., Lee, J., Nguyen, T. B., Kumar, V., Ishida, K., Chen, L., Chu, X., Lai, Y., Salphati, L., Hop, C. E. C. A., Xiao, G., Liao, M., & Unadkat, J. D. (2019). Positron Emission Tomography Imaging of [11 C]Rosuvastatin Hepatic Concentrations and Hepatobiliary Transport in Humans in the Absence and Presence of Cyclosporin A. *Clinical Pharmacology and Therapeutics*, *106*(5), 1056–1066. https://doi.org/10.1002/cpt.1506

Borst, P., Evers, R., Kool, M., & Wijnholds, J. (1999). The multidrug resistance protein family. *Biochimica Et Biophysica Acta*, *1461*(2), 347–357. https://doi.org/10.1016/s0005-2736(99)00167-4

Bosgra, S., van de Steeg, E., Vlaming, M. L., Verhoeckx, K. C., Huisman, M. T., Verwei, M., & Wortelboer, H. M. (2014). Predicting carrier-mediated hepatic disposition of rosuvastatin in man by scaling from individual transfected cell-lines in vitro using absolute transporter protein quantification and PBPK modeling. *European Journal of Pharmaceutical Sciences: Official Journal of the European Federation for Pharmaceutical Sciences*, *65*, 156–166. https://doi.org/10.1016/j.ejps.2014.09.007

Bow, D. A. J., Perry, J. L., Miller, D. S., Pritchard, J. B., & Brouwer, K. L. R. (2008). Localization of P-gp (Abcb1) and Mrp2 (Abcc2) in freshly isolated rat hepatocytes. *Drug Metabolism and Disposition: The Biological Fate of Chemicals*, *36*(1), 198–202. https://doi.org/10.1124/dmd.107.018200

Bowman, C. M., & Benet, L. Z. (2016). Hepatic Clearance Predictions from In Vitro-In Vivo Extrapolation and the Biopharmaceutics Drug Disposition Classification System. *Drug Metabolism and Disposition: The Biological Fate of Chemicals*, *44*(11), 1731–1735. https://doi.org/10.1124/dmd.116.071514

Bowman, C. M., & Benet, L. Z. (2018). An examination of protein binding and protein-facilitated uptake relating to in vitro-in vivo extrapolation. *European Journal of Pharmaceutical Sciences: Official Journal of the European Federation for Pharmaceutical Sciences*, *123*, 502–514. https://doi.org/10.1016/j.ejps.2018.08.008

Bowman, C. M., Okochi, H., & Benet, L. Z. (2019). The Presence of a Transporter-Induced Protein Binding Shift: A New Explanation for Protein-Facilitated Uptake and Improvement for In Vitro-In

Vivo Extrapolation. *Drug Metabolism and Disposition: The Biological Fate of Chemicals*, *47*(4), 358–363. https://doi.org/10.1124/dmd.118.085779

Britz, H., Hanke, N., Taub, M. E., Wang, T., Prasad, B., Fernandez, É., Stopfer, P., Nock, V., & Lehr, T. (2020). Physiologically Based Pharmacokinetic Models of Probenecid and Furosemide to Predict Transporter Mediated Drug-Drug Interactions. *Pharmaceutical Research*, *37*(12), 250. https://doi.org/10.1007/s11095-020-02964-z

Brouwer, K. L. R., Keppler, D., Hoffmaster, K. A., Bow, D. a. J., Cheng, Y., Lai, Y., Palm, J. E., Stieger, B., Evers, R., & International Transporter Consortium. (2013). In vitro methods to support transporter evaluation in drug discovery and development. *Clinical Pharmacology and Therapeutics*, *94*(1), 95–112. https://doi.org/10.1038/clpt.2013.81

Brown, C. D. A., Sayer, R., Windass, A. S., Haslam, I. S., De Broe, M. E., D'Haese, P. C., & Verhulst, A. (2008). Characterisation of human tubular cell monolayers as a model of proximal tubular xenobiotic handling. *Toxicology and Applied Pharmacology*, *233*(3), 428–438. https://doi.org/10.1016/j.taap.2008.09.018

Bteich, M., Poulin, P., & Haddad, S. (2019). The potential protein-mediated hepatic uptake: Discussion on the molecular interactions between albumin and the hepatocyte cell surface and their implications for the in vitro-to-in vivo extrapolations of hepatic clearance of drugs. *Expert Opinion on Drug Metabolism & Toxicology*, *15*(8), 633–658. https://doi.org/10.1080/17425255.2019.1640679

Burt, H. J., Neuhoff, S., Almond, L., Gaohua, L., Harwood, M. D., Jamei, M., Rostami-Hodjegan, A., Tucker, G. T., & Rowland-Yeo, K. (2016). Metformin and cimetidine: Physiologically based pharmacokinetic modelling to investigate transporter mediated drug-drug interactions. *European Journal of Pharmaceutical Sciences: Official Journal of the European Federation for Pharmaceutical Sciences*, *88*, 70–82. https://doi.org/10.1016/j.ejps.2016.03.020

Burt, H. J., Riedmaier, A. E., Harwood, M. D., Crewe, H. K., Gill, K. L., & Neuhoff, S. (2016). Abundance of Hepatic Transporters in Caucasians: A Meta-Analysis. *Drug Metabolism and Disposition*, *44*(10), 1550–1561. https://doi.org/10.1124/dmd.116.071183

Camenisch, G., & Umehara, K. (2012). Predicting human hepatic clearance from in vitro drug metabolism and transport data: A scientific and pharmaceutical perspective for assessing drug-drug

interactions. *Biopharmaceutics & Drug Disposition*, *33*(4), 179–194. https://doi.org/10.1002/bdd.1784

Cecchelli, R., Aday, S., Sevin, E., Almeida, C., Culot, M., Dehouck, L., Coisne, C., Engelhardt, B., Dehouck, M.-P., & Ferreira, L. (2014). A stable and reproducible human blood-brain barrier model derived from hematopoietic stem cells. *PloS One*, *9*(6), e99733. https://doi.org/10.1371/journal.pone.0099733

Chang, S.-Y., Weber, E. J., Van Ness, K. P., Eaton, D. L., & Kelly, E. J. (2016). Liver and Kidney on Chips: Microphysiological Models to Understand Transporter Function. *Clinical Pharmacology and Therapeutics*, *100*(5), 464–478. https://doi.org/10.1002/cpt.436

Chen, W.-Y., Evangelista, E. A., Yang, J., Kelly, E. J., & Yeung, C. K. (2021). Kidney Organoid and Microphysiological Kidney Chip Models to Accelerate Drug Development and Reduce Animal Testing. *Frontiers in Pharmacology*, *12*, 695920. https://doi.org/10.3389/fphar.2021.695920

Chen, X., Unadkat, J. D., & Mao, Q. (2021). Tetrahydrocannabinol and Its Major Metabolites Are Not (or Are Poor) Substrates or Inhibitors of Human P-Glycoprotein [ATP-Binding Cassette (ABC) B1] and Breast Cancer Resistance Protein (ABCG2). *Drug Metabolism and Disposition: The Biological Fate of Chemicals*, *49*(10), 910–918. https://doi.org/10.1124/dmd.121.000505

Chen, Y., Ma, F., Jones, N. S., Yoshida, K., Chiang, P.-C., Durk, M. R., Wright, M. R., Jin, J. Y., & Chinn, L. W. (2020). Physiologically-Based Pharmacokinetic Model-Informed Drug Development for Fenebrutinib: Understanding Complex Drug-Drug Interactions. *CPT: Pharmacometrics & Systems Pharmacology*, *9*(6), 332–341. https://doi.org/10.1002/psp4.12515

Chen, Y., Zhu, R., Ma, F., Mao, J., Chen, E. C., Choo, E. F., Sahasranaman, S., & Liu, L. (2018). Assessment of OATP transporter-mediated drug-drug interaction using physiologically-based pharmacokinetic (PBPK) modeling—A case example. *Biopharmaceutics & Drug Disposition*, *39*(9), 420–430. https://doi.org/10.1002/bdd.2159

Chiney, M. S., Ng, J., Gibbs, J. P., & Shebley, M. (2020). Quantitative Assessment of Elagolix Enzyme-Transporter Interplay and Drug-Drug Interactions Using Physiologically Based Pharmacokinetic Modeling. *Clinical Pharmacokinetics*, *59*(5), 617–627. https://doi.org/10.1007/s40262-019-00833-6

Chothe, P. P., Wu, S.-P., Ye, Z., & Hariparsad, N. (2018). Assessment of Transporter-Mediated and Passive Hepatic Uptake Clearance Using Rifamycin-SV as a Pan-Inhibitor of Active Uptake. *Molecular Pharmaceutics*, *15*(10), 4677–4688. https://doi.org/10.1021/acs.molpharmaceut.8b00654

Chu, X., Bleasby, K., & Evers, R. (2013). Species differences in drug transporters and implications for translating preclinical findings to humans. *Expert Opinion on Drug Metabolism & Toxicology*, *9*(3), 237–252. https://doi.org/10.1517/17425255.2013.741589

Costales, C., Lin, J., Kimoto, E., Yamazaki, S., Gosset, J. R., Rodrigues, A. D., Lazzaro, S., West, M. A., West, M., & Varma, M. V. S. (2021). Quantitative prediction of breast cancer resistant protein mediated drug-drug interactions using physiologically-based pharmacokinetic modeling. *CPT: Pharmacometrics & Systems Pharmacology*, *10*(9), 1018–1031. https://doi.org/10.1002/psp4.12672

Czuba, L. C., Hillgren, K. M., & Swaan, P. W. (2018). Post-translational modifications of transporters. *Pharmacology & Therapeutics*, *192*, 88–99. https://doi.org/10.1016/j.pharmthera.2018.06.013

De Bruyn, T., Ufuk, A., Cantrill, C., Kosa, R. E., Bi, Y.-A., Niosi, M., Modi, S., Rodrigues, A. D., Tremaine, L. M., Varma, M. V. S., Galetin, A., & Houston, J. B. (2018). Predicting Human Clearance of Organic Anion Transporting Polypeptide Substrates Using Cynomolgus Monkey: In Vitro-In Vivo Scaling of Hepatic Uptake Clearance. *Drug Metabolism and Disposition: The Biological Fate of Chemicals*, *46*(7), 989–1000. https://doi.org/10.1124/dmd.118.081315

De Bruyn, T., Ye, Z.-W., Peeters, A., Sahi, J., Baes, M., Augustijns, P. F., & Annaert, P. P. (2011). Determination of OATP-, NTCP- and OCT-mediated substrate uptake activities in individual and pooled batches of cryopreserved human hepatocytes. *European Journal of Pharmaceutical Sciences: Official Journal of the European Federation for Pharmaceutical Sciences*, *43*(4), 297–307. https://doi.org/10.1016/j.ejps.2011.05.002

Deng, F., Tuomi, S.-K., Neuvonen, M., Hirvensalo, P., Kulju, S., Wenzel, C., Oswald, S., Filppula, A. M., & Niemi, M. (2021). Comparative Hepatic and Intestinal Efflux Transport of Statins. *Drug Metabolism and Disposition*, *49*(9), 750–759. https://doi.org/10.1124/dmd.121.000430

Dixit, V., Hariparsad, N., Li, F., Desai, P., Thummel, K. E., & Unadkat, J. D. (2007). Cytochrome P450 enzymes and transporters induced by anti-human immunodeficiency virus protease inhibitors in human hepatocytes: Implications for predicting clinical drug interactions. *Drug Metabolism and Disposition: The Biological Fate of Chemicals*, *35*(10), 1853–1859. https://doi.org/10.1124/dmd.107.016089

Dixit, V., Moore, A., Tsao, H., & Hariparsad, N. (2016). Application of Micropatterned Cocultured Hepatocytes to Evaluate the Inductive Potential and Degradation Rate of Major Xenobiotic Metabolizing Enzymes. *Drug Metabolism and Disposition: The Biological Fate of Chemicals*, *44*(2), 250–261. https://doi.org/10.1124/dmd.115.067173

Elsby, R., Martin, P., Surry, D., Sharma, P., & Fenner, K. (2016). Solitary Inhibition of the Breast Cancer Resistance Protein Efflux Transporter Results in a Clinically Significant Drug-Drug Interaction with Rosuvastatin by Causing up to a 2-Fold Increase in Statin Exposure. *Drug Metabolism and Disposition: The Biological Fate of Chemicals*, *44*(3), 398–408. https://doi.org/10.1124/dmd.115.066795

Eyal, S., Ke, B., Muzi, M., Link, J. M., Mankoff, D. A., Collier, A. C., & Unadkat, J. D. (2010). Regional P-glycoprotein activity and inhibition at the human blood-brain barrier as imaged by positron emission tomography. *Clinical Pharmacology and Therapeutics*, *87*(5), 579–585. https://doi.org/10.1038/clpt.2010.11

Feng, B., Hurst, S., Lu, Y., Varma, M. V., Rotter, C. J., El-Kattan, A., Lockwood, P., & Corrigan, B. (2013). Quantitative prediction of renal transporter-mediated clinical drug-drug interactions. *Molecular Pharmaceutics*, *10*(11), 4207–4215. https://doi.org/10.1021/mp400295c

Feng, B., Pemberton, R., Dworakowski, W., Ye, Z., Zetterberg, C., Wang, G., Morikawa, Y., & Kumar, S. (2021). Evaluation of the Utility of PXB Chimeric Mice for Predicting Human Liver Partitioning of Hepatic Organic Anion-Transporting Polypeptide Transporter Substrates. *Drug Metabolism and Disposition*, *49*(3), 254–264. https://doi.org/10.1124/dmd.120.000276

Fowler, S., Chen, W. L. K., Duignan, D. B., Gupta, A., Hariparsad, N., Kenny, J. R., Lai, W. G., Liras, J., Phillips, J. A., & Gan, J. (2020). Microphysiological systems for ADME-related applications:

Current status and recommendations for system development and characterization. *Lab on a Chip*, *20*(3), 446–467. https://doi.org/10.1039/c9lc00857h

Francis, L. J., Houston, J. B., & Hallifax, D. (2021). Impact of Plasma Protein Binding in Drug Clearance Prediction: A Data Base Analysis of Published Studies and Implications for In Vitro-In Vivo Extrapolation. *Drug Metabolism and Disposition: The Biological Fate of Chemicals*, *49*(3), 188–201. https://doi.org/10.1124/dmd.120.000294

Gerk, P. M., Li, W., & Vore, M. (2004). Estradiol 3-glucuronide is transported by the multidrug resistance-associated protein 2 but does not activate the allosteric site bound by estradiol 17-glucuronide. *Drug Metabolism and Disposition: The Biological Fate of Chemicals*, *32*(10), 1139–1145. https://doi.org/10.1124/dmd.104.000372

Gertz, M., Cartwright, C. M., Hobbs, M. J., Kenworthy, K. E., Rowland, M., Houston, J. B., & Galetin, A. (2013). Cyclosporine inhibition of hepatic and intestinal CYP3A4, uptake and efflux transporters: Application of PBPK modeling in the assessment of drug-drug interaction potential. *Pharmaceutical Research*, *30*(3), 761–780. https://doi.org/10.1007/s11095-012-0918-y

Gillette, J. R., & Pang, K. S. (1977). Theoretic aspects of pharmacokinetic drug interactions. *Clinical Pharmacology and Therapeutics*, *22*(5 Pt 2), 623–639. https://doi.org/10.1002/cpt1977225part2623

Greiner, B., Eichelbaum, M., Fritz, P., Kreichgauer, H. P., von Richter, O., Zundler, J., & Kroemer, H. K. (1999). The role of intestinal P-glycoprotein in the interaction of digoxin and rifampin. *The Journal of Clinical Investigation*, *104*(2), 147–153. https://doi.org/10.1172/JCI6663

Hafey, M. J., Houle, R., Tanis, K. Q., Knemeyer, I., Shang, J., Chen, Q., Baudy, A., Monroe, J., Sistare, F. D., & Evers, R. (2020). A Two-Tiered In Vitro Approach to De-Risk Drug Candidates for Potential Bile Salt Export Pump Inhibition Liabilities in Drug Discovery. *Drug Metabolism and Disposition: The Biological Fate of Chemicals*, *48*(11), 1147–1160. https://doi.org/10.1124/dmd.120.000086

Hanke, N., Frechen, S., Moj, D., Britz, H., Eissing, T., Wendl, T., & Lehr, T. (2018a). PBPK Models for CYP3A4 and P-gp DDI Prediction: A Modeling Network of Rifampicin, Itraconazole, Clarithromycin, Midazolam, Alfentanil, and Digoxin. *CPT: Pharmacometrics & Systems Pharmacology*, *7*(10), 647–659. https://doi.org/10.1002/psp4.12343

Hanke, N., Frechen, S., Moj, D., Britz, H., Eissing, T., Wendl, T., & Lehr, T. (2018b). PBPK Models for CYP3A4 and P-gp DDI Prediction: A Modeling Network of Rifampicin, Itraconazole, Clarithromycin, Midazolam, Alfentanil, and Digoxin. *CPT: Pharmacometrics & Systems Pharmacology*, *7*(10), 647–659. https://doi.org/10.1002/psp4.12343

Hanke, N., Gómez-Mantilla, J. D., Ishiguro, N., Stopfer, P., & Nock, V. (2021). Physiologically Based Pharmacokinetic Modeling of Rosuvastatin to Predict Transporter-Mediated Drug-Drug Interactions. *Pharmaceutical Research*, *38*(10), 1645–1661. https://doi.org/10.1007/s11095-021-03109-6

Harwood, M. D., Achour, B., Neuhoff, S., Russell, M. R., Carlson, G., Warhurst, G., & Amin Rostami-Hodjegan. (2016). In Vitro-In Vivo Extrapolation Scaling Factors for Intestinal P-Glycoprotein and Breast Cancer Resistance Protein: Part I: A Cross-Laboratory Comparison of Transporter-Protein Abundances and Relative Expression Factors in Human Intestine and Caco-2 Cells. *Drug Metabolism and Disposition: The Biological Fate of Chemicals*, *44*(3), 297–307. https://doi.org/10.1124/dmd.115.067371

Harwood, M. D., Neuhoff, S., Carlson, G. L., Warhurst, G., & Rostami-Hodjegan, A. (2013). Absolute abundance and function of intestinal drug transporters: A prerequisite for fully mechanistic in vitro-in vivo extrapolation of oral drug absorption. *Biopharmaceutics & Drug Disposition*, *34*(1), 2–28. https://doi.org/10.1002/bdd.1810

Hay, M., Thomas, D. W., Craighead, J. L., Economides, C., & Rosenthal, J. (2014). Clinical development success rates for investigational drugs. *Nature Biotechnology*, *32*(1), 40–51. https://doi.org/10.1038/nbt.2786

Hernández Lozano, I., Karch, R., Bauer, M., Blaickner, M., Matsuda, A., Wulkersdorfer, B., Hacker, M., Zeitlinger, M., & Langer, O. (2019). Towards Improved Pharmacokinetic Models for the Analysis of Transporter-Mediated Hepatic Disposition of Drug Molecules with Positron Emission Tomography. *The AAPS Journal*, *21*(4), 61. https://doi.org/10.1208/s12248-019-0323-0

Hernández Lozano, I., & Langer, O. (2020). Use of imaging to assess the activity of hepatic transporters. *Expert Opinion on Drug Metabolism & Toxicology*, *16*(2), 149–164. https://doi.org/10.1080/17425255.2020.1718107

Hickman, D., Wang, J. P., Wang, Y., & Unadkat, J. D. (1998). Evaluation of the selectivity of In vitro probes and suitability of organic solvents for the measurement of human cytochrome P450 monooxygenase activities. *Drug Metabolism and Disposition: The Biological Fate of Chemicals*, *26*(3), 207–215.

Houston, J. B., & Galetin, A. (2008). Methods for predicting in vivo pharmacokinetics using data from in vitro assays. *Current Drug Metabolism*, *9*(9), 940–951. https://doi.org/10.2174/138920008786485164

Hwang, S., Lee, S. G., Kim, K. H., Park, K. M., Ahn, C. S., Moon, D. B., Chu, C. W., Lee, Y. J., & Min, P. C. (2002). Correlation of blood-free graft weight and volumetric graft volume by an analysis of blood content in living donor liver grafts. *Transplantation Proceedings*, *34*(8), 3293–3294. https://doi.org/10.1016/s0041-1345(02)03603-5

Imaoka, T., Huang, W., Shum, S., Hailey, D. W., Chang, S.-Y., Chapron, A., Yeung, C. K., Himmelfarb, J., Isoherranen, N., & Kelly, E. J. (2021). Bridging the gap between in silico and in vivo by modeling opioid disposition in a kidney proximal tubule microphysiological system. *Scientific Reports*, *11*(1), 21356. https://doi.org/10.1038/s41598-021-00338-y

Ishida, K., Ullah, M., Tóth, B., Juhasz, V., & Unadkat, J. D. (2018). Successful Prediction of In Vivo Hepatobiliary Clearances and Hepatic Concentrations of Rosuvastatin Using Sandwich-Cultured Rat Hepatocytes, Transporter-Expressing Cell Lines, and Quantitative Proteomics. *Drug Metabolism and Disposition*, *46*(1), 66–74. https://doi.org/10.1124/dmd.117.076539

Izumi, S., Nozaki, Y., Komori, T., Maeda, K., Takenaka, O., Kusano, K., Yoshimura, T., Kusuhara, H., & Sugiyama, Y. (2013). Substrate-Dependent Inhibition of Organic Anion Transporting Polypeptide 1B1: Comparative Analysis with Prototypical Probe Substrates Estradiol-17 β -Glucuronide, Estrone-3-Sulfate, and Sulfobromophthalein. *Drug Metabolism and Disposition*, *41*(10), 1859–1866. https://doi.org/10.1124/dmd.113.052290

Izumi, S., Nozaki, Y., Kusuhara, H., Hotta, K., Mochizuki, T., Komori, T., Maeda, K., & Sugiyama, Y. (2018). Relative Activity Factor (RAF)-Based Scaling of Uptake Clearance Mediated by Organic Anion Transporting Polypeptide (OATP) 1B1 and OATP1B3 in Human Hepatocytes. *Molecular Pharmaceutics*, *15*(6), 2277–2288. https://doi.org/10.1021/acs.molpharmaceut.8b00138

Izumi, S., Nozaki, Y., Lee, W., & Sugiyama, Y. (2022). Experimental and modeling evidence supporting the trans-inhibition mechanism for preincubation time-dependent, long-lasting inhibition of organic anion transporting polypeptide (OATP) 1B1 by cyclosporine A. *Drug Metabolism and Disposition: The Biological Fate of Chemicals*, DMD-AR-2021-000783. https://doi.org/10.1124/dmd.121.000783

Jang, K.-J., Otieno, M. A., Ronxhi, J., Lim, H.-K., Ewart, L., Kodella, K. R., Petropolis, D. B., Kulkarni, G., Rubins, J. E., Conegliano, D., Nawroth, J., Simic, D., Lam, W., Singer, M., Barale, E., Singh, B., Sonee, M., Streeter, A. J., Manthey, C., … Hamilton, G. A. (2019). Reproducing human and cross-species drug toxicities using a Liver-Chip. *Science Translational Medicine*, *11*(517), eaax5516. https://doi.org/10.1126/scitranslmed.aax5516

Jenkinson, S. E., Chung, G. W., van Loon, E., Bakar, N. S., Dalzell, A. M., & Brown, C. D. A. (2012). The limitations of renal epithelial cell line HK-2 as a model of drug transporter expression and function in the proximal tubule. *Pflügers Archiv - European Journal of Physiology*, *464*(6), 601–611. https://doi.org/10.1007/s00424-012-1163-2

Jones, H. M., Barton, H. A., Lai, Y., Bi, Y.-A., Kimoto, E., Kempshall, S., Tate, S. C., El-Kattan, A., Houston, J. B., Galetin, A., & Fenner, K. S. (2012). Mechanistic pharmacokinetic modeling for the prediction of transporter-mediated disposition in humans from sandwich culture human hepatocyte data. *Drug Metabolism and Disposition: The Biological Fate of Chemicals*, *40*(5), 1007–1017. https://doi.org/10.1124/dmd.111.042994

Kaddoumi, A., Choi, S.-U., Kinman, L., Whittington, D., Tsai, C.-C., Ho, R. J. Y., Anderson, B. D., & Unadkat, J. D. (2007). Inhibition of P-glycoprotein activity at the primate blood-brain barrier increases the distribution of nelfinavir into the brain but not into the cerebrospinal fluid. *Drug Metabolism and Disposition: The Biological Fate of Chemicals*, *35*(9), 1459–1462. https://doi.org/10.1124/dmd.107.016220

Kameyama, Y., Yamashita, K., Kobayashi, K., Hosokawa, M., & Chiba, K. (2005). Functional characterization of SLCO1B1 (OATP-C) variants, SLCO1B1*5, SLCO1B1*15 and SLCO1B1*15+C1007G, by using transient expression systems of HeLa and HEK293 cells.

Pharmacogenetics and Genomics, *15*(7), 513–522. https://doi.org/10.1097/01.fpc.0000170913.73780.5f

Kaneko, K.-I., Tanaka, M., Ishii, A., Katayama, Y., Nakaoka, T., Irie, S., Kawahata, H., Yamanaga, T., Wada, Y., Miyake, T., Toshimoto, K., Maeda, K., Cui, Y., Enomoto, M., Kawamura, E., Kawada, N., Kawabe, J., Shiomi, S., Kusuhara, H., … Watanabe, Y. (2018). A Clinical Quantitative Evaluation of Hepatobiliary Transport of [11C]Dehydropravastatin in Humans Using Positron Emission Tomography. *Drug Metabolism and Disposition: The Biological Fate of Chemicals*, *46*(5), 719–728. https://doi.org/10.1124/dmd.118.080408

Karlgren, M., Simoff, I., Backlund, M., Wegler, C., Keiser, M., Handin, N., Müller, J., Lundquist, P., Jareborg, A.-C., Oswald, S., & Artursson, P. (2017). A CRISPR-Cas9 Generated MDCK Cell Line Expressing Human MDR1 Without Endogenous Canine MDR1 (cABCB1): An Improved Tool for Drug Efflux Studies. *Journal of Pharmaceutical Sciences*, *106*(9), 2909–2913. https://doi.org/10.1016/j.xphs.2017.04.018

Keemink, J., Deferm, N., De Bruyn, T., Augustijns, P., Bouillon, T., & Annaert, P. (2018). Effect of Cryopreservation on Enzyme and Transporter Activities in Suspended and Sandwich Cultured Rat Hepatocytes. *The AAPS Journal*, *20*(2), 33. https://doi.org/10.1208/s12248-018-0188-7

Kesselheim, A. S., Hwang, T. J., & Franklin, J. M. (2015). Two decades of new drug development for central nervous system disorders. *Nature Reviews. Drug Discovery*, *14*(12), 815–816. https://doi.org/10.1038/nrd4793

Kikuchi, R., Chiou, W. J., Durbin, K. R., Savaryn, J. P., Ma, J., Emami Riedmaier, A., de Morais, S. M., Jenkins, G. J., & Bow, D. A. J. (2021). Quantitation of Plasma Membrane Drug Transporters in Kidney Tissue and Cell Lines Using a Novel Proteomic Approach Enabled a Prospective Prediction of Metformin Disposition. *Drug Metabolism and Disposition: The Biological Fate of Chemicals*, *49*(10), 938–946. https://doi.org/10.1124/dmd.121.000487

Kim, S.-J., Lee, K.-R., Miyauchi, S., & Sugiyama, Y. (2019). Extrapolation of In Vivo Hepatic Clearance from In Vitro Uptake Clearance by Suspended Human Hepatocytes for Anionic Drugs with High Binding to Human Albumin: Improvement of In Vitro-to-In Vivo Extrapolation by Considering the “Albumin-Mediated” Hepatic Uptake Mechanism on the Basis of the “Facilitated-Dissociation

Model.” *Drug Metabolism and Disposition: The Biological Fate of Chemicals*, *47*(2), 94–103. https://doi.org/10.1124/dmd.118.083733

Kimoto, E., Bi, Y.-A., Kosa, R. E., Tremaine, L. M., & Varma, M. V. S. (2017a). Hepatobiliary Clearance Prediction: Species Scaling From Monkey, Dog, and Rat, and In Vitro-In Vivo Extrapolation of Sandwich-Cultured Human Hepatocytes Using 17 Drugs. *Journal of Pharmaceutical Sciences*, *106*(9), 2795–2804. https://doi.org/10.1016/j.xphs.2017.04.043

Kimoto, E., Bi, Y.-A., Kosa, R. E., Tremaine, L. M., & Varma, M. V. S. (2017b). Hepatobiliary Clearance Prediction: Species Scaling From Monkey, Dog, and Rat, and In Vitro-In Vivo Extrapolation of Sandwich-Cultured Human Hepatocytes Using 17 Drugs. *Journal of Pharmaceutical Sciences*, *106*(9), 2795–2804. https://doi.org/10.1016/j.xphs.2017.04.043

Kimoto, E., Vourvahis, M., Scialis, R. J., Eng, H., Rodrigues, A. D., & Varma, M. V. S. (2019). Mechanistic Evaluation of the Complex Drug-Drug Interactions of Maraviroc: Contribution of Cytochrome P450 3A, P-Glycoprotein and Organic Anion Transporting Polypeptide 1B1. *Drug Metabolism and Disposition: The Biological Fate of Chemicals*, *47*(5), 493–503. https://doi.org/10.1124/dmd.118.085241

Kindla, J., Müller, F., Mieth, M., Fromm, M. F., & König, J. (2011). Influence of non-steroidal anti-inflammatory drugs on organic anion transporting polypeptide (OATP) 1B1- and OATP1B3-mediated drug transport. *Drug Metabolism and Disposition: The Biological Fate of Chemicals*, *39*(6), 1047–1053. https://doi.org/10.1124/dmd.110.037622

Kodaira, H., Kusuhara, H., Fujita, T., Ushiki, J., Fuse, E., & Sugiyama, Y. (2011). Quantitative evaluation of the impact of active efflux by p-glycoprotein and breast cancer resistance protein at the blood-brain barrier on the predictability of the unbound concentrations of drugs in the brain using cerebrospinal fluid concentration as a surrogate. *The Journal of Pharmacology and Experimental Therapeutics*, *339*(3), 935–944. https://doi.org/10.1124/jpet.111.180398

Korjamo, T., Heikkinen, A. T., & Mönkkönen, J. (2009). Analysis of unstirred water layer in in vitro permeability experiments. *Journal of Pharmaceutical Sciences*, *98*(12), 4469–4479. https://doi.org/10.1002/jps.21762

Korjamo, T., Heikkinen, A. T., Waltari, P., & Mönkkönen, J. (2008). The asymmetry of the unstirred water layer in permeability experiments. *Pharmaceutical Research*, *25*(7), 1714–1722. https://doi.org/10.1007/s11095-008-9573-8

Korzekwa, K. R., Nagar, S., Tucker, J., Weiskircher, E. A., Bhoopathy, S., & Hidalgo, I. J. (2012). Models to predict unbound intracellular drug concentrations in the presence of transporters. *Drug Metabolism and Disposition: The Biological Fate of Chemicals*, *40*(5), 865–876. https://doi.org/10.1124/dmd.111.044289

Kotani, N., Maeda, K., Debori, Y., Camus, S., Li, R., Chesne, C., & Sugiyama, Y. (2012). Expression and Transport Function of Drug Uptake Transporters in Differentiated HepaRG Cells. *Molecular Pharmaceutics*, *9*(12), 3434–3441. https://doi.org/10.1021/mp300171p

Kotani, N., Maeda, K., Watanabe, T., Hiramatsu, M., Gong, L., Bi, Y., Takezawa, T., Kusuhara, H., & Sugiyama, Y. (2011). Culture period-dependent changes in the uptake of transporter substrates in sandwich-cultured rat and human hepatocytes. *Drug Metabolism and Disposition: The Biological Fate of Chemicals*, *39*(9), 1503–1510. https://doi.org/10.1124/dmd.111.038968

Kreisl, W. C., Liow, J. S., Kimura, N., Seneca, N., Zoghbi, S. S., Morse, C. L., Herscovitch, P., Pike, V. W., & Innis, R. B. (2010). P-Glycoprotein Function at the Blood-Brain Barrier in Humans Can Be Quantified with the Substrate Radiotracer 11C-N-Desmethyl-Loperamide. *Journal of Nuclear Medicine*, *51*(4), 559–566. https://doi.org/10.2967/jnumed.109.070151

Kumar, A. R., Prasad, B., Bhatt, D. K., Mathialagan, S., Varma, M. V. S., & Unadkat, J. D. (2021). IVIVE of Transporter-Mediated Renal Clearance: Relative Expression Factor (REF) vs Relative Activity Factor (RAF) Approach. *Drug Metabolism and Disposition: The Biological Fate of Chemicals*. https://doi.org/10.1124/dmd.121.000367

Kumar, V., Li, C. Y., Ishida, K., Kis, E., Gáborik, Z., & Unadkat, J. D. (2020). Pitfalls in Predicting Hepatobiliary Drug Transport Using Human Sandwich-Cultured Hepatocytes. *The AAPS Journal*, *22*(5), 110. https://doi.org/10.1208/s12248-020-00496-3

Kumar, V., Nguyen, T. B., Tóth, B., Juhasz, V., & Unadkat, J. D. (2017). Optimization and Application of a Biotinylation Method for Quantification of Plasma Membrane Expression of Transporters in Cells. *The AAPS Journal*, *19*(5), 1377–1386. https://doi.org/10.1208/s12248-017-0121-5

Kumar, V., Prasad, B., Patilea, G., Gupta, A., Salphati, L., Evers, R., Hop, C. E. C. A., & Unadkat, J. D. (2015). Quantitative transporter proteomics by liquid chromatography with tandem mass spectrometry: Addressing methodologic issues of plasma membrane isolation and expression-activity relationship. *Drug Metabolism and Disposition: The Biological Fate of Chemicals*, *43*(2), 284–288. https://doi.org/10.1124/dmd.114.061614

Kumar, V., Salphati, L., Hop, C. E. C. A., Xiao, G., Lai, Y., Mathias, A., Chu, X., Humphreys, W. G., Liao, M., Heyward, S., & Unadkat, J. D. (2019). A Comparison of Total and Plasma Membrane Abundance of Transporters in Suspended, Plated, Sandwich-Cultured Human Hepatocytes Versus Human Liver Tissue Using Quantitative Targeted Proteomics and Cell Surface Biotinylation. *Drug Metabolism and Disposition: The Biological Fate of Chemicals*, *47*(4), 350–357. https://doi.org/10.1124/dmd.118.084988

Kumar, V., Yin, J., Billington, S., Prasad, B., Brown, C. D. A., Wang, J., & Unadkat, J. D. (2018). The Importance of Incorporating OCT2 Plasma Membrane Expression and Membrane Potential in IVIVE of Metformin Renal Secretory Clearance. *Drug Metabolism and Disposition*, *46*(10), 1441–1445. https://doi.org/10.1124/dmd.118.082313

Kumar, V., Yin, M., Ishida, K., Salphati, L., Hop, C. E. C. A., Rowbottom, C., Xiao, G., Lai, Y., Mathias, A., Chu, X., Humphreys, W. G., Liao, M., Nerada, Z., Szilvásy, N., Heyward, S., & Unadkat, J. D. (2020). Prediction of Transporter-Mediated Rosuvastatin Hepatic Uptake Clearance and Drug Interaction in Humans Using Proteomics-Informed REF Approach. *Drug Metabolism and Disposition*, DMD-AR-2020-000204. https://doi.org/10.1124/dmd.120.000204

Kunze, A., Huwyler, J., Poller, B., Gutmann, H., & Camenisch, G. (2014). In vitro-in vivo extrapolation method to predict human renal clearance of drugs. *Journal of Pharmaceutical Sciences*, *103*(3), 994–1001. https://doi.org/10.1002/jps.23851

Lauwers, F., Cassot, F., Lauwers-Cances, V., Puwanarajah, P., & Duvernoy, H. (2008). Morphometry of the human cerebral cortex microcirculation: General characteristics and space-related profiles. *NeuroImage*, *39*(3), 936–948. https://doi.org/10.1016/j.neuroimage.2007.09.024

Lee, W., Ha, J., & Sugiyama, Y. (2020). Post-translational regulation of the major drug transporters in the families of organic anion transporters and organic anion–transporting polypeptides. *The Journal of Biological Chemistry*, *295*(50), 17349–17364. https://doi.org/10.1074/jbc.REV120.009132

Lei, Y. D., Wania, F., Shiu, W. Y., & Boocock, D. G. B. (2000). HPLC-Based Method for Estimating the Temperature Dependence of n-Octanol−Water Partition Coefficients. *Journal of Chemical & Engineering Data*, *45*(5), 738–742. https://doi.org/10.1021/je9902488

Li, C. Y., Basit, A., Gupta, A., Gáborik, Z., Kis, E., & Prasad, B. (2019). Major glucuronide metabolites of testosterone are primarily transported by MRP2 and MRP3 in human liver, intestine and kidney. *The Journal of Steroid Biochemistry and Molecular Biology*, *191*, 105350. https://doi.org/10.1016/j.jsbmb.2019.03.027

Li, J., Wu, J., Bao, X., Honea, N., Xie, Y., Kim, S., Sparreboom, A., & Sanai, N. (2017). Quantitative and Mechanistic Understanding of AZD1775 Penetration across Human Blood-Brain Barrier in Glioblastoma Patients Using an IVIVE-PBPK Modeling Approach. *Clinical Cancer Research: An Official Journal of the American Association for Cancer Research*, *23*(24), 7454–7466. https://doi.org/10.1158/1078-0432.CCR-17-0983

Li, N., Badrinarayanan, A., Li, X., Roberts, J., Hayashi, M., Virk, M., & Gupta, A. (2020). Comparison of In Vitro to In Vivo Extrapolation Approaches for Predicting Transporter-Mediated Hepatic Uptake Clearance Using Suspended Rat Hepatocytes. *Drug Metabolism and Disposition*, *48*(10), 861–872. https://doi.org/10.1124/dmd.120.000064

Li, R., Barton, H. A., Yates, P. D., Ghosh, A., Wolford, A. C., Riccardi, K. A., & Maurer, T. S. (2014). A “middle-out” approach to human pharmacokinetic predictions for OATP substrates using physiologically-based pharmacokinetic modeling. *Journal of Pharmacokinetics and Pharmacodynamics*, *41*(3), 197–209. https://doi.org/10.1007/s10928-014-9357-1

Li, R., Bi, Y.-A., Lai, Y., Sugano, K., Steyn, S. J., Trapa, P. E., & Di, L. (2014). Permeability comparison between hepatocyte and low efflux MDCKII cell monolayer. *The AAPS Journal*, *16*(4), 802–809. https://doi.org/10.1208/s12248-014-9616-5

Li, R., Ghosh, A., Maurer, T. S., Kimoto, E., & Barton, H. A. (2014). Physiologically based pharmacokinetic prediction of telmisartan in human. *Drug Metabolism and Disposition: The Biological Fate of Chemicals*, *42*(10), 1646–1655. https://doi.org/10.1124/dmd.114.058461

Liang, X., Park, Y., DeForest, N., Hao, J., Zhao, X., Niu, C., Wang, K., Smith, B., & Lai, Y. (2020). In Vitro Hepatic Uptake in Human and Monkey Hepatocytes in the Presence and Absence of Serum Protein and Its In Vitro to In Vivo Extrapolation. *Drug Metabolism and Disposition: The Biological Fate of Chemicals*, *48*(12), 1283–1292. https://doi.org/10.1124/dmd.120.000163

Lin, W., Ji, T., Einolf, H., Ayalasomayajula, S., Lin, T.-H., Hanna, I., Heimbach, T., Breen, C., Jarugula, V., & He, H. (2017). Evaluation of Drug-Drug Interaction Potential Between Sacubitril/Valsartan (LCZ696) and Statins Using a Physiologically Based Pharmacokinetic Model. *Journal of Pharmaceutical Sciences*, *106*(5), 1439–1451. https://doi.org/10.1016/j.xphs.2017.01.007

Loe, D. W., Almquist, K. C., Deeley, R. G., & Cole, S. P. (1996). Multidrug resistance protein (MRP)-mediated transport of leukotriene C4 and chemotherapeutic agents in membrane vesicles. Demonstration of glutathione-dependent vincristine transport. *The Journal of Biological Chemistry*, *271*(16), 9675–9682. https://doi.org/10.1074/jbc.271.16.9675

Loryan, I., Hammarlund-Udenaes, M., & Syvänen, S. (2020). *Brain Distribution of Drugs: Pharmacokinetic Considerations* (pp. 1–30). Springer. https://doi.org/10.1007/164_2020_405

Lundquist, P., Lööf, J., Sohlenius-Sternbeck, A.-K., Floby, E., Johansson, J., Bylund, J., Hoogstraate, J., Afzelius, L., & Andersson, T. B. (2014). The impact of solute carrier (SLC) drug uptake transporter loss in human and rat cryopreserved hepatocytes on clearance predictions. *Drug Metabolism and Disposition: The Biological Fate of Chemicals*, *42*(3), 469–480. https://doi.org/10.1124/dmd.113.054676

Maeda, K., Ohnishi, A., Sasaki, M., Ikari, Y., Aita, K., Watanabe, Y., Kusuhara, H., Sugiyama, Y., & Senda, M. (2019). Quantitative investigation of hepatobiliary transport of [11C]telmisartan in humans by PET imaging. *Drug Metabolism and Pharmacokinetics*, *34*(5), 293–299. https://doi.org/10.1016/j.dmpk.2019.02.004

Markus, J., Landry, T., Stevens, Z., Scott, H., Llanos, P., Debatis, M., Armento, A., Klausner, M., & Ayehunie, S. (2021). Human small intestinal organotypic culture model for drug permeation,

inflammation, and toxicity assays. *In Vitro Cellular & Developmental Biology - Animal*, *57*(2), 160–173. https://doi.org/10.1007/s11626-020-00526-6

Mateus, A., Matsson, P., & Artursson, P. (2013). Rapid Measurement of Intracellular Unbound Drug Concentrations. *Molecular Pharmaceutics*, *10*(6), 2467–2478. https://doi.org/10.1021/mp4000822

Mathialagan, S., Piotrowski, M. A., Tess, D. A., Feng, B., Litchfield, J., & Varma, M. V. (2017a). Quantitative Prediction of Human Renal Clearance and Drug-Drug Interactions of Organic Anion Transporter Substrates Using In Vitro Transport Data: A Relative Activity Factor Approach. *Drug Metabolism and Disposition: The Biological Fate of Chemicals*, *45*(4), 409–417. https://doi.org/10.1124/dmd.116.074294

Mathialagan, S., Piotrowski, M. A., Tess, D. A., Feng, B., Litchfield, J., & Varma, M. V. (2017b). Quantitative Prediction of Human Renal Clearance and Drug-Drug Interactions of Organic Anion Transporter Substrates Using In Vitro Transport Data: A Relative Activity Factor Approach. *Drug Metabolism and Disposition: The Biological Fate of Chemicals*, *45*(4), 409–417. https://doi.org/10.1124/dmd.116.074294

Matsunaga, N., Ufuk, A., Morse, B. L., Bedwell, D. W., Bao, J., Mohutsky, M. A., Hillgren, K. M., Hall, S. D., Houston, J. B., & Galetin, A. (2019). Hepatic Organic Anion Transporting Polypeptide-Mediated Clearance in the Beagle Dog: Assessing In Vitro-In Vivo Relationships and Applying Cross-Species Empirical Scaling Factors to Improve Prediction of Human Clearance. *Drug Metabolism and Disposition: The Biological Fate of Chemicals*, *47*(3), 215–226. https://doi.org/10.1124/dmd.118.084194

Mitchell, W., Alam, N., Amaral, K., Ho, D., & Li, A. P. (2019, July). *Effect of organic solvents on pravastatin uptake in human hepatocytes*. International Society for the Study of Xenobiotics (ISSX) 12th International Meeting 2019, Portland, USA.

Mitra, P., Weinheimer, S., Michalewicz, M., & Taub, M. E. (2018). Prediction and Quantification of Hepatic Transporter-Mediated Uptake of Pitavastatin Utilizing a Combination of the Relative Activity Factor Approach and Mechanistic Modeling. *Drug Metabolism and Disposition: The Biological Fate of Chemicals*, *46*(7), 953–963. https://doi.org/10.1124/dmd.118.080614

Miyauchi, S., Masuda, M., Kim, S.-J., Tanaka, Y., Lee, K.-R., Iwakado, S., Nemoto, M., Sasaki, S., Shimono, K., Tanaka, Y., & Sugiyama, Y. (2018). The Phenomenon of Albumin-Mediated Hepatic Uptake of Organic Anion Transport Polypeptide Substrates: Prediction of the In Vivo Uptake Clearance from the In Vitro Uptake by Isolated Hepatocytes Using a Facilitated-Dissociation Model. *Drug Metabolism and Disposition: The Biological Fate of Chemicals*, *46*(3), 259–267. https://doi.org/10.1124/dmd.117.077115

Moore, A., Chothe, P. P., Tsao, H., & Hariparsad, N. (2016). Evaluation of the Interplay between Uptake Transport and CYP3A4 Induction in Micropatterned Cocultured Hepatocytes. *Drug Metabolism and Disposition: The Biological Fate of Chemicals*, *44*(12), 1910–1919. https://doi.org/10.1124/dmd.116.072660

Morgan, P., Van Der Graaf, P. H., Arrowsmith, J., Feltner, D. E., Drummond, K. S., Wegner, C. D., & Street, S. D. A. (2012). Can the flow of medicines be improved? Fundamental pharmacokinetic and pharmacological principles toward improving Phase II survival. *Drug Discovery Today*, *17*(9–10), 419–424. https://doi.org/10.1016/j.drudis.2011.12.020

Nagar, S., Tucker, J., Weiskircher, E. A., Bhoopathy, S., Hidalgo, I. J., & Korzekwa, K. (2014). Compartmental models for apical efflux by P-glycoprotein--part 1: Evaluation of model complexity. *Pharmaceutical Research*, *31*(2), 347–359. https://doi.org/10.1007/s11095-013-1164-7

Nagaya, Y., Katayama, K., Kusuhara, H., & Nozaki, Y. (2020). Impact of P-glycoprotein-mediated active efflux on drug distribution into lumbar cerebrospinal fluid in nonhuman primates. *Drug Metabolism and Disposition: The Biological Fate of Chemicals*. https://doi.org/10.1124/dmd.120.000099

Nakakariya, M., Ono, M., Amano, N., Moriwaki, T., Maeda, K., & Sugiyama, Y. (2012). In vivo biliary clearance should be predicted by intrinsic biliary clearance in sandwich-cultured hepatocytes. *Drug Metabolism and Disposition: The Biological Fate of Chemicals*, *40*(3), 602–609. https://doi.org/10.1124/dmd.111.042101

Nakaoka, T., Kaneko, K., Irie, S., Mawatari, A., Igesaka, A., Uetake, Y., Ochiai, H., Niwa, T., Yamano, E., Wada, Y., Tanaka, M., Kotani, K., Kawahata, H., Kawabe, J., Miki, Y., Doi, H., Hosoya, T., Kazuya, M., Kusuhara, H., … Watanabe, Y. (2022). Clinical evaluation of [18F]pitavastatin for

quantitative analysis of hepatobiliary transporter activity. *Drug Metabolism and Pharmacokinetics*, 100449. https://doi.org/10.1016/j.dmpk.2022.100449

Neal, E. H., Marinelli, N. A., Shi, Y., McClatchey, P. M., Balotin, K. M., Gullett, D. R., Hagerla, K. A., Bowman, A. B., Ess, K. C., Wikswo, J. P., & Lippmann, E. S. (2019). A Simplified, Fully Defined Differentiation Scheme for Producing Blood-Brain Barrier Endothelial Cells from Human iPSCs. *Stem Cell Reports*, *12*(6), 1380–1388. https://doi.org/10.1016/j.stemcr.2019.05.008

Nicolaï, J., Chapy, H., Gillent, E., Saunders, K., Ungell, A.-L., Nicolas, J.-M., & Chanteux, H. (2020). Impact of In Vitro Passive Permeability in a P-gp-transfected LLC-PK1 Model on the Prediction of the Rat and Human Unbound Brain-to-Plasma Concentration Ratio. *Pharmaceutical Research*, *37*(9), 175. https://doi.org/10.1007/s11095-020-02867-z

Niessen, J., Jedlitschky, G., Grube, M., Bien, S., Schwertz, H., Ohtsuki, S., Kawakami, H., Kamiie, J., Oswald, S., Starke, K., Strobel, U., Siegmund, W., Rosskopf, D., Greinacher, A., Terasaki, T., & Kroemer, H. K. (2009). Human platelets express organic anion-transporting peptide 2B1, an uptake transporter for atorvastatin. *Drug Metabolism and Disposition: The Biological Fate of Chemicals*, *37*(5), 1129–1137. https://doi.org/10.1124/dmd.108.024570

Nozaki, Y., & Izumi, S. (2020). Recent advances in preclinical in vitro approaches towards quantitative prediction of hepatic clearance and drug-drug interactions involving organic anion transporting polypeptide (OATP) 1B transporters. *Drug Metabolism and Pharmacokinetics*, *35*(1), 56–70. https://doi.org/10.1016/j.dmpk.2019.11.004

Onozato, D., Yamashita, M., Nakanishi, A., Akagawa, T., Kida, Y., Ogawa, I., Hashita, T., Iwao, T., & Matsunaga, T. (2018). Generation of Intestinal Organoids Suitable for Pharmacokinetic Studies from Human Induced Pluripotent Stem Cells. *Drug Metabolism and Disposition*, *46*(11), 1572–1580. https://doi.org/10.1124/dmd.118.080374

Ozawa, T., Takayama, K., Okamoto, R., Negoro, R., Sakurai, F., Tachibana, M., Kawabata, K., & Mizuguchi, H. (2015). Generation of enterocyte-like cells from human induced pluripotent stem cells for drug absorption and metabolism studies in human small intestine. *Scientific Reports*, *5*(1), 16479. https://doi.org/10.1038/srep16479

Pahwa, S., Alam, K., Crowe, A., Farasyn, T., Neuhoff, S., Hatley, O., Ding, K., & Yue, W. (2017). Pretreatment With Rifampicin and Tyrosine Kinase Inhibitor Dasatinib Potentiates the Inhibitory Effects Toward OATP1B1- and OATP1B3-Mediated Transport. *Journal of Pharmaceutical Sciences*, *106*(8), 2123–2135. https://doi.org/10.1016/j.xphs.2017.03.022

Palaiokostas, M., Ding, W., Shahane, G., & Orsi, M. (2018). Effects of lipid composition on membrane permeation. *Soft Matter*, *14*(42), 8496–8508. https://doi.org/10.1039/c8sm01262h

Pang, K. S., Han, Y. R., Noh, K., Lee, P. I., & Rowland, M. (2019). Hepatic clearance concepts and misconceptions: Why the well-stirred model is still used even though it is not physiologic reality? *Biochemical Pharmacology*, *169*, 113596. https://doi.org/10.1016/j.bcp.2019.07.025

Park, J. E., Shitara, Y., Lee, W., Morita, S., Sahi, J., Toshimoto, K., & Sugiyama, Y. (2021). Improved Prediction of the Drug-Drug Interactions of Pemafibrate Caused by Cyclosporine A and Rifampicin via PBPK Modeling: Consideration of the Albumin-Mediated Hepatic Uptake of Pemafibrate and Inhibition Constants With Preincubation Against OATP1B. *Journal of Pharmaceutical Sciences*, *110*(1), 517–528. https://doi.org/10.1016/j.xphs.2020.10.016

Patilea-Vrana, G., & Unadkat, J. D. (2016). Transport vs. Metabolism: What Determines the Pharmacokinetics and Pharmacodynamics of Drugs? Insights From the Extended Clearance Model. *Clinical Pharmacology and Therapeutics*, *100*(5), 413–418. https://doi.org/10.1002/cpt.437

Peng, J., Ladumor, M. K., & Unadkat, J. D. (2021). Prediction of Pregnancy-Induced Changes in Secretory and Total Renal Clearance of Drugs Transported by Organic Anion Transporters. *Drug Metabolism and Disposition: The Biological Fate of Chemicals*, *49*(10), 929–937. https://doi.org/10.1124/dmd.121.000557

Pfeifer, N. D., Yang, K., & Brouwer, K. L. R. (2013). Hepatic basolateral efflux contributes significantly to rosuvastatin disposition I: Characterization of basolateral versus biliary clearance using a novel protocol in sandwich-cultured hepatocytes. *The Journal of Pharmacology and Experimental Therapeutics*, *347*(3), 727–736. https://doi.org/10.1124/jpet.113.207472

Prasad, B., Achour, B., Artursson, P., Hop, C. E. C. A., Lai, Y., Smith, P. C., Barber, J., Wisniewski, J. R., Spellman, D., Uchida, Y., Zientek, M. A., Unadkat, J. D., & Rostami-Hodjegan, A. (2019). Toward a Consensus on Applying Quantitative Liquid Chromatography-Tandem Mass Spectrometry

Proteomics in Translational Pharmacology Research: A White Paper. *Clinical Pharmacology and Therapeutics*, *106*(3), 525–543. https://doi.org/10.1002/cpt.1537

Prasad, B., & Unadkat, J. D. (2015). The concept of fraction of drug transported (ft) with special emphasis on BBB efflux of CNS and antiretroviral drugs. *Clinical Pharmacology and Therapeutics*, *97*(4), 320–323. https://doi.org/10.1002/cpt.72

Purushothaman, S., Cama, J., & Keyser, U. F. (2016). Dependence of norfloxacin diffusion across bilayers on lipid composition. *Soft Matter*, *12*(7), 2135–2144. https://doi.org/10.1039/c5sm02371h

Qiu, X., Zhang, Y., Liu, T., Shen, H., Xiao, Y., Bourner, M. J., Pratt, J. R., Thompson, D. C., Marathe, P., Humphreys, W. G., & Lai, Y. (2016). Disruption of BSEP Function in HepaRG Cells Alters Bile Acid Disposition and Is a Susceptive Factor to Drug-Induced Cholestatic Injury. *Molecular Pharmaceutics*, *13*(4), 1206–1216. https://doi.org/10.1021/acs.molpharmaceut.5b00659

Ramsden, D., Tweedie, D. J., Chan, T. S., Taub, M. E., & Li, Y. (2014). Bridging in vitro and in vivo metabolism and transport of faldaprevir in human using a novel cocultured human hepatocyte system, HepatoPac. *Drug Metabolism and Disposition: The Biological Fate of Chemicals*, *42*(3), 394–406. https://doi.org/10.1124/dmd.113.055897

Riccardi, K. A., Tess, D. A., Lin, J., Patel, R., Ryu, S., Atkinson, K., Di, L., & Li, R. (2019). A Novel Unified Approach to Predict Human Hepatic Clearance for Both Enzyme- and Transporter-Mediated Mechanisms Using Suspended Human Hepatocytes. *Drug Metabolism and Disposition: The Biological Fate of Chemicals*, *47*(5), 484–492. https://doi.org/10.1124/dmd.118.085639

Riccardi, K., Lin, J., Li, Z., Niosi, M., Ryu, S., Hua, W., Atkinson, K., Kosa, R. E., Litchfield, J., & Di, L. (2017). Novel Method to Predict In Vivo Liver-to-Plasma Kpuu for OATP Substrates Using Suspension Hepatocytes. *Drug Metabolism and Disposition: The Biological Fate of Chemicals*, *45*(5), 576–580. https://doi.org/10.1124/dmd.116.074575

Rodrigues, A. D., Lai, Y., Shen, H., Varma, M. V. S., Rowland, A., & Oswald, S. (2020). Induction of Human Intestinal and Hepatic Organic Anion Transporting Polypeptides: Where Is the Evidence for Its Relevance in Drug-Drug Interactions? *Drug Metabolism and Disposition: The Biological Fate of Chemicals*, *48*(3), 205–216. https://doi.org/10.1124/dmd.119.089615

Rowland, M., Roberts, M. S., & Pang, K. S. (2022). In Defense of Current Concepts and Applications of Clearance in Drug Development and Therapeutics. *Drug Metabolism and Disposition: The Biological Fate of Chemicals*, *50*(2), 187–190. https://doi.org/10.1124/dmd.121.000637

Sachar, M., Kumar, V., Gormsen, L. C., Munk, O. L., & Unadkat, J. D. (2020). Successful Prediction of Positron Emission Tomography-Imaged Metformin Hepatic Uptake Clearance in Humans Using the Quantitative Proteomics-Informed Relative Expression Factor Approach. *Drug Metabolism and Disposition: The Biological Fate of Chemicals*, *48*(11), 1210–1216. https://doi.org/10.1124/dmd.120.000156

Sanoh, S., Naritomi, Y., Kitamura, S., Shinagawa, A., Kakuni, M., Tateno, C., & Ohta, S. (2020). Predictability of human pharmacokinetics of drugs that undergo hepatic organic anion transporting polypeptide (OATP)-mediated transport using single-species allometric scaling in chimeric mice with humanized liver: Integration with hepatic drug metabolism. *Xenobiotica*, *50*(11), 1370–1379. https://doi.org/10.1080/00498254.2020.1769229

Sarkar, U., Ravindra, K. C., Large, E., Young, C. L., Rivera-Burgos, D., Yu, J., Cirit, M., Hughes, D. J., Wishnok, J. S., Lauffenburger, D. A., Griffith, L. G., & Tannenbaum, S. R. (2017). Integrated Assessment of Diclofenac Biotransformation, Pharmacokinetics, and Omics-Based Toxicity in a Three-Dimensional Human Liver-Immunocompetent Coculture System. *Drug Metabolism and Disposition: The Biological Fate of Chemicals*, *45*(7), 855–866. https://doi.org/10.1124/dmd.116.074005

Sasongko, L., Link, J. M., Muzi, M., Mankoff, D. A., Yang, X., Collier, A. C., Shoner, S. C., & Unadkat, J. D. (2005). Imaging P-glycoprotein transport activity at the human blood-brain barrier with positron emission tomography. *Clinical Pharmacology and Therapeutics*, *77*(6), 503–514. https://doi.org/10.1016/j.clpt.2005.01.022

Sato, S., Matsumiya, K., Tohyama, K., & Kosugi, Y. (2021a). Translational CNS Steady-State Drug Disposition Model in Rats, Monkeys, and Humans for Quantitative Prediction of Brain-to-Plasma and Cerebrospinal Fluid-to-Plasma Unbound Concentration Ratios. *The AAPS Journal*, *23*(4), 81. https://doi.org/10.1208/s12248-021-00609-6

Sato, S., Matsumiya, K., Tohyama, K., & Kosugi, Y. (2021b). Translational CNS Steady-State Drug Disposition Model in Rats, Monkeys, and Humans for Quantitative Prediction of Brain-to-Plasma and Cerebrospinal Fluid-to-Plasma Unbound Concentration Ratios. *The AAPS Journal*, *23*(4), 81. https://doi.org/10.1208/s12248-021-00609-6

Shen, D. D., Artru, A. A., & Adkison, K. K. (2004). Principles and applicability of CSF sampling for the assessment of CNS drug delivery and pharmacodynamics. *Advanced Drug Delivery Reviews*, *56*(12), 1825–1857. https://doi.org/10.1016/j.addr.2004.07.011

Shitara, Y., Horie, T., & Sugiyama, Y. (2006a). Transporters as a determinant of drug clearance and tissue distribution. *European Journal of Pharmaceutical Sciences: Official Journal of the European Federation for Pharmaceutical Sciences*, *27*(5), 425–446. https://doi.org/10.1016/j.ejps.2005.12.003

Shitara, Y., Horie, T., & Sugiyama, Y. (2006b). Transporters as a determinant of drug clearance and tissue distribution. *European Journal of Pharmaceutical Sciences: Official Journal of the European Federation for Pharmaceutical Sciences*, *27*(5), 425–446. https://doi.org/10.1016/j.ejps.2005.12.003

Simoff, I., Karlgren, M., Backlund, M., Lindström, A.-C., Gaugaz, F. Z., Matsson, P., & Artursson, P. (2016). Complete Knockout of Endogenous Mdr1 (Abcb1) in MDCK Cells by CRISPR-Cas9. *Journal of Pharmaceutical Sciences*, *105*(2), 1017–1021. https://doi.org/10.1016/S0022-3549(15)00171-9

Sirianni, G. L., & Pang, K. S. (1997). Organ clearance concepts: New perspectives on old principles. *Journal of Pharmacokinetics and Biopharmaceutics*, *25*(4), 449–470. https://doi.org/10.1023/a:1025792925854

Smietana, K., Siatkowski, M., & Møller, M. (2016). Trends in clinical success rates. *Nature Reviews. Drug Discovery*, *15*(6), 379–380. https://doi.org/10.1038/nrd.2016.85

Soars, M. G., McGinnity, D. F., Grime, K., & Riley, R. J. (2007). The pivotal role of hepatocytes in drug discovery. *Chemico-Biological Interactions*, *168*(1), 2–15. https://doi.org/10.1016/j.cbi.2006.11.002

Sprowl, J. A., Ong, S. S., Gibson, A. A., Hu, S., Du, G., Lin, W., Li, L., Bharill, S., Ness, R. A., Stecula, A., Offer, S. M., Diasio, R. B., Nies, A. T., Schwab, M., Cavaletti, G., Schlatter, E., Ciarimboli, G., Schellens, J. H. M., Isacoff, E. Y., … Pabla, N. (2016). A phosphotyrosine switch regulates organic cation transporters. *Nature Communications*, *7*, 10880. https://doi.org/10.1038/ncomms10880

Stieger, B., & Hagenbuch, B. (2014). Organic anion-transporting polypeptides. *Current Topics in Membranes*, *73*, 205–232. https://doi.org/10.1016/B978-0-12-800223-0.00005-0

Storelli, F., Anoshchenko, O., & Unadkat, J. D. (2021). Successful Prediction of Human Steady-State Unbound Brain-to-Plasma Concentration Ratio of P-gp Substrates Using the Proteomics-Informed Relative Expression Factor Approach. *Clinical Pharmacology & Therapeutics*, *110*(2), 432–442. https://doi.org/10.1002/cpt.2227

Storelli, F., Billington, S., Kumar, A. R., & Unadkat, J. D. (2021). Abundance of P-Glycoprotein and Other Drug Transporters at the Human Blood-Brain Barrier in Alzheimer's Disease: A Quantitative Targeted Proteomic Study. *Clinical Pharmacology and Therapeutics*, *109*(3), 667–675. https://doi.org/10.1002/cpt.2035

Storelli, F., Li, C. Y., Sachar, M., Kumar, V., Heyward, S., Sáfár, Z., Kis, E., & Unadkat, J. D. (2022a). Prediction of Hepatobiliary Clearances and Hepatic Concentrations of Transported Drugs in Humans Using Rosuvastatin as a Model Drug. *Clinical Pharmacology and Therapeutics*. https://doi.org/10.1002/cpt.2556

Storelli, F., Li, C. Y., Sachar, M., Kumar, V., Heyward, S., Sáfár, Z., Kis, E., & Unadkat, J. D. (2022b). Prediction of Hepatobiliary Clearances and Hepatic Concentrations of Transported Drugs in Humans Using Rosuvastatin as a Model Drug. *Clinical Pharmacology and Therapeutics*. https://doi.org/10.1002/cpt.2556

Tachibana, T., Kitamura, S., Kato, M., Mitsui, T., Shirasaka, Y., Yamashita, S., & Sugiyama, Y. (2010). Model analysis of the concentration-dependent permeability of P-gp substrates. *Pharmaceutical Research*, *27*(3), 442–446. https://doi.org/10.1007/s11095-009-0026-9

Takashima, T., Hashizume, Y., Katayama, Y., Murai, M., Wada, Y., Maeda, K., Sugiyama, Y., & Watanabe, Y. (2011). The involvement of organic anion transporting polypeptide in the hepatic

uptake of telmisartan in rats: PET studies with [^{11}C]telmisartan. *Molecular Pharmaceutics*, *8*(5), 1789–1798. https://doi.org/10.1021/mp200160t

Takashima, T., Kitamura, S., Wada, Y., Tanaka, M., Shigihara, Y., Ishii, H., Ijuin, R., Shiomi, S., Nakae, T., Watanabe, Y., Cui, Y., Doi, H., Suzuki, M., Maeda, K., Kusuhara, H., Sugiyama, Y., & Watanabe, Y. (2012). PET imaging-based evaluation of hepatobiliary transport in humans with (15R)-11C-TIC-Me. *Journal of Nuclear Medicine: Official Publication, Society of Nuclear Medicine*, *53*(5), 741–748. https://doi.org/10.2967/jnumed.111.098681

Tournier, N., Bauer, M., Pichler, V., Nics, L., Klebermass, E.-M., Bamminger, K., Matzneller, P., Weber, M., Karch, R., Caillé, F., Auvity, S., Marie, S., Jäger, W., Wadsak, W., Hacker, M., Zeitlinger, M., & Langer, O. (2019). Impact of P-Glycoprotein Function on the Brain Kinetics of the Weak Substrate ^{11} C-Metoclopramide Assessed with PET Imaging in Humans. *Journal of Nuclear Medicine*, *60*(7), 985–991. https://doi.org/10.2967/jnumed.118.219972

Tournier, N., Stieger, B., & Langer, O. (2018). Imaging techniques to study drug transporter function in vivo. *Pharmacology & Therapeutics*, *189*, 104–122. https://doi.org/10.1016/j.pharmthera.2018.04.006

Trapa, P. E., Troutman, M. D., Lau, T. Y., Wager, T. T., Maurer, T. S., Patel, N. C., West, M. A., Umland, J. P., Carlo, A. A., Feng, B., & Liras, J. L. (2019). In Vitro-In Vivo Extrapolation of Key Transporter Activity at the Blood-Brain Barrier. *Drug Metabolism and Disposition: The Biological Fate of Chemicals*, *47*(4), 405–411. https://doi.org/10.1124/dmd.118.083279

Ulvestad, M., Björquist, P., Molden, E., Asberg, A., & Andersson, T. B. (2011). OATP1B1/1B3 activity in plated primary human hepatocytes over time in culture. *Biochemical Pharmacology*, *82*(9), 1219–1226. https://doi.org/10.1016/j.bcp.2011.07.076

Varma, M. V. S., Lin, J., Bi, Y., Kimoto, E., & Rodrigues, A. D. (2015). Quantitative Rationalization of Gemfibrozil Drug Interactions: Consideration of Transporters-Enzyme Interplay and the Role of Circulating Metabolite Gemfibrozil 1-O-β-Glucuronide. *Drug Metabolism and Disposition: The Biological Fate of Chemicals*, *43*(7), 1108–1118. https://doi.org/10.1124/dmd.115.064303

Varma, M. V. S., Scialis, R. J., Lin, J., Bi, Y.-A., Rotter, C. J., Goosen, T. C., & Yang, X. (2014). Mechanism-based pharmacokinetic modeling to evaluate transporter-enzyme interplay in drug

interactions and pharmacogenetics of glyburide. *The AAPS Journal*, *16*(4), 736–748. https://doi.org/10.1208/s12248-014-9614-7

Varma, M. V., Steyn, S. J., Allerton, C., & El-Kattan, A. F. (2015). Predicting Clearance Mechanism in Drug Discovery: Extended Clearance Classification System (ECCS). *Pharmaceutical Research*, *32*(12), 3785–3802. https://doi.org/10.1007/s11095-015-1749-4

Verscheijden, L. F. M., Litjens, C. H. C., Koenderink, J. B., Mathijssen, R. H. J., Verbeek, M. M., de Wildt, S. N., & Russel, F. G. M. (2021). Physiologically based pharmacokinetic/pharmacodynamic model for the prediction of morphine brain disposition and analgesia in adults and children. *PLoS Computational Biology*, *17*(3), e1008786. https://doi.org/10.1371/journal.pcbi.1008786

Vildhede, A., Mateus, A., Khan, E. K., Lai, Y., Karlgren, M., Artursson, P., & Kjellsson, M. C. (2016). Mechanistic Modeling of Pitavastatin Disposition in Sandwich-Cultured Human Hepatocytes: A Proteomics-Informed Bottom-Up Approach. *Drug Metabolism and Disposition: The Biological Fate of Chemicals*, *44*(4), 505–516. https://doi.org/10.1124/dmd.115.066746

Wang, L., Prasad, B., Salphati, L., Chu, X., Gupta, A., Hop, C. E. C. A., Evers, R., & Unadkat, J. D. (2015). Interspecies variability in expression of hepatobiliary transporters across human, dog, monkey, and rat as determined by quantitative proteomics. *Drug Metabolism and Disposition: The Biological Fate of Chemicals*, *43*(3), 367–374. https://doi.org/10.1124/dmd.114.061580

Wang, L., Zhu, Z., Tran, D., Seo, S. K., & Pan, X. (2021). Advancing Estimation of Hepatobiliary Clearances in Physiologically Based Pharmacokinetic Models of Rosuvastatin Using Human Hepatic Concentrations. *Pharmaceutical Research*. https://doi.org/10.1007/s11095-021-03138-1

Wang, Q., Zheng, M., & Leil, T. (2017). Investigating Transporter-Mediated Drug-Drug Interactions Using a Physiologically Based Pharmacokinetic Model of Rosuvastatin: Investigating DDI Using a Rosuvastatin PBPK Model. *CPT: Pharmacometrics & Systems Pharmacology*, *6*(4), 228–238. https://doi.org/10.1002/psp4.12168

Watanabe, T., Kusuhara, H., Maeda, K., Shitara, Y., & Sugiyama, Y. (2009). Physiologically Based Pharmacokinetic Modeling to Predict Transporter-Mediated Clearance and Distribution of Pravastatin in Humans. *Journal of Pharmacology and Experimental Therapeutics*, *328*(2), 652–662. https://doi.org/10.1124/jpet.108.146647

Watanabe, T., Kusuhara, H., Watanabe, T., Debori, Y., Maeda, K., Kondo, T., Nakayama, H., Horita, S., Ogilvie, B. W., Parkinson, A., Hu, Z., & Sugiyama, Y. (2011). Prediction of the overall renal tubular secretion and hepatic clearance of anionic drugs and a renal drug-drug interaction involving organic anion transporter 3 in humans by in vitro uptake experiments. *Drug Metabolism and Disposition: The Biological Fate of Chemicals*, *39*(6), 1031–1038. https://doi.org/10.1124/dmd.110.036129

Wegler, C., Gazit, M., Issa, K., Subramaniam, S., Artursson, P., & Karlgren, M. (2021). Expanding the Efflux In Vitro Assay Toolbox: A CRISPR-Cas9 Edited MDCK Cell Line with Human BCRP and Completely Lacking Canine MDR1. *Journal of Pharmaceutical Sciences*, *110*(1), 388–396. https://doi.org/10.1016/j.xphs.2020.09.039

Wood, F. L., Houston, J. B., & Hallifax, D. (2017). Clearance Prediction Methodology Needs Fundamental Improvement: Trends Common to Rat and Human Hepatocytes/Microsomes and Implications for Experimental Methodology. *Drug Metabolism and Disposition: The Biological Fate of Chemicals*, *45*(11), 1178–1188. https://doi.org/10.1124/dmd.117.077040

Woolbright, B. L., McGill, M. R., Yan, H., & Jaeschke, H. (2016). Bile Acid-Induced Toxicity in HepaRG Cells Recapitulates the Response in Primary Human Hepatocytes. *Basic & Clinical Pharmacology & Toxicology*, *118*(2), 160–167. https://doi.org/10.1111/bcpt.12449

Yang, Y., Li, P., Zhang, Z., Wang, Z., Liu, L., & Liu, X. (2020). Prediction of Cyclosporin-Mediated Drug Interaction Using Physiologically Based Pharmacokinetic Model Characterizing Interplay of Drug Transporters and Enzymes. *International Journal of Molecular Sciences*, *21*(19), E7023. https://doi.org/10.3390/ijms21197023

Yin, M., Storelli, F., & Unadkat, J. D. (2022). Is The Protein-Mediated Uptake Of Drugs By OATPs A Real Phenomenon Or An Artifact? *Drug Metabolism and Disposition: The Biological Fate of Chemicals*, DMD-AR-2022-000849. https://doi.org/10.1124/dmd.122.000849

Yoshikado, T., Lee, W., Toshimoto, K., Morita, K., Kiriake, A., Chu, X., Lee, N., Kimoto, E., Varma, M. V. S., Kikuchi, R., Scialis, R. J., Shen, H., Ishiguro, N., Lotz, R., Li, A. P., Maeda, K., Kusuhara, H., & Sugiyama, Y. (2021). Evaluation of Hepatic Uptake of OATP1B Substrates by Short Term-

Cultured Plated Human Hepatocytes: Comparison With Isolated Suspended Hepatocytes. *Journal of Pharmaceutical Sciences*, *110*(1), 376–387. https://doi.org/10.1016/j.xphs.2020.10.041

Yoshikado, T., Yoshida, K., Kotani, N., Nakada, T., Asaumi, R., Toshimoto, K., Maeda, K., Kusuhara, H., & Sugiyama, Y. (2016). Quantitative Analyses of Hepatic OATP-Mediated Interactions Between Statins and Inhibitors Using PBPK Modeling With a Parameter Optimization Method. *Clinical Pharmacology and Therapeutics*, *100*(5), 513–523. https://doi.org/10.1002/cpt.391

Zamek-Gliszczynski, M. J., Kalvass, J. C., Pollack, G. M., & Brouwer, K. L. R. (2009). Relationship between drug/metabolite exposure and impairment of excretory transport function. *Drug Metabolism and Disposition: The Biological Fate of Chemicals*, *37*(2), 386–390. https://doi.org/10.1124/dmd.108.023648

Zamek-Gliszczynski, M. J., Lee, C. A., Poirier, A., Bentz, J., Chu, X., Ellens, H., Ishikawa, T., Jamei, M., Kalvass, J. C., Nagar, S., Pang, K. S., Korzekwa, K., Swaan, P. W., Taub, M. E., Zhao, P., Galetin, A., & International Transporter Consortium. (2013). ITC recommendations for transporter kinetic parameter estimation and translational modeling of transport-mediated PK and DDIs in humans. *Clinical Pharmacology and Therapeutics*, *94*(1), 64–79. https://doi.org/10.1038/clpt.2013.45

Zhang, Y., Panfen, E., Fancher, M., Sinz, M., Marathe, P., & Shen, H. (2019). Dissecting the Contribution of OATP1B1 to Hepatic Uptake of Statins Using the OATP1B1 Selective Inhibitor Estropipate. *Molecular Pharmaceutics*, *16*(6), 2342–2353. https://doi.org/10.1021/acs.molpharmaceut.8b01226